Aus dem Institut für Transfusionsmedizin und Immunologie

der Medizinischen Fakultät Mannheim

Direktor: Prof. Dr. med. Harald Klüter

Analysis of the effect of SI-CLP on tumor growth and on the composition of tumor microenvironment

Inauguraldissertation

zur Erlangung des Doctor scientiarum humanarum (Dr. sc. hum)

der

Medizinischen Fakultät Mannheim

der Ruprecht-Karls-Universität

zu Heidelberg

Vorgelegt von

Shuiping Yin

aus Anhui, China

2016

Dekan: Prof. Dr. med. Sergij Goerdt

Referentin: Prof. Dr. rer. nat. Julia Kzhyshkowska

Contents

Abbreviations

°C	Degrees Celsius
A	Ampere
AKT	Protein kinase B
AMCase	Acidic mammalian chitinase
APC	Allophycocyanin
APS	Ammonium persulfate
BSA	Bovine serum albumin
CCL	Chemokine (C-C motif) ligand
CCR	Chemokine (C-C motif) receptor
CD	Cluster of differentiation
cDNA	Complementary deoxyribonucleic acid
CLP	Chitinase-like proteins
cm	centimeter
CO_2	Carbon dioxide
CR	Complement receptors
CSF	Colony stimulating factors
CXCL	Chemokine (C-X-C motif) ligand
DAPI	4', 6-Diamidino-2-phenylindole
ddH_2O	double distilled H_2O
DMEM	Dulbecco´s modified Eagle's medium
DMSO	Dimethyl sulfoxide
DNA	Deoxyribonucleic acid
DNase	Deoxyribonuclease
dNTP	Deoxynucleotides
E. coli	Escherichia coli
ECF	Eosinophil chemotactic cytokine
ECM	Extracellular matrix
EDTA	Ethylenediaminetetraacetic acid
EGF	Epidermal growth factor
ERK	Extracellular signal-regulated kinase
F	Forward
FACS	Fluorescence-Activated Cell Sorting
FCS	Fetal Calf Serum
FGF	Fibroblast growth factor
GlcNAc	N-Acetylglucosamine
g	gram(s)
h	hour(s)
HCl	Hydrochloric acid
HLA	Human leukocyte antigen (Histocompatibility antigen)
HMVECs	Human microvascular endothelial cells
HRP	Horseradish peroxide

IFN	Interferon
Ig	Immunoglobulin
IHC	Immunohistochemistry
IL	Interleukin
kb	kilobase
kDa	Kilodalton
ko	knockout
LB	Lysogeny broth
LPS	Lipopolysaccharides
M	Molar
mA	milliampere
MAPK	Mitogen-activated protein kinase
MCP	Monocyte chemoattractant protein
mg	milligrams
MHC	Major histocompatibility complex
mi	micro
MIF	Macrophage migration inhibitory factor
min	minute(s)
MIP	Macrophage Inflammatory Protein
ml	milliliter
mM	millimolar
MMP	Metalloproteinase
mRNA	messenger ribonucleic acid
MW	Molecular weight
NA	Not Applicable
NF-κB	Nuclear factor 'Kappa-light-chain-enhancer' of activated B cells
ng	nanogram(s)
NK	Natural killer
NOS	Nitric oxide synthases
P/S	Penicillin/Streptomycin
PAGE	Polyacrylamide gel electrophoresis
PBS	Phosphate-buffered saline
PD	Programmed cell death
PDGF	Platelet-derived growth factor
PFA	Paraformaldehyde
Pr	Probe
R	Reverse
RCF	Relative Centrifugal Force
RNA	Ribonucleic acid
rpm	revolutions per min
RT-PCR	Real-time polymerase chain reaction
S100A9	S100 calcium-binding protein A9
SDF	Stromal cell-derived factor

SDS	Sodium dodecyl sulfate
sec	second(s)
SFM	Serum-free medium
sh	small hairpin
si	short interfering
SI-CLP	Stabilin-1-interacting chitinase-like protein
st	stock concentration
STAT	Signal transducers and activators of transcription
TAE	Tris-Acetate-EDTA
TAM	Tumor-associated macrophages
TEMED	Tetramethylethylenediamine
TGF	Transforming growth factor
TGS	Tris-Glycine-SDS
Th	Helper T
TNF	Tumor necrosis factor
Tris	(hydroxymethyl) aminomethane
uPA	Urokinase-type plasminogen activator
VEGF	Vascular endothelial growth factor
VSMC	Vascular smooth muscle cells
wd	working dilution
wt	wide type
µg	microgram(s)
µl	microliter
µM	micromolar

1   Introduction

1.1   Chitinase-like protein family

1.1.1   Structure and properties of chitinase-like proteins

Chitinases and chitinase-like proteins, characterized by the presence of an 18-times α/β barrel structure, are widely found in bacteria, fungi, insects, protozoan parasites, plants and mammals, and serve as a component of the host defense mechanism against chitin-containing organisms[1,2]. Some plants increase the production of chitinases to inhibit fungal growth by degrading part of their cell walls containing chitin[3]. Chitin, composed of N-acetylglucosamine repeats of β-(1-4)-poly-N-acetyl D-glucosamine, is mainly found in lower life forms, including mushrooms, as well as the cell walls of fungi and bacteria, the exoskeleton of insects and crustaceans, and the microfilaria sheath of parasitic nematodes[1,4].

In mammals, true chitinases are represented by acidic mammalian chitinase (AMCase) and chitotriosidase that possess a chitin binding domain and enzymatic activity, and are able to hydrolyze chitin into oligosaccharides of varying sizes[5]. Similar to the true chitinases, chitinase-like proteins also contain a typical Glyco_18 domain, but they do not possess enzymatic activity doe to the substitution of glutamic acid at the end of the DxxDxDxE conserved motif with either leucine, isoleucine or tryptophan (Figure 1A)[6,7]. In total, six Glyco_18 domain-containing proteins have been found in human, including AMCase, chitotriosidase, oviductin, stabilin-1-interacting chitinase-like protein (SI-CLP), chitinase-3-like protein 1 (YKL-40) and chitinase-3-like protein 2 (YKL-39)[7].

Even though mammalian chitinase-like proteins do not hydrolyze chitin, they can bind chitin due to their lectin properties as summarized in the Table 1. The lectin properties of chitinase-like proteins are important for their interaction with specific carbohydrate polymer components of extracellular matrix (ECM) or cell surface glycoproteins[7,8]. For example, YKL-40 induces the interaction of αvβ3 integrin and syndecan-1 on human microvascular endothelial cells (HMVECs) through its heparin binding activity, which results in enhanced tube formation in vitro and increased angiogenesis in vivo[9]. SI-CLP demonstrates the strongest binding affinity to N-acetylglucosamine tetramer $(GlcNAc)_4$, which is a component of chitin[10]. Moreover, SI-CLP protein purified from E. coli bind with lipopolysaccharides (LPS) and neutralizes the toxic effect of endotoxin[11]. Human YKL-39 protein purified from Pichia pastoris yeast demonstrates the strongest interaction with $(GlcNAc)_5$ and $(GlcNAc)_6$ via hydrogen bonds and hydrophobic interactions[12]. YM1 specifically binds saccharides with

a free amino group, such as glucosamine, galactosamine or glucosamine polymers, but fails to bind chitin fragments[4].

A
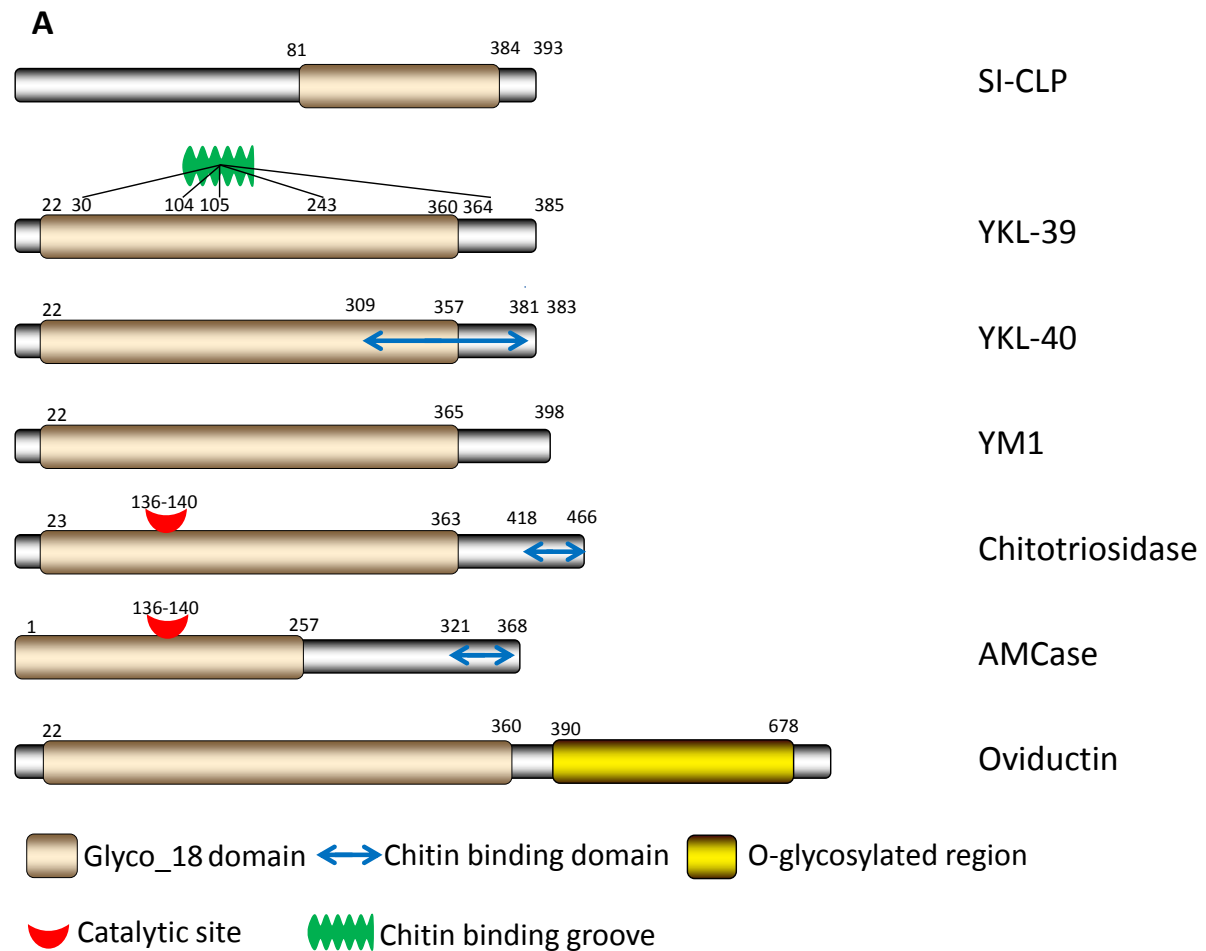
B

```
      FDGIDIDWEYP            Glyco_18 prototype catalytic domain
1-186-FDGFVVEVMNQ-393        SI-CLP
1-131-FDGLDVSWIYP-385        YKL-39
1-131-FDGLDLAWLYP-383        YKL-40
1-131-FDGLNLDWQYP-398        YM-1
1-131-FDGLDLDWEYP-466        Chitotriosidase
1-131-FDGLDFDWEYP-368        AMCase
1-132-FDGLDLFFLYP-678        Oviductin
```

Figure 1. Structure of mammalian chitinases and chitinase-like proteins. Domain organization of mammalian Glyco_18 domain-containing proteins (Kzhyshkowska, J. et al., 2016), Copyright Portland Press Limited[7].

Table 1. Lectin properties of chitinase-like proteins

Chitinase-like protein	Source of the protein	Carbohydrate binding	Functions mediated by interaction with carbohydrates	Reference
YKL-40	Bovine nasal cartilage and chondrocytes	Collagen type I	Facilitates type I collagen fibril formation	(Bigg et al.,2006)[13]
	Human YKL-40 transfected CHO cells	Chitooligosaccharides, $(GlcNac)_5$ and $(GlcNac)_4$	Involved in defense against chitin-containing organisms	(Fusetti et al., 2003)[8]
	Human peripheral blood monocyte-derived macrophages	Chitin	Interfere with hyphal growth of fungi	(Renkema et al., 1998)[14]
	Nodular smooth muscle cell	Heparin	Enhancing ECM-cell interaction	(Shackelton et al., 1995)[15]
YKL-39	Pichia pastoris yeast cells	Chitooligosaccharides, $(GlcNac)_5$ and $(GlcNac)_6$	unknown	(Rank et al., 2015; Schimpl et al., 2012)[12,16]
SI-CLP	E. coli	Galactosamine, Glucosamine, ribose, $(GlcNac)_4$, mannose, Ghitooligosacharide	LPS sensing	(Meng et al., 2010)[10]
YM1	Mouse peritoneal exudate fluid	Galactosamine, Glucosamine polymers and heparin	Preventing inflammation via competing for binding sites on local ECM occupied by infiltrating leukocytes	(Chang et al., 2001)[4]

1.1.2 Identification and cell specific expression of chitinase-like proteins

In mammals, chitinase-like proteins are expressed in various cell types, and elevated expression of chitinase-like proteins is associated with several pathological processes (Table 2). YKL-40, a secreted glycoprotein of 40 kDa molecular weight, was initially isolated from conditioned medium of cultured human chondrocytes using heparin-agarose affinity chromatography[17]. In vitro, the expression of YKL-40 in human monocyte-derived macrophages is elevated under IFN-γ stimulation[6]. YKL-40 expression in bronchial epithelium cells is increased under strong mechanical stress[18]. In serum and synovial fluid of rheumatoid arthritis patients, increased YKL-40 expression is due to its production by chondrocytes, macrophages and neutrophils[19,20]. Endogenous expression of YKL-40 in glioblastoma cell lines (MG-63 and U-87 MG) is vital for tumor proliferation, migration and angiogenesis[21,22].

Similarly to YKL-40, YKL-39 was also purified out of human articular cartilage chondrocytes using heparin-agarose affinity chromatography[23]. Expression of YKL-39 was found in human macrophages, chondrocytes and synoviocytes[23-25]. In comparison with normal chondrocytes, YKL-39 expression is up-regulated in osteoarthritic chondrocytes[25]. In human monocytes-derived macrophages expression of YKL-39 was significantly increased under stimulation with IL-4 and TGF-β[26].

YM1 gene is present in rodents, but absent in human[27]. YM1 protein was found in mouse macrophages, neutrophils and bone marrow derived mast cells[4,28-31]. In vitro, YM1 expression in macrophages was induced by IL-4 or IL-13 via STAT-6 dependent signaling pathway, and IFN-γ antagonized the stimulating effect of IL-4[29,32]. However, YM1 protein was also found in wound-healing macrophages where IL-4 was absent[31]. It was hypothesized that YM1 originates from neutrophils that were phagocytosed by macrophages during late stages of infection or inflammation[28].

SI-CLP, a stabilin-1 interacting chitinase-like protein, was identified as a ligand for the multifunctional receptor stabilin-1 using yeast two-hybrid screening[6]. Endogenous SI-CLP expression was found in various cell lines including those of monocytic, T-cell, B-cell and epithelial origin. Expression of SI-CLP is strongly up-regulated in primary human monocyte-derived macrophages stimulated by IL-4 and dexamethasone and suppressed by IFN-γ[6]. IL-12 slightly enhances the expression of SI-CLP gene in mouse bone marrow derived-macrophages, whereas IL-4 fails to increase SI-CLP expression[11].

Table 1. Expression profile of chitinase-like proteins

Chitinase-like protein	Cell type	Biological activity, mechanism	Associated disorder or pathological process	Reference
YKL-40	Human chondrocytes	Promotes chondrocyte proliferation	Rheumatoid arthritis and osteoarthritis	(Petersson et al., 2006)[19]
	Human bronchial epithelial cells	Induces airway hyper-responsiveness	Asthma	(Park et al., 2010)[33]
	Human colonic epithelial cells	Enhances the migration and proliferation of colonic epithelial cells	Neoplastic progression of the colon	(Chen et al., 2011)[34]
	Human peripheral blood monocyte-derived macrophages	Unknown	Inflammation	(Kzhyshkowska et al., 2006)[6]
	Human neutrophils	Suggested function in degradation of ECM	Rheumatoid arthritis	(Volck et al., 1998)[20]
	Human synovial cells	Not available	Rheumatoid arthritis	(Hakala et al., 1993)[17]
	Vascular smooth muscle cells (VSMC)	Promotes migration of vascular endothelial cell	Promotes tumor angiogenesis	(Malinda et al., 1999)[35]
	U-87 MG cells	Promotes proliferation and migration of tumor cells	Promotes tumor progression	(Ku et al., 2011)[21]
	MG-63 cells	Promotes angiogenesis	Promotes tumor progression	(Faibish et al., 2011)[22]
YKL-39	Human osteoarthritic chondrocytes	Unknown	Osteoarthritis	(Knorr et al., 2003)[24]
	Human monocyte-derived macrophages	Unknown	Unknown	(Kzhyshkowska et al., 2008)[26]
SI-CLP	Cell lines: Raji, MonoMac-6, THP-1, U937, Jurkat, A549, HEK293	Unknown	Unknown	(Kzhyshkowska et al., 2006)[6]
	Human monocyte-derived macrophages	Unknown	Unknown	(Kzhyshkowska et al., 2006)[6]
	Peripheral blood mononuclear cells derived from rheumatoid arthritis patients	Aggregates inflammation	Rheumatoid arthritis	(Xiao et al., 2014)[11]
YM1	Mouse macrophages	Biomarker of alternatively activation macrophages	Infection and allergic peritonitis	(Welch et al., 2012)[36]
	Mouse neutrophils	Suggested function in the digestion of glycosaminoglycans	Mouse chronic granulomatous disease	(Harbord et al., 2002)[28]
	Mouse bone marrow-derived mast cells	Unknown	Unknown	(Lee et al., 2005)[30]

1.2 Biological activities of chitinase-like proteins

1.2.1 Cytokine-like activity

Chitinase-like proteins exert direct or indirect chemotactic activity towards various cells as summarized in the Table 3. For the first time the chemotactic activity of chitinase-like proteins was demonstrated for murine YM1 protein (originally named ECF-L) that induced the recruitment of eosinophils, T lymphocytes and bone marrow cells[37]. The chemotactic activity of YM1 protein was concentration dependent and was abrogated by a specific anti-YM1 antibody[37]. The presence of a CXC motif on the N-terminus of the YM1 protein was suggested to mediate its chemotaxic activity.

Table 2. Chemotactic activity of chitinase-like proteins

Chitinase-like protein	Chemotaxis for cell types	Concentration	In vitro model	Mechanism	Reference
YM1	Eosinophils, T lymphocytes, bone marrow cells	1×10^{-8} M	Microchemotaxis Transwell (3 μm for eosinophils and bone marrow cells, 8 μm for T lymphocytes)	CXC motif in N-terminus	(Owhashi et al., 2000)[37]
YKL-40	VSMC	1 ng/ml	Microchemotaxis Transwell with polycarbonate membrane of 12 μm pore size	Binding with integrin on the VSMC	(Nishikawa and Millis, 2003)[38]
YKL-40	THP-1	80 ng/ml	Transwell with 8 μm pore size membrane pre-coated with fibronectin	YKL-40 induced IL-8 and MCP-1 secretion in SW480 cells	(Kawada et al., 2012)[39]
YKL-40	Bronchial smooth muscle cells	100 ng/ml	Chemicon Transwell with 8 μm pore size polycarbonate membrane	YKL-40 stimulated IL-8 secretion in BEAS-2B and HBECs	(Tang et al., 2013)[40]

Unlike ECF-L, YKL-40 does not contain typical CXC or CC sequences on its N-terminus[37]. The chemotactic activity of YKL-40 can be direct and indirect. Purified YKL-40 protein used at the concentration 80 ng/ml directly induces chemotaxis of human monocyte-like THP-1 cells[39]. Indirect effect was shown for YKL-40-transfected SW480 cells (human colon carcinoma cell line) that secreted elevated levels of IL-8 and MCP-1, that in turn exerted a chemotactic effect on THP-1 cells[39]. Similarly, bronchial epithelial cells stimulated with YKL-40 secreted elevated levels of IL-8 that mediated enhanced chemotaxis of human

bronchial smooth muscle cells[40]. Moreover, the adhesion and migration of VSMC was enhanced under stimulation of YKL-40[38].

1.2.2   Growth factor-like activity

Growth factors are secreted mediators that induce cellular growth and proliferation through their binding to specific growth factor receptors on the cell surface. Growth factors can activate ERK1/2-MAPK and AKT signaling pathways that participate in various cellular activities including cell survival, cell cycle progression and cell migration. Growth factor activities were also reported for the chitinase-like proteins. Purified YKL-40 protein directly promotes the proliferation of HEK-293 and U-373 MG cells via the activation of the ERK1/2-MAPK signaling pathway[41]. However, the effect of YKL-40 on the stimulation of proliferation was not limited to the tumor cells. YKL-40-stimulated proliferation was demonstrated for human synovial cells and skin fibroblasts, and was mediated by the direct activation of ERK1/2-MAPK and AKT signaling pathways[42]. YKL-40 can also promote cell proliferation indirectly. For instance, YKL-40 increases the secretion of IL-8 in human bronchial epithelial cells via the activation of the MAPK pathway, and IL-8 induces the proliferation of human bronchial smooth muscle cells[43]. In addition, purified YKL-39 protein can also activate the ERK1/2-MAPK signaling pathway in HEK-293 and U-373 MG cells, but it leads to the inhibition of proliferation of HEK-293 and U-373 MG cells[41]. The stimulation with YKL-40 and YKL-39 results in opposite effect in the proliferation of HEK-293 and U-373 MG cells, however the mechanism of such opposite effects remains to be unknown. SI-CLP protein was reported to activate the ERK signaling pathway in PMA treated THP-1 cells, but it was unknown whether the activation of ERK signaling pathway affects cell proliferation[11].

1.3   Role of chitinase-like proteins in tumor progression

Among all chitinases and chitinase-like proteins, the function of YKL-40 in cancer progression is the best investigated. Increased expression of YKL-40 was found in the circulation of various solid tumors including glioblastoma, esophageal squamous cell carcinoma, breast, bladder, colon, head and neck, liver, lung, pancreas, prostate, stomach and endometrial cancers, and high YKL-40 levels in the serum of tumor patients are positively associated with a poor outcome or short disease-free survival[39,44-54]. As illustrated by Figure 2, YKL-40 participates in the tumor progression by affecting the tumor initiation, tumor growth and metastasis[22,55]. Preliminary data produced in our laboratory suggested that SI-CLP can

have an inhibitory effect on the tumor growth of TS/A breast adenocarcinoma in a mouse model (Nan Wang, PhD thesis 2014), however the mechanism of SI-CLP suppression of tumor growth remains to be identified. The role of YKL-39 in tumour progression also remains to be invesigated.
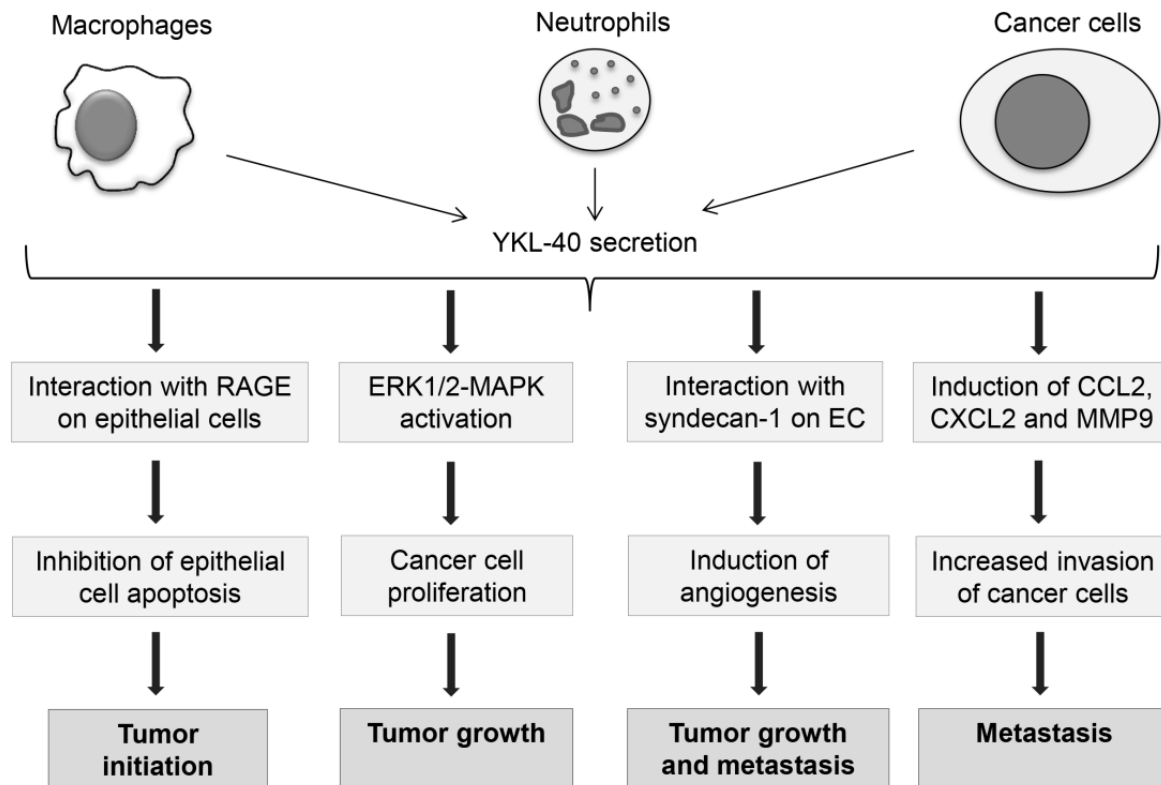
Figure 2. YKL-40 supports tumor progression. YKL-40 involves tumor progression via affecting tumor initiation, tumor growth, tumor angiogenesis and metastasis (Kzhyshkowska, J. et al., 2016), Copyright Portland Press Limited[7].

1.3.1 Effects of chitinase-like proteins on the survival of tumor cells

Endogenous YKL-40 was shown to support the survival of tumor cells[21,39]. The colony forming ability of U-87 MG (human primary glioblastoma cell line) was shown to be suppressed when YKL-40 gene expression was silenced, while the colony forming ability of U-373 MG cells (human primary glioblastoma cell line) was increased when YKL-40 was over-expressed in vitro[21]. YKL-40 protein exerts an anti-apoptotic effect in U-87 MG cells through activating the AKT signaling pathway[55]. In addition, YKL-40 is also able to attenuate ionizing irradiation induced tumor death through enhancing angiogenesis and proliferation of tumor cells[56]. YKL-40 antagonizes S100A9-regulated apoptosis through competitive binding with RAGE on mouse intestinal epithelial cells[57]. Overall, YKL-40 enhances the survival of tumor cells by promoting proliferation and inhibiting apoptosis of tumor cells (Figure 2).

1.3.2   Effects of chitinase-like proteins on tumor angiogenesis

Besides direct proliferation of tumor cells, neovascularization is vital for tumor growth. The positive correlation between YKL-40 expression and blood vessel density was found in the abundantly vascularized tumors such as human breast cancer and glioblastoma by immunohistochemical analysis[9,56]. Recombinant YKL-40 protein was shown to increase the migration and tube formation of HMVECs in vitro[9,39]. By comparison to empty vector transfected MDA-MB-231 and HCT-116 cells, the conditioned medium of YKL-40 transfected MDA-MB-231 and HCT-116 cells increased the migration and tube formation of HMVECs[9]. U-87 MG cells expressing endogenous YKL-40 protein enhance the tube formation of HMVECs through increasing VEGF production[55], while tumor angiogenesis is suppressed when the YKL-40 gene in U-87 MG cells was silenced in vivo[9]. Transient suppression of VEGF protein in U-87 MG cells significantly enhanced YKL-40 expression, which promoted tumor angiogenesis and was associated with poor prognosis in glioblastoma[55,58]. However, pro-angiogenic effects of YKL-40 on HMVECs are not affected by VEGF since anti-VEGF neutralizing antibody failed to abrogate enhanced tube formation and migration of HMVECs induced by YKL-40[9]. The effects of SI-CLP and YKL-39 on tumor angiogenesis was not analyzed up to date.

1.3.3   Effects of chitinase-like proteins on tumor metastasis

Evidence accumulate that YKL-40 can support metastatic process. Elevated serum YKL-40 levels were found to positively correlate with tumor metastasis in breast cancer and glioblastoma[44,45,59]. The adhesion ability of U-87 MG cells to ECM substrates is suppressed after the YKL-40 gene in U-87 MG cells is silenced[21]. Knockdown of YKL-40 gene leads to decreased invasion and MMP-2 expression in U-87 MG cells[21], which are important for glioblastoma metastasis[60]. On another side, the adhesion and invasion ability of tumor cells is enhanced when YKL-40 gene in U-373 MG cells is overexpressed[21]. The ability of YKL-40 to promote tumor metastasis was also demonstrated in melanoma animal models with lung metastasis. Increased lung metastasis was observed in YKL-40 transgenic mice injected by B16 cells from tail-vein, and pulmonary metastasis was decreased in YKL-40 ko mice[61,62]. In mammary tumor-bearing mice, increased YKL-40 expression in the metastasized lung induces the secretion of CCL2, CXCL2 and MMP9 by alveolar macrophages and lung interstitial macrophages[63], and CCL2 recruited macrophages to the tumor microenvironment facilitating tumor metastasis into lungs[64].

1.4 Macrophages

1.4.1 Overview

Macrophages are differentiated phagocytic cells of the mononuclear phagocyte system[65]. Macrophages are widely distributed in various organs and tissues, including the bone, central nervous system, gastrointestinal tract, liver, lymphoid organs, lungs, serous cavities, synovium and skin, and are key innate immune cells that control tissue homeostasis and inflammation[66]. Macrophages are regulate multiple physiological and pathological processes due to their ability to secrete various cytokines and chemokines, phagocytose pathogens and cellular debris, and activate non-specific and specific immunity[67]. Monocytes in peripheral blood circulation enter extra vascular tissues under specific signals, and differentiate into specific tissue macrophages to maintain tissue homeostasis (Table 4).

Table 3. Terminology of tissue macrophages

Tissue	Name of macrophages
Bone	Osteoclasts
Central nervous system	Microglia
Connective tissue	Histiocytes
Chorion villi of the placenta	Hofbauer cells
Kidney	Mesangial cells
Liver	Kupffer cells
Lung	Alveolar macrophages
Peritoneal cavity	Peritoneal macrophages
Skin and mucosa	Langerhans cells
Spleen	White-pulp macrophages, red-pulp macrophages, marginal-zone macrophages
Tumor	Tumor-associated macrophages

1.4.2 Selected biological activities of macrophages

1.4.2.1 Endocytosis and phagocytosis

Endocytosis is one of the key biological processes applied by macrophages to acquire nutrients from the extracellular microenvironment and initiate non-specific innate immunity. Macrophages utilize different internalsation pathways depending on their targets, including clathrin-mediated endocytosis, caveolae-mediated endocytosis, macropinocytosis and phagocytosis. Engulfed vacuoles are directed to early endosomes, late endosomes and lysosomes for digestion. Macrophages are characterized by pronounced phagocytosis of apoptotic cells and cellular debris[68], foreign microorganisms (bacteria, viruses, fungi and protozoa) and soluble antigens[69]. The process of phagocytosis includes several stages including sensing of pathogens, formation of phagosomes and intracellular digestion of pathogens. Pathogens are recognized via interacting with multiple surface receptors of macrophages, such as Fc receptors, complement receptors (CR1, CR3 and CR4), mannose receptors (CD205 and CD206) and scavenger receptors (CD36, MARCO and stabilin-1). Macrophages extend pseudopodia to capture and ingest pathogens followed by receptor-mediated internalization and reorganization of the actin based cytoskeleton[69,70]. Ingested pathogens fuse with lysosomes to form macrophage phagosomes, where pathogens are degraded by multiple hydrolytic enzymes. Digested pathogens can be expelled to extracellular space or presented in the form of foreign peptides to immune cells to initiate adaptive immunity.

Recently, endocytic function of TAM was demonstrated to regulate tumor growth in a mouse model of TS/A breast adenocarcinoma where tumor growth was impaired in stabilin-1 knockout mice[68]. The tumor supportive role of multifunctional scavenging receptor stabilin-1 was linked to the efficient endocytosis of the soluble component of extracellular matrix SPARC, that was shown to have an inhibitory effect of progression of breast cancer, while impaired SPARC clearance by stabilin-1 ko TAM correlated with the decrease of the tumor growth[68].

1.4.2.2 Secretion

Macrophages participate in a broad range of physiological and pathological processes via secreting multiple substances, including immunity-associated cytokines, chemotaxis associated chemokines and cytokine inhibitors, complement components, coagulation factors and extracellular matrix components, enzymes, reactive oxygen and Glyco_18 domain

containing proteins[71]. Functionally, the cytokines secreted by macrophages could be divided into three groups: (a) cytokines that promote inflammatory response, e.g., IL-1β, TNF-α, IL-8, IL-12; (b) cytokines that suppress inflammation response, e.g., IL-10, TGF-β; (c) cytokines that regulate cell activation of natural killer and T cells, e.g., IL-1ra, IL-12, IL-18. Chitinase-like proteins secreted by activated macrophages, including SI-CLP, YKL-39, YKL-40, YM1 and chitotriosidase, play an important role in innate immunity, tumor progression and chronic inflammation[6,26,72]. Interestingly, transport of SI-CLP in the secretory pathway in alternatively activated macrophage is mediated by stabilin-1, frequently expressed on TAM in different types of tumors[6,73].

1.4.2.3 Antigen presentation and T cell activation

Macrophages along with B cells and dendritic cells belong to professional antigen-presenting cells which present antigens in the context of MHC class I and MHC class II molecules. Endogenous antigens are presented by macrophages in the context of MHC class I molecules, which are specifically targeted by CD8+ cytotoxic T cells. Extracellular antigens are internalized and re-presented by macrophages in association with MHC II molecule, which along with co-stimulatory signals activate immature CD4+ T cells or B cells[74].

1.4.3 Macrophage activation

Macrophages are activated by a range of signals including various cytokines, immune complexes, glucocorticoids, LPS and interferon in the microenvironment. The activation states of macrophages are determined by intracellular signaling cascades, transcription factors, cytokines, chemokines, scavenger receptors and metabolic pathways (Figure 3). IFN-γ and IL-4 induce clear-cut antagonistic effects on macrophage polarization, which are designated as type I and type II activation respectively[75]. Mouse macrophages activated by IL-4 are characterized by increased expression of STAT6, Arg1 and chemokines such as CCL17, CCL22 and CCL24, while human macrophages stimulated by IL-4 are characterized by increased expression of IRF4, SOCS1, GATA3 and chemokines CCL4, CCL13, CCL17 and CCL18[75]. Specific membrane receptors (CD206 and stabilin-1) were found in IL-4 activated human macrophages, which are widely found in Th2 responses, type II inflammation and allergy reactions[76]. IFN-γ or LPS induces the up-regulation of transcription factors STAT1 and NF-κB mediating the production of iNOS and the secretion of pro-inflammatory cytokines (TNF-α, IL-1β and IL-6)[77]. Macrophages under stimulation of LPS or IFN-γ are characterized by reduced phagocytic activity, enhanced Type I inflammatory response and

enhanced killing of intracellular pathogens[78]. Macrophages differentiated from mouse bone marrow precursors or human peripheral blood monocytes using CSF-1 or GM-CSF are widely used in vitro. Macrophages are innate immune cells with extreme phenotypic plasticity and can be polarized and re-polarized by multiple factors[79,80]. Recently, it has been found that each stimuli potentially induces a unique transcriptional program in macrophages which may reveal a certain degree of similarity with M1 (IFN-γ) and M2 (IL-4) macrophages[81].
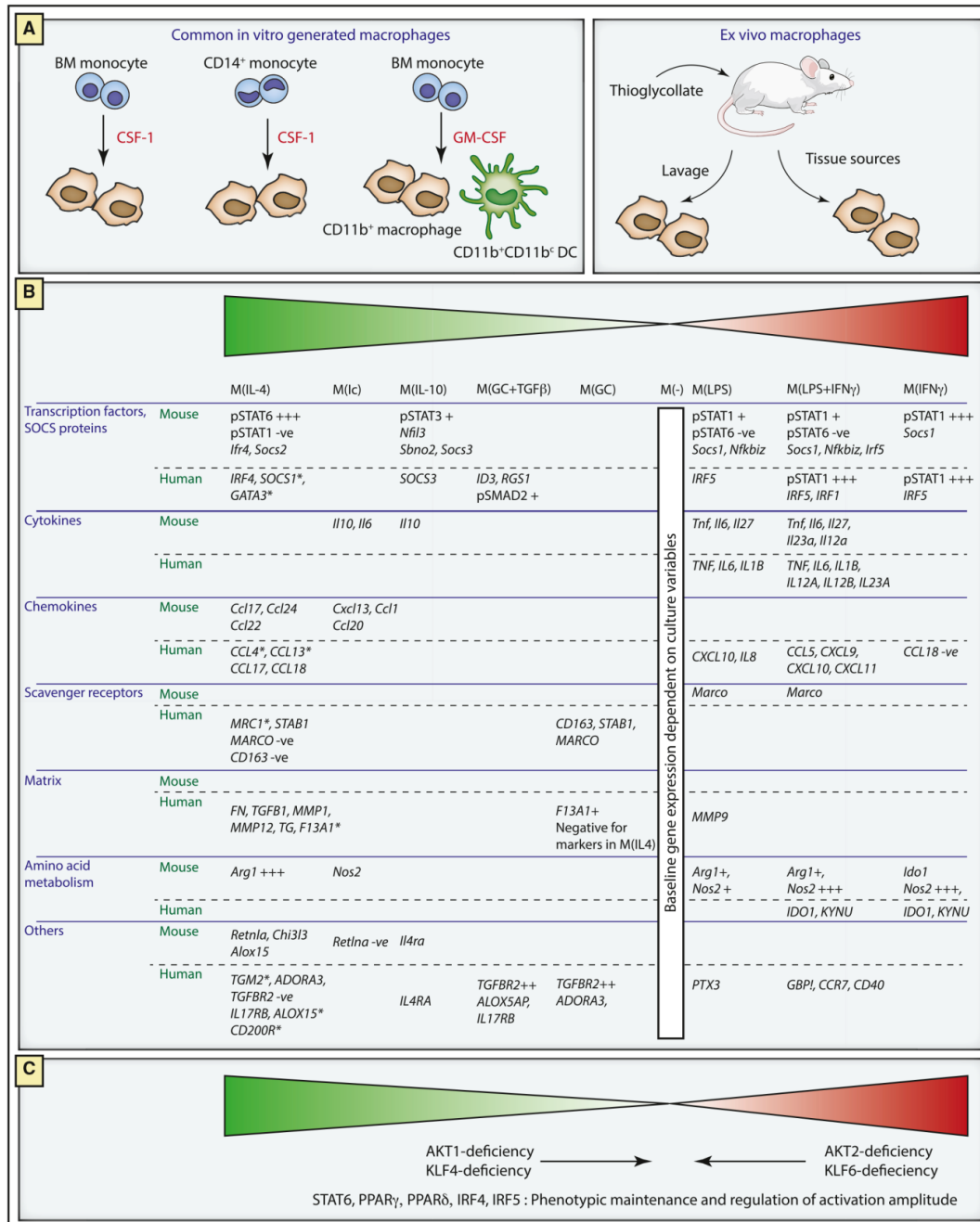
Figure 3. Macrophage activation under different stimulations. (A) Widely used macrophage preparations in vitro and ex vivo. (B) The status of macrophage activation were indicated by transcription factors, cytokines, chemokines, scavenger receptors, matrix, amino acid metabolism and so on. (C) Genetics was used to aid in macrophage-activation studies. (Murray, P. J. et al., 2014), Copyright Elsevier[75].

1.4.4   Role of tumor-associated macrophages in tumor progression.

Most of solid tumor tissues are highly infiltrated by macrophages, and the amounts of tumor-associated macrophages (TAM) are positively associated with poor prognosis in most of published research[82]. TAM participate in all stages of tumor progression from tumor initiation to remote metastasis (Figure 4).
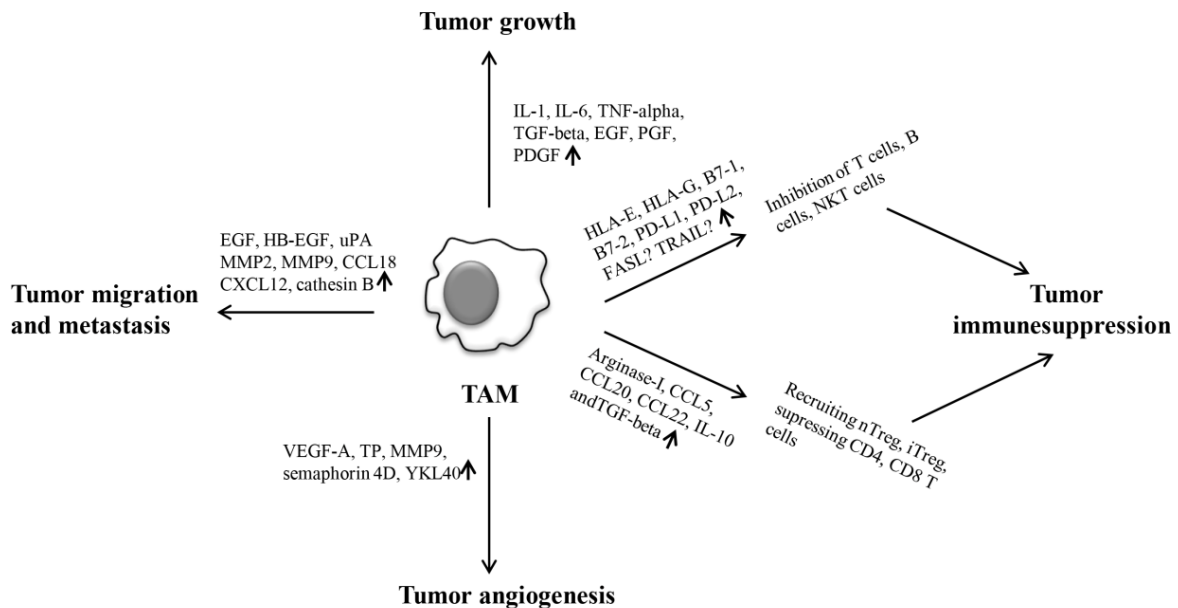
Figure 4. The role of TAM in tumor progression. Major effects of TAM on tumor progression include: tumor growth, tumor migration and metastasis, tumor angiogenesis and tumor immune suppression. TAM expresses an array of cytokines, chemokines, enzymes and cell surface receptors to affect tumor progression.

1.4.4.1   TAM and angiogenesis

Extensive studies in mouse model of breast demonstrated that TAM are crucial cells for the angiogenic switch required for efficient primary tumor growth[83,84]. Macrophages are recruited into tumor tissue by chemokines such as CSF-1, MCP-1 and SDF-1[85]. CSF-1 ko mice are characterized by reduced macrophage infiltration in tumor tissue, which was associated with attenuated angiogenesis and tumor growth[83]. Recruited macrophages increase the secretion of VEGF-A, thymidine phosphorylase, Semaphorin-4D, MMPs and YKL-40 to promote angiogenesis[86]. In human lung cancer, YKL-40 mRNA was detected in TAM of the peritumoral stroma[87]. The positive correlation between TAM density and tumor vessel abundance was demonstrated by the extensive analysis of animal study and clinical material[88-93]. VEGF-A is the most common cytokine secreted by TAM to promote tumor angiogenesis, and hypoxia-inducible factors are the most important regulators of VEGF-A production in

TAM[86]. However, targeting of -VEGF-A was not always successful in suppressing neovascularization, which can be partially explained by compensatory up-regulation of YKL-40[58]. The application of anti-VEGF and anti-YKL-40 blocking antibodies was demonstrated to be more efficient in restricting growth of glioblastoma in the animal model and in reducing neo-angiogenesis in tumor tissue in comparison with single anti-VEGF or anti-YKL-40 therapy[55]. Thymidine phosphorylases are abundantly found in many human solid tumor tissues, and its expression is positively associated with tumor angiogenesis and metastasis[94]. Thymidine phosphorylases derived from human monocyte cells (U937 and THP-1) enhance the migration of human umbilical vein endothelial cells in vitro and tumor angiogenesis in vivo through the intracellular metabolism of thymidine and subsequent extracellular release of 2-deoxyribose[95]. In Semaphorin-4D ko mice, tumor growth and metastasis were impaired, accompanied by reduced tumor neo-angiogenesis[96]. MMP9 produced by TAM can enhance neovascularization in vivo via cleaving VEGF-A from its ECM-bound form[97]. Targeting MMP9 expressing macrophages is effective in impairing cervical carcinogenesis through inducing the apoptosis of neoplastic epithelial and endothelial cell[98].

1.4.4.2 TAM and tumor growth

The supporting role of TAM in tumor growth was demonstrated in number of animal models. For example, the reduction of TAM in an animal tumor model bases on the subcutaneous injection of human A673 rhabdomyosarcoma demonstrates inhibition of tumor growth and progression[99]. Depleting TAM by injecting the bacterial pathogen inducing specific apoptosis of TAM suppressed tumor growth in animal breast cancer model [100]. The infiltration of monocytes into the tumor microenvironment is mediated by CCL2 and CCL5, and targeting of CCL2 by siRNA or application of CCR5 antagonist was efficient in the inhibiting of tumor growth due to the reduction of the amount of TAM[101,102]. The tumor promoting effect of TAM is related to the increased secretion of soluble mediators, e.g., IL-1, IL-6, TNF-α, TGF-β, EGF (epidermal growth factor), FGF (fibroblast growth factor) and PDGF (platelet-derived growth factor)[97]. Tumor cells express abundant receptors for growth factors and cytokines, including EGFR, FGFR and PDGFR, and that respond to TAM-mediators by enhanced proliferation. In vitro, IL-1β released by macrophages induces the proliferation of colon cancer cells through the activation of Wnt signaling[103]. IL-6 can induce the proliferation of glioma stem cells via STAT3 activation, and silencing IL-6 receptor in glioma stem cells with shRNA increases the apoptosis of glioblastoma stem cells leading to the suppression of glioblastoma growth[104]. High IL-6 serum levels in human ductal breast

carcinoma predict poor prognosis, and the application of anti-IL-6 monoclonal antibody inhibits the mammosphere formation of primary human breast cancer tissue and MCF7 tumor cells in Notch-3 dependent mechanism[105]. TNF-α released by TAM binds with TNFR1 and TNFR2 expressed by tumor cells, which improves the survival of tumor cells via elevating the expression of anti-apoptotic molecules[106].

1.4.4.3 TAM and tumor metastasis

Tumor metastasis was shown to be significantly impaired when TAM in the tumor microenvironment were depleted or reduced[99,101]. Intra-vital and multi-photon imaging clearly demonstrated the coordination of TAM and tumor cells in case of inducing metastasis through the formation of a EGF/CSF-1 paracrine signaling loop[107,108]. Inhibition of EGF or CSF-1 in mammary tumor bearing mice reduces the amount of metastatic tumor cells[109]. TAM modulate the extracellular matrix to promote the migration and metastasis of tumor cells through increasing the production of MMPs, uPA, Cathepsin B and other factors[110]. MMP2 and MMP9 are the most common proteases secreted by TAM, and the role of MMPs in promoting tumor metastasis has been widely revealed[111]. Tumor invasion and metastasis was inhibited when Cathepsin B from TAM was depleted in an autonomous breast tumor model[112]. Moreover, TAM can enhance tumor metastasis via other soluble cytokines or miRNA[113-116]. CCL18 released by TAM enhances the metastasis of breast cancer by interacting with its receptor expressed on breast cancer cells, and blocking the specific receptor of CCL18 reverses the pro-metastasis effect of CCL18[114]. CXCL12 was secreted by TAM in a breast tumor model, and the binding of CXCL12 with CXCR7 enhanced the migration of tumor cells through up-regulation of vascular cell adhesion molecule 1 and MMPs[115]. Heparin binding EGF-like growth factor and Oncostatin M derived from TAM enhance the migration of tumor cells, and high heparin binding EGF-like growth factor levels in breast carcinoma patients positively correlate with TAM infiltration and tumor metastasis[116].

1.4.4.4 TAM and immune suppression

TAM express various effector factors to suppress anti-tumor immune responses in the tumor microenvironment (Figure 5). The interaction between TAM and other immune cells is pivotal for tumor progression. TAM induce apoptosis of cytotoxic T cells by up-regulating the expression of FASL[117]. Some tumor cells up-regulate HLA molecules, e.g., HLA-C, HLA-G and HLA-E to inhibit the activity of NK cells and some subsets of activated T cells[84]. HLA negative tumor cells can induce the expression of HLA molecules on TAM, which inhibit the

migration of NK cells to the lymph nodes via HLA-E-CD94 binding[118]. HLA-G expressed by TAM can interact with ILT2, the co-stimulatory receptor of T cells, to suppress the function of T cells[84]. PD-1 expression on T cells, NKT cells and B cells is a safety mechanism to down-regulate exaggerated immune reactions[119]. However, TAM strategically suppress the function of activated T cells, NKT cells and B cells in the tumor microenvironment by elevating PD-L1 and PD-L2 production[120]. Increased expression of arginase-I is a typical property of alternatively activated macrophages, and TAM impair T cell function by decreasing the expression of the CD3 ζ-chain[121]. IL-10 and TGF-β secreted by TAM enhance the regulatory functions of CD4+ T cells by up-regulating FoxP3 expression, known as Treg cells[122]. TAM recruit natural regulatory T cells by increasing the secretion of CCL5, CCL20 and CCL22, which inhibit the non-specific and specific tumor killing function of NKT and T cells[84].
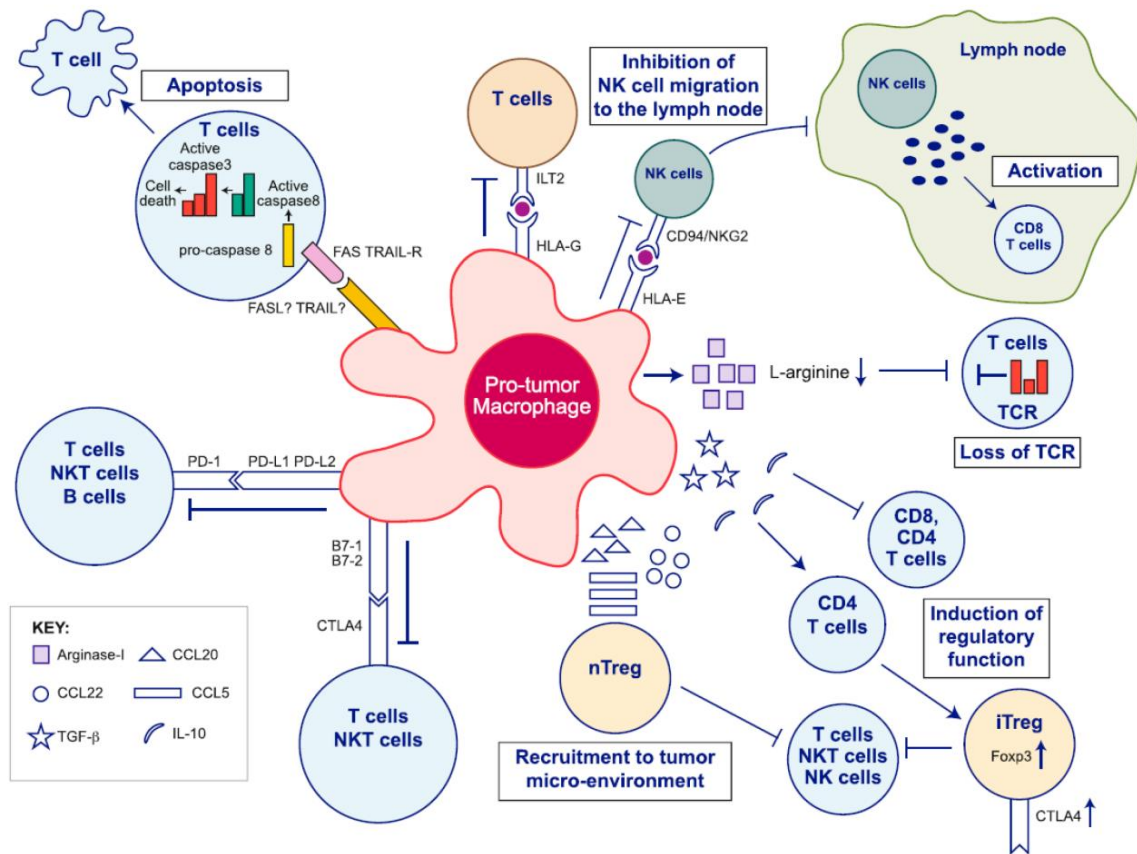
Figure 5. TAM regulate anti-tumor immune responses. TAM express various effector molecules, including cytokines, chemokines, enzymes and cells surface receptors to suppress the anti-tumor immune responses mediate by innate and adaptive immune cells (Noy, R. and Pollard, J.W. 2014), Copyright Elsevier[84].

1.4.5 Immunotherapy of targeting tumor-associated macrophages

Depleting TAM and interfering TAM derived pro-tumor cytokines are the most investigated strategies for targeting TAM. It is known that the recruitment of monocytes from the blood vessels to tumor tissue strongly depends on cytokine signals such as CCL2, CCL3, CCL4, CCL7, CCL8 and MIF[97]. Blocking CCL2-CCR2 interaction is efficient in reducing the infiltration of monocytes which suppressed tumor metastasis[64]. Even though majority of publications demonstrated that high TAM density predicts a poor prognosis for cancer patients, evidence accumulate that TAM density can also correlate with a good prognosis[97]. For example, the amount of CD68+ macrophages in the gaps of tumor ductal structures in human breast cancer was negatively associated with lymph node metastasis[123]. Roles of TAM in tumor progression are versatile, and in human tumor tissue TAM are represented by heterogeneous subpopulations; suggesting that, targeting tumor-supportive TAM subpopulations or their secreted factors as a promising therapeutic approach. Qian and Pollard proposed six phenotypes of TAM in mouse and human tumor tissue based on their function, including activated macrophages (IL-12$^+$, MHC II^{hi}, iNOS$^+$, TNF-α^+, CD80/86$^+$), immunosuppressive macrophages (Arginase$^+$, MARCO$^+$, IL-10$^+$, CCL22$^+$), angiogenic macrophages (VEGFR1$^+$, VEGF$^+$, CXCR4$^+$, Tie2$^+$), metastasis-associated macrophages (VEGFR1$^+$, CCR2$^+$, CXCR4$^-$, Tie2$^-$), invasive macrophage (Wnt signaling, CTS B&S$^+$, EGF$^+$) and perivascular macrophages[110]. It was anticipated that reprogramming pro-tumor macrophages to anti-tumor macrophages can improve the anti-tumor response. However, such reprogramming in vivo is complicated due to the plasticity of the macrophage phenotype. An alternative approach is to silence the function of pro-tumor TAM specifically in the tumor microenvironment.

Another approach for targeting TAM is the neutralization of the tumor-promoting soluble factors produced by TAM. TAM produce various cytokines to exert pro-tumor function, and blocking of these cytokines was found to be a promising strategy in some tumor models[93,96]. Tumor cell derived CSF-1 is important for monocyte chemotaxis, and TAM programmed by tumor cells facilitate their proliferation by secreting EGF[109]. Interrupting the CSF-1-EGF positive cycle has proved to be effective in inhibiting tumor growth and metastasis[124]. Targeting of CSF-1/CSF-1R signaling pathway was demonstrated to delay tumor initiation and to attenuate tumor growth in various mouse tumor models[110,125]. Similarly, inhibiting EGF secretion from TAM reduces tumor metastasis in mammary tumor bearing mice[107].

In summary targeting of TAM by blocking of activity of TAM-released factors or depletion of TAM subpopulations is a very promising direction in anti-tumor therapy development. Chitinase-like proteins are known to be released by various subpopulations of macrophages, and our preliminary observations demonstrated that SI-CLP, in contrast to known activities of YKL-40, is able to suppress tumor growth in animal model for breast cancer (Nan Wang, PhD thesis 2014). However, the effect of SI-CLP on TAM and other components of tumor microenvironment remained to be investigated.

1.5 Aims and objectives of the thesis

The major aims of the thesis project were to identify the functional role and possible mechanism of SI-CLP in breast cancer development using mouse model for breast adenocarcinoma.

Specific objectives included:

1) To investigate the effect of SI-CLP on tumor growth of mouse model for breast adenocarcinoma;

2) To investigate the effect of SI-CLP on proliferation and migration of tumor cells in vitro;

3) To analyze the effect of SI-CLP on tumor angiogenesis in vivo;

4) To analyze the effect of purified SI-CLP on the migration of human monocytes and mouse bone marrow derived macrophages in vitro;

5) To investigate the effect of SI-CLP on recruitment and phenotype of TAM;

6) To investigate the effect of SI-CLP on recruitment of other immune cells in tumor microenvironment in vivo.

2 <u>Materials and Methods</u>

2.1 Chemicals, reagents and kits

2.1.1 Chemicals and reagents

Product	Company
0.22 μm filter	Carl Roth
3MM blotting papers	GE Healthcare
Acetic acid	Merck
Acetone	Sigma-Aldrich
Acrylamide / bis acrylamilde solution 30%	Bio-Rad
AEC+high sensitivity substrate chromogen	Dako
Agarose	Bioron
Amersham Hyperfilm ECL	GE Healthcare
Ammonium persulfate (APS)	Merck
Bovine serum albumin	Sigma-Aldrich
CD11b MicroBeads, human and mouse	Miltenyi Biotec
CD14 MicroBeads, human	Miltenyi Biotec
Cell strainer	Corning
Collagenase IV	Santa Cruz Biotechnology
Dako Pen	Dako
DAPI	Roche Diagnostics
DMEM medium + GlutaMAX	Thermo Fisher Scientific
DMSO	Sigma-Aldrich
DNA ladder	Thermo Fisher Scientific
DNA Loading Dye (6x)	Thermo Fisher Scientific
DNase	Thermo Fisher Scientific
dNTP	Thermo Fisher Scientific
DPBS (sterile 1x)	Thermo Fisher Scientific
EDTA (0.5 M)	Thermo Fisher Scientific
Ethanol	Merck
Faramount Mounting Medium, Aqueous	Dako
Fetal calf serum	Biochrom
Fluorescent Mounting Medium	Dako
Glycerol	Sigma-Aldrich
Isoflurane	CP Pharmaceuticals
Isopropanol	Merck
Laemmli sample buffer	Bio-Rad
LB broth with agar	Sigma-Aldrich
Macrophage-SFM medium	Thermo Fisher Scientific
Methanol	Merck
Mouse Genome 430 2.0 Array	Affymetrix

Nitrocellulose blotting membrane	GE Healthcare
Non-Fat Dry Milk	Bio-Rad
O.C.T compound	VWR
PageRuler Plus prestained Protein ladder	Thermo Fisher Scientific
Paraformaldehyde (PFA)	Sigma-Aldrich
Penicillin / Streptomycin	Biochrom
Percoll	Biochrom
Peroxidase-Blocking Solution	Dako
Ponceau S solution	Sigma-Aldrich
Protein G Sepharose 4 Fast Flow	GE healthcare
Recombinant human MCP-1 (CCL2)	Peprotech
Recombinant human SI-CLP protein	Cusabio
Recombinant murine MCP-1 (CCL2)	Peprotech
Recombinant murine M-CSF	Peprotech
Recombinant murine MIP-3β (CCL19)	Peprotech
Recombinant murine SI-CLP protein	Cusabio
Red blood cell lysis buffer	Sigma-Aldrich
Reduced serum medium+ GlutaMAX	Thermo Fisher Scientific
RPMI medium +GlutaMAX	Thermo Fisher Scientific
Saponin	VWR
Sodium azide	Sigma-Aldrich
Sodium dodecyl sulphate (SDS) 10%	Bio-Rad
TaqMan Probe	MWG Biotech
TEMED	Sigma-Aldrich
Tris/Glycine/SDS electrophoresis buffer (10x)	Bio-Rad
Triton X-100	Sigma-Aldrich
Trypan blue solution	Sigma-Aldrich
Trypsin-EDTA solution (sterile 1x)	Sigma-Aldrich
Tween 20	Biochrom
β-mercaptoethanol	Sigma-Aldrich

2.1.2   Kits

Product	Company
Click-iT EdU Alexa Fluor 488 Flow Cytometry Assay Kit	Thermo Fisher Scientific
E.Z.N.A Total RNA Kit I	Omega Biotech Corp
Pan T Cell Isolation Kit II, mouse	Miltenyi Biotec
RevertAid H Minus First Strand cDNA Synthesis Kit	Thermo Fisher Scientific
RNeasy Mini Kit	QIAGEN
SensiFAST Probe No-ROX Kit	Bioline
Streptavidin/Biotin Blocking Kit	Vector Laboratories

2.2 Equipment

Product	Company
Agarose electrophoresis unit	VWR
Balance	Kern
Blot chambers	VWR
Cell counter + Analyser System	OMNI Life Science
Cell culture hood	Thermo Fisher Scientific
Cell culture incubator	Heraeus instruments
Centrifuge 5804 R	Eppendorf
Centrifuge Universal 320	Hettich
Confocal laser scanning microscope SP8	Leica Microsystems
Cryostat microtome	Leica Biosystems
Digital caliper	Fixpoint
FACS Canto II	BD Biosciences
Freezer (-20°C)	Kirsch
Freezer (-80°C)	Sanyo
Fridge (4°C)	Liebherr
Ice machine AF100	Scotsman
Inverted microscope	Leica Microsystems
LightCycler 480 Instrument	Roche Diagnostics
MACS manual cell separator	Miltenyi Biotec
Magnetic stirrer MR3001	Heidolph
Micro Centrifuge	Carl Roth
Microwave oven	Sharp
Mini-vortex MS3 basic	IKA
Neubauer Chamber	Glaswarenfabrik Karl Hecht
Orbital shaker 7-0031	NeoLab Migge
PH meter 211	Sigma-Aldrich
Roller	Ortho Diagnostic Systems
Rotator	Neolab
SDS-PAGE power unit Power-Pac 200	Bio-Rad
SDS-PAGE unit	VWR
Spectrophotometer infinite M200	TECAN
Thermomixer comfort	Eppendorf
Universal turning device	VivaScience
Veterinary anesthesia evaporator	MIDMARK
Vortex Genie 2	Scientific Industries
Water bath VWB12	VWR
X-ray film processor CAWOMEN 2000 IR	CAWO Solutions

2.3 Buffers and solutions

2.3.1 Running buffer for agarose gel electrophoresis

1) 242 g Tris free base were dissolved in 750 ml ddH2O.

2) 57.1 ml acetic acid and 100 ml of EDTA solution (0.5M) were added to the solution and the volume was adjusted to 1 L with ddH2O.

3) 20 ml of the solution was dissolved in 980 ml of ddH2O to make 1x TAE buffer for agarose gel electrophoresis

2.3.2 Buffers and solutions for cell fixation, immunohistochemical and immunofluorescent staining.

2.3.2.1 Solution for cell fixation

1) 40 g of paraformaldehyde (PFA) was dissolved in 700 ml of PBS.

2) The pH was adjusted to 11.4 with 1 N NaOH.

3) The solution was stirred at room temperature for 1 h to dissolve PFA completely.

4) The pH was adjusted to 7.4 with HCl and the volume was adjusted to 1 L with PBS.

5) The solution was filtered, aliquoted and stored at -20°C.

2.3.2.2 Solution for cell permeabilization

1) 2.5 ml of Triton X-100 was mixed with 500 ml of PBS.

2) The solution was stirred by placing on top of a magnetic stirrer for 1 h.

3) The solution was stored at room temperature.

2.3.2.3 Blocking Solution

1) 1.5 g BSA powder was weighed and poured into a 50ml falcon tube.

2) 50 ml of PBS was added to dissolve BSA powder.

3) The falcon tube was placed on a Tube Roller Mixers at 15-20 rpm/min overnight.

4) The solution was stored at 4°C for no more than one month.

2.3.2.4 Solution for diluting antibody

Blocking solution prepared according to above protocol was diluted with PBS in a ratio of 1:3 to make solutions for diluting antibody.

2.3.2.5 Solution for washing

1) 10 ml of Tween-20 was added to 90 ml of PBS.

2) The PBS/Tween-20 solution was mixed by placing on top of a magnetic stirrer for 1 h.

3) 10 ml of the PBS/Tween-20 solution was mixed with 10 L of PBS to make washing solution.

2.3.3 Buffers for SDS-PAGE and Western Blot

2.3.3.1 10% APS

1 g ammonium persulfate was weighed and dissolved in 10 ml of ddH$_2$O, which was aliquoted and stored in -20°C.

2.3.3.2 Running buffer for SDS-PAGE

100 ml of 10x TGS was dissolved in 900 ml of ddH$_2$O.

2.3.3.3 Blotting buffer for SDS-PAGE

1) 100 ml of 10x TGS solution and 200 ml of methanol were added to 600 ml of ddH$_2$O.
2) The final volume was adjusted to 1 L with ddH$_2$O.

2.3.3.4 Loading buffer for SDS-PAGE

50 µl of β-mercaptoethanol was mixed with 950 µl of 2x Laemmli sample buffer.

2.3.3.5 Blocking solution for SDS-PAGE

1) 3 g of non-fat milk powder was dissolved in 20 ml of PBS.
2) The final volume was adjusted to 50 ml with PBS.

2.3.3.6 Antibody dilution solution for SDS-PAGE

1 g of non-fat milk powder was dissolved in 20 ml of PBS and the final volume was adjusted to 100 ml with PBS.

2.3.4 Buffer for flow cytometry analysis

2.3.4.1 FACS buffer

1) 10 ml of FCS was mixed with 1 L of PBS.
2) Sodium azide was added to the solution, and the final concentration of sodium azide was adjusted to 0.1%.

2.3.5 MACS buffer

1) 2.5 g of BSA powder and 2 ml of 0.5 M EDTA were dissolved in 500 ml of PBS.
2) The solution was mixed by shaking at room temperature for 3 h, and then it was filtered through the 0.22 µm filter.

2.3.6   Solution for cell cryopreservation

DMSO was dissolved in FCS at the ratio 1:10, which was then filtered through a 0.22 µm filter.

2.3.7   Buffer for RNA isolation

20 µl of β-mercaptoethanol was added to 1 ml of the TRK buffer to make lysis buffer for RNA isolation.

2.4   Animal techniques

2.4.1   Mice used in the study

Wild type BALB/c female mice at the age of 8-10 weeks were bought from Janvier Labs, and the mice were housed at least one week in animal core facility before performing injection. Stabilin-1 knockout (ko) in BALB/c female mice were generated by Dr. Kai Schledzewski (Department of Dermatology, Venerology and Allergy, Medical Faculty Mannheim, University of Heidelberg) and Prof. Bernd Arnold (German Cancer Research Center)[126]. 30 BALB/C stabilin-1 ko mice at the age of 8-12 weeks offered by Dr. Kai Schledzewski were used in the study. TS/A clones stably transfected with mChid1 (TS/A-SI-CLP) and TS/A clones stably transfected with empty vector (TS/A-EV) were generated in our lab by previous PhD student (Nan Wang, PhD thesis 2014). The ethic approval numbers of murine tumor model (TS/A tumor in stabilin-1 ko mice) are 35-9185.81/G-115/07 and 35-9185.81/G-208/10. The ethic approval number for isolating TAM from BALB/c mice injected by TS/A-EV and TS/A-SI-CLP cells is 35-9185.81/G-228/15.

2.4.2   Preparation of tumor cells

1)   Freshly thawed TS/A-EV and TS/A-SI-CLP cells were passaged 2-3 times to maintain them in the exponential growth phase before performing tumor injection.

2) 2×10^6 TS/A-EV and TS/A-SI-CLP cells were grown in RPMI complete medium supplemented with 400 µg/ml G418 until the cell confluence in T75 flasks reached 80-90%.

3)   Tumor cells were harvested according to the standard protocol for adherent cells, and 3×10^6 cells were plated into a new T175 flask.

4)   The expression of SI-CLP protein in TS/A-EV and TS/A-SI-CLP cells was determined by performing immunofluorescent staining and Western Blot at the same time.

5) The medium was changed one day before performing *in vivo* injection.

6) On the day of harvesting cells for tumor injection the cell confluence was 70-90%.

7) The cells were washed once with PBS (without Ca^{2+}, Mg^{2+}).

8) 3 ml of 1x Trypsin/EDTA solution was added to the T175 flask and incubated at 37°C for 2 min to detach the cells.

9) 10 ml of RPMI complete medium was added to the flask for neutralizing the effect of trypsin.

10) The cell suspension was collected and transferred to a 50ml falcon tube.

11) The cells were pelleted after centrifugation at 1,300 rpm, 4°C for 5 min.

12) The cell pellet was washed twice with PBS and re-suspended in 20 ml of PBS.

13) The cell suspension was passed through 70 µm cell strainers to remove cell clumps.

14) A 10 µl aliquot was applied for determining the total cell amount and cell viability with a Neubauer Chamber. Formula of quantification: cell quantity (cells/ml) = cell amount in 4 quadrants/4 $\times$ dilution factor $\times 10^4$

15) The cells were pelleted and re-suspended with an appropriate amount of PBS to reach a final concentration (25×10^6 cells/ml PBS).

16) The cell suspension was placed on ice and transported to the animal house in 5 min.

2.4.3 Subcutaneous injection of tumor cells

1) The hairs on right flank area of mice were shaved one day before injecting tumor cells.

2) The mice were anesthetized by inhaling isoflurane.

3) The mice were placed on the top of a mouse cage with the right flank upwards.

4) The skin on the right flank of anesthetized mice was disinfected.

5) Loose skins of the right flank were lifted up by two fingers, and 100 µl of the cell suspension in a 1 ml insulin syringe was injected into one mouse subcutaneously. Any air-bubbles or leaking should be avoided during injection. The injection of TS/A-EV and TS/A-SI-CLP cells was as homogenous as possible.

6) The mice were put back to the cage after recovering from anaesthesia.

2.4.4 Measurement of tumor growth

The tumor volume was measured on day 7, 10, 14, 18 and 21 after injection of tumor cells. The greatest longitudinal diameter (length), the greatest transverse diameter (width) and tumor thickness were measured by calliper. Tumor volume (in mm^3) was calculated using the formula for an ellipsoid: Tumor volume = $0.52 \times$ length $\times$ width $\times$ thickness

Mice were sacrificed by cervical dislocation on the day 21 post-injection. Tumor were excised and weighed. Freshly excised tumor tissues were used for isolating TAM or snap-frozen in liquid nitrogen. Frozen tumor tissues were kept in a -80°C freezer and used for immunohistochemical and immunofluorescent staining.

2.5 Cell Culture

2.5.1 Cell line and primary cells

Table 4. List of cell line and primary cells used in the study.

Name of the cell line or primary cells	Growth/cultivation medium (P/S: penicillin/streptomycin)	Growth condition
CD14+ human monocytes	Macrophage SFM medium	37°C, 7,5% CO_2
Murine bone marrow cells	DMEM supplemented with 10% FCS and 100 µg/ml P/S	37°C, 7,5% CO_2
Murine TAM	DMEM supplemented with 10% FCS and 100 µg/ml P/S	37°C, 7,5% CO_2
SI-CLP transfected TS/A clones (P1D5, P1C8, P1F10, P2B7 and P2G7)	RPMI medium supplemented with 10% FCS, 100 µg/ml P/S and 400 µg/ml G418	37°C, 5% CO_2
Empty vector transfected TS/A clones (CL-1, CL-A1, CL-A3, CL-A4 and CL-A6)	RPMI medium supplemented with 10% FCS, 100 µg/ml P/S and 400 µg/ml G418	37°C, 5% CO_2
TS/A cells	RPMI medium supplemented with 10% FCS and 100 µg/ml P/S	37°C, 5% CO_2

2.5.2 Propagation of cells

2.5.2.1 *Harvesting adherent cells*

1) The medium in T75 flask was aspirated and 5 ml of PBS (without Ca^{2+} and Mg^{2+}) was added to remove all traces of the serum containing trypsin inhibitors.

2) 2 ml of 1x Trypsin/EDTA solution was added to the flask, which was incubated at 37°C for 3 min to detach the cells.

3) 8 ml of RPMI complete medium was added to stop the reaction and all cells in suspension were collected.

4) The cell suspension was centrifuged at 1,200 rpm for 8 min to pellet cells.

5) The cell pellet was re-suspended in 1 ml of RPMI complete medium.

6) An appropriate aliquot of the cell suspension was applied for determining the cell amount.

7) 2×10^6 tumor cells were plated in a new T75 flask for propagation.

2.5.2.2 *Cryopreservation of cells*

1) Tumor cells were harvested according to the protocol described above.

2) After last centrifugation, an appropriate aliquot of the cell suspension was applied for determining the cell amount and cell viability.

3) $3\text{-}5 \times 10^6$ tumor cells were re-suspended in 1 ml of frozen medium.

4) The cell suspension was placed into an Mr. Frosty freezing container, which was stored at -80°C overnight and transferred to a liquid nitrogen tank for long-term storage.

2.5.2.3 *Thawing cells*

1) Frozen aliquot of tumor cells was taken out from a liquid nitrogen tank and thawed rapidly in a 37°C water bath.

2) Thawed tumor cells were re-suspended in 10 ml of sterile PBS (without Ca^{2+} and Mg^{2+}).

3) The cell suspension was centrifuged at 1,200 rpm for 8 min to get rid of residual DMSO.

4) The cell pellet was re-suspended in 10 ml of fresh complete medium and transferred to the sterile culture flask.

2.5.3 Isolation of CD14+ human monocytes from buffy coats

Fresh buffy coats in protective bags of 30 ml were provided by the German Red Cross Blood Donor Service Baden-Württemberg–Hessen. A unique number was given for each individual donor.

1) 15 ml of Biocoll separating solution was poured into a 50ml falcon tube.

2) The blood from the buffy coat package was poured into a sterile T75 flask and mixed with the same amount of PBS (without Ca^{2+} and Mg^{2+}).

3) 30 ml of diluted blood was slowly added to the falcon tube with Biocoll separating solution inside.

4) The falcon tube was centrifuged at 420 RCF, 20°C for 30 min without breaks.

5) Enriched peripheral blood mononuclear cells fraction (white ring) was collected in a new 50ml falcon tube, which was filled with PBS until 50 ml and centrifuged at 420 RCF, 20°C for 10 min with break.

6) The supernatant was aspirated and the cell pellet was re-suspended in 5 ml of PBS.

7) The cell suspension was filled with PBS until 50 ml and centrifuged at 420 RCF, 20°C for 10 min.

8) The supernatant was aspirated and the cell pellet was re-suspended again in 5 ml of PBS. The cell suspension was filled with PBS until 50 ml and a 10 µl aliquot was applied for cell counting.

9) The cell suspension was centrifuged at 420 RCF, 20°C for 10 min.

10) 30 ml of Percoll gradient solution was prepared by mixing 13.5 ml Percoll, 15 ml MEM Spinner modification and 1.5 ml 10x Earle´s salt solution in a 50ml falcon tube.

11) The supernatant of cell suspension was aspirated and the cell pellet was re-suspended in 3 ml of PBS.

12) The cell suspension was carefully added on top of the Percoll gradient solution in 50ml falcon tube, which was centrifuged at 420 RCF, 20°C for 30 min without breaks.

13) The upper layer containing the mononuclear cells was carefully collected and transferred into a new 50ml falcon tube.

14) The total volume in falcon tube was filled up to 50 ml with PBS and the falcon tube was centrifuged at 420 RCF, 20 °C for 10 min with breaks.

15) The supernatant was aspirated and the cell pellet was re-suspended in 5 ml of PBS.

16) The cell suspension was transferred into a 15ml falcon tube and the total volume of cell suspension was filled up to 10 ml.

17) 10 µl of cell suspension was applied for cell counting and the rest of cell suspension was centrifuged at 420 RCF, 20 °C for 10 min

18) The supernatant was carefully aspirated and the cell pellet was re-suspended in 95 µl of MACS buffer + 5 µl CD14 micro beads per 10^7 cells.

19) The cells were incubated at 4°C for 20 min on a rotator.

20) The final volume was made up to 10 ml with MACS buffer and centrifuged at 420 RCF, 20°C for 10 min.

21) The cell pellet was re-suspended in 1 ml of MACS buffer.

22) An LS separation column was placed in the magnetic separation unit and washed once with 3 ml of MACS buffer.

23) A fresh collecting tube was placed beneath the LS separation column and the cell suspension was added to the LS column.

24) The LS column was washed three times with 3 ml of MACS buffer before removing from magnetic separation unit.

25) The column was placed on top of a fresh 15ml falcon tube and 5 ml of MACS buffer was added to elute CD14+ monocytes from the column.

26) 10 µl of aliquot was applied for cell counting and the cell suspension was centrifuged at 420 RCF, 20°C for 10 min.

27) The cell pellet was re-suspended in appropriate macrophage SFM medium to reach a final concentration of $1X10^6$ cells/ml.

2.5.4 Isolation of bone marrow cells from BALB/c female mice.

1) BALB/c female mice were sacrificed by cervical dislocation.

2) The abdominal part of the mice was sterilized with 70% ethanol.

3) The legs close to the hip were cut off with scissors.

4) The skin was removed from the legs and the foot link was broken.

5) The muscles were totally removed from the bones with scissors and forceps. The femur and tibia were separated after the knee joint was broken.

6) The bones were sterilized with 70% ethanol for 1 min and transferred to a Petri dish filled with cold PBS.

7) A hole was made on both ends of the bones to allow flushing of bone marrow with the needle of a syringe.

8) A 10ml syringe coupled with a 22 G needle was filled with PBS and bone marrow was expelled from both sides of the bone into a 50ml falcon tube.

9) The cells were mixed by pipetting 5-8 times to break cell aggregates and passed through a 70 µm Cell Strainer.

10) The cell suspension was centrifuged at 400 RCF for 10 min and the cell pellet was re-suspended in 1 ml of Red Blood Cell Lysis Buffer.

11) The cell suspension was transferred to a new 15ml falcon tube and incubated at room temperature for 2 min.

12) 3 ml of DMEM complete medium was added to the cell suspension, followed by centrifuging samples at 400 RCF for 6 min.

13) The cell supernatant was aspirated and the cell pellet was re-suspended in 5 ml of DMEM complete medium supplemented with 30 ng/ml M-CSF.

14) 10 µl of the cell suspension was applied for cell counting and the cell suspension was adjusted to $1X10^6$ cells/ml with murine bone marrow medium.

15) The cells were plated in 6 wells plate and cultured for four days in murine bone marrow medium at 37°C in 7.5% CO_2 incubator.

2.5.5   Isolation of murine TAM

TAM were isolated from mammary adenocarcinoma tumors generated by subcutaneous injection of $2.5X10^6$ TS/A-EV and TS/A-SI-CLP cells in BALB/c female mice. 2.5 mg DNase I and 8.5 mg collagenase IV were dissolved in 10 ml of Reduced Serum Medium, which was filtered through a 0.22 μm filter into a 15ml falcon tube. 10 ml of enzyme mix was applied for digesting up to 2 g TS/A tumors.

1) Mice were anaesthetized with isoflurane and sacrificed by cervical dislocation.

2) The hair over the tumors was shaved and the area was disinfected.

3) The tumor was carefully excised with scissors and placed in a 10 cm Petri dish.

4) The tumor was carefully skinned and weighed.

5) The necrosis area was removed from the tumor tissue, and the rest of tumor was chopped to tiny pieces in the Petri dish.

6) Chopped tumor pieces were transferred to a falcon tube filled with the corresponding amount of enzyme mix.

7) Falcon tube containing tumor tissues was incubated at 37°C for 1.5 h on a rotating shaker.

8) Digested tumor tissues were passed through a 100 μm Cell Strainer into a 50ml falcon tube, and the cell strainer was rinsed once with cold PBS.

9) The total volume of digested tumor tissue was adjusted to 50 ml with cold PBS.

10) The falcon tube was centrifuged at 4°C, 1,600 rpm for 10 min.

11) The cell supernatant was aspirated and the cell pellet was re-suspended in 10 ml of cold MACS buffer.

12) The cell suspension was passed through a 40 μm cell strainer into 50ml falcon tubes and counted with a Neubauer Chamber.

13) The cell suspension was centrifuged at 1,500 rpm, 4°C for 10 min.

14) The cell supernatant was carefully aspirated and the cell pellet was re-suspended in 10 ml of cold MACS buffer.

15) The falcon tubes were centrifuged at 1,500 rpm, 4°C for 10 min.

16) The cell supernatant was aspirated and the cell pellet were re-suspended in 90 μl of MACS buffer per 10^7 total cells.

17) 10 μl of mouse CD11b microbeads were added to the cell suspension per 10^7 total cells.

18) The cell suspension was mixed well and incubated at 4°C for 15 min.

19) 2 ml of MACS buffer per 10^7 cells was added to the cell suspension, which was centrifuged for 10 min at 1,500 rpm, 4°C.

20) The cell supernatant was aspirated and up to 10^8 cells was re-suspended in 500 µl of MACS buffer.

21) The LS columns were placed in the magnetic field of a MACS separator, and 3 ml of MACS buffer was added to rinse each column.

22) The cell suspension was applied on the column, and the column was washed three times once the column reservoir was empty.

23) The column was removed from the MACS separator and placed on a clean 15 ml falcon tube.

24) 5 ml of MACS buffer was pipetted on the column to flush CD14 positive cells.

25) 10 µl of the cell suspension were taken for counting cells in a Neubauer chamber after MACS separation.

26) The cell suspension was centrifuged at 1,300 rpm 4°C for 8 min.

27) The supernatant was aspirated and pre-warmed DMEM complete medium was added to get a final concentration of $1X10^6$/ml medium.

28) $4X10^6$ isolated TAM were added to one well of 6 wells plates, which was placed in 37°C, 5% CO_2 incubator.

29) After 30 min, non-adherent cells in 6 wells plates or Petri dishes were washed away by adding DMEM medium.

30) 350 µl of RNA lysis buffer was added to adherent TAM in one well of 6 wells plates, and the RNA lysates were used for RNA isolation and Microarray gene chip analysis. Moreover, $2X10^6$ TAM was seeded on top of a coverslip and used for staining CD68 protein.

31) $4X10^6$ TAM were maintained in DMEM complete medium for 16 h, and the conditioned supernatant from TAM were harvested.

2.5.6 Isolation of spleen T cells from BALB/c mice

1) The mice were sacrificed by cervical dislocation.

2) The abdominal part of the mice was sterilized with 70% ethanol.

3) The abdominal cavity was opened and the whole spleen was taken out.

4) The spleen tissue was cut into small pieces with a fine scissor and smeared with the end of a 5ml syringe.

5) The tissue suspension was passed through a 70 μm Cell Strainer, which was washed three times with sterile PBS.

6) The cell suspensions were centrifuged at 400 RCF for 10 min and the cell pellet was re-suspended in 1 ml of red blood cell lysis buffer. The cell suspension was transferred to a 15ml falcon tube and incubated at room temperature for 2 min.

7) 8 ml of RPMI medium was added to the cell suspension, which was centrifuged for 6 min at 400 RCF.

8) The supernatant was aspirated after centrifugation and the cell pellet was re-suspended in 5 ml of RPMI medium.

9) A 10 μl of aliquot was taken for cell counting and the cell suspension was centrifuged at 400 RCF for 6 min.

10) The supernatant was aspirated and the cell pellet was re-suspended in 40 μl of FACS buffer per 10^7 total cells.

11) 10 μl of biotin conjugated antibody cocktail was added to the cell suspension per 10^7 total cells.

12) The cell suspension was incubated on ice for 5 min, and then 30 μl of FACS buffer was added per 10^7 total cells.

13) 20 μl of anti-biotin microbeads was added to the cell suspension per 10^7 total cells.

14) The cell suspension was fully mixed and incubated on ice for 10 min.

15) The LS columns were placed in the magnetic field of a MACS separator, and 3 ml of MACS buffer was added to rinse each column.

16) The cell suspension was added to each column, which was washed three times by adding 3 ml of MACS buffer.

17) Spleen T cells were eluted from the column and collected in a 15ml falcon tube.

18) The falcon tube was centrifuged at 4°C, 1,300 rpm for 8 min.

19) The cell pellet was re-suspended in 1 ml of RPMI medium, and 10 μl of the cell suspension was used for determining the cell amount.

20) The purity of mouse spleen T cells was determined by staining CD3 antigen and analyzed by flow cytometry.

21) The spleen T cells were plated in 6 wells plates and maintained at 37°C, 7.5% CO_2 incubator for 4 h before performing chemotaxis assay.

2.6 Immunological techniques

2.6.1 Primary antibodies

Table 5. List of primary antibodies used in this study. (st: stock concentration; wd: working dilution; NA: Not Applicable).

Antigen name	Catalog number	Company (St)	Species,	IF wd	WB wd	IHC wd	FACS wd
CD206	MCA2235GA	AbD-Serotec st: 1.0 mg/ml	Rat-IgG2a	N/A	N/A	1:1000	N/A
CD3	14-0031-85	eBioscience st: 0.5 mg/ml	Armenian Hamster IgG	N/A	N/A	1:200	N/A
CD31	MCA2388	AbD-Serotec st: 1.0 mg/ml	Rat-IgG2a	N/A	N/A	1:400	N/A
CD3-APC	100312	BioLegend st: 0.5 mg/ml	Rat IgG2c	N/A	N/A	N/A	1:100
CD4 biotin	100507	BioLegend st: 0.5 mg/ml	Rat IgG2a	N/A	N/A	1:200	N/A
CD68	SM1550P	Acris st: 1.0 mg/ml	Rat IgG2a	1:200	N/A	1:200	N/A
CD8a	558733	eBioscience st: 0.5 mg/ml	Rat IgG2a	N/A	N/A	1:200	N/A
FoxP3 biotin	135773	eBioscience st: 0.5 mg/ml	Rat IgG2a	N/A	N/A	1:200	N/A
Gr-1	Ab25377	Abcam st: 0.5 mg/ml	Rat IgG2b	N/A	N/A	1:400	N/A
LYVE-1 biotin	103-PA50AG	Relia-tech st: 1.0 mg/ml	Rabbit	N/A	N/A	1:400	N/A
PD-1	AF1021-SP	Techne Corporation st: 0.2 mg/ml	Goat IgG	N/A	N/A	1:200	N/A
SI-CLP	1B8	Our laboratory	Rat-IgG2a Hybridoma supernatant	1:3	1:3	1:3	N/A
Siglec-F	552125	eBioscience st: 0.5 mg/ml	Rat IgG2a	N/A	N/A	1:200	N/A
Stabilin-1	RS-1	Our laboratory	Rabbit IgG Immunserum	N/A	N/A	1:800	N/A

2.6.2   Secondary antibodies, conjugates, and fluorescent dyes

Table 6. List of secondary antibodies, conjugates and fluorescent dyes used in the study. (st: stock concentration; wd: working dilution; NA: Not Applicable)

Antibody conjugated	Catalog number	Company, (st)	IF (wd)	WB (wd)	IHC (wd)
Alexa Fluor 488 conjugated donkey anti-rat IgG	712-546-153	Jackson ImmunoResearch st: 1.4 mg/ml	1:400	NA	NA
DAPI	236276	Roche Diagnostics st: 1 mg/ml	1:1000	NA	NA
DRAQ5	4084	Cell Signaling Technology st: 5mM	1:1000	NA	NA
HRP conjugated streptavidin	016-030-084	Jackson ImmunoResearch st: 1.0 mg/ml	NA	NA	1:400
HRP conjugated goat anti-Armenian Hamster IgG	Sc-2443	Santa Cruz Biotechnology st: 0.4 mg/ml	NA	NA	1:200
HRP conjugated goat anti-rabbit IgG	R1364	Acris Pharmaceutics st: 1.0mg/ml	NA	NA	1:400
HRP conjugated goat anti-rat IgG	Sc-2065	Santa Cruz Biotechnology st: 0.4 mg/ml	NA	1:5000	1:400

2.6.3   Immunofluorescent staining and confocal microscopy analysis

2.6.3.1   Cell fixation with PFA

All procedures were performed at room temperature. The following protocol was used to fix cells grown on coverslips in 6 wells plates.

1)   The cells in 6 wells plates were washed two times with 1 ml of PBS.

2)   The cells were fixed with 1 ml 2% PFA in PBS for 10 min.

3)   PFA solution was aspirated.

4)   2 ml of 0.5% Triton X-100 in PBS was added to each well.

5)   0.5% Triton X-100/PBS solution was aspirated 15 min later.

6)   The cells were fixed with 1 ml of 4% PFA in PBS for 10 min.

7)   PFA solution was aspirated and the cells were washed 4 x 10 min with PBS on a shaker.

8)   Plates were dried in the hood.

9)   Plates were sealed with Parafilm and stored at -80°C.

2.6.3.2   Immunofluorescent staining

1)   The cells in 6 wells plates were washed two times with 2 ml of PBS and each washing was performed for 5 min on a shaker.

2)   The cells were washed with 1 ml of 0.1 % Tween 20 in PBS for 30 sec.

3)   The cells were incubated with 1 ml of 3% BSA in PBS for 1 h and then briefly washed with 1 ml of 0.1 % Tween 20 in PBS for 30 sec.

4)   Primary antibody was diluted in 1% BSA/PBS solution according to the Table 7.

5)   100 µl of primary antibody solution were dropped exactly on top of each coverslip to cover the cells area and incubated with the cells at room temperature for 1.5 h.

6)   The cells were washed 3 x 5 min with PBS on a shaker.

7)   The cells were washed briefly with 2 ml of 0.1 % Tween 20 in PBS for 30 sec.

8)   Secondary antibody along with DRAQ5 for nuclear staining was diluted in 1% BSA/PBS and 100 µl of secondary antibody solution was dropped exactly on the top of each coverslip.

9)   The cells were incubated with secondary antibody solution for 45 min at room temperature. During and after this process plates were kept in the dark environment.

10)   The cells were washed 4 x 5 min with PBS on a shaker.

11)   A drop of fluorescent mounting medium was added to each glass slide and the coverslips with stained cells were in contact with mounting medium directly without causing visible air bubbles.

12)   The mounted samples were stored at 4°C in darkness for at least 24 h before analyzed using Confocal Laser Scanning Microscope.

2.6.3.3   Confocal microscopy analysis

Confocal microscopy analysis was performed using a Leica Microsystems TCS SP8 laser scanning spectral confocal microscope, equipped with a 63×1.32 objective. As a source of excitation an argon laser emitting at 488 nm, a krypton laser emitting at 568 nm and a helium/neon laser emitting at 633 nm were used. Data were acquired and analyzed with Leica Microsystems Confocal Software.

2.6.4 Immunohistochemical analysis of frozen tissue sections

2.6.4.1 Preparation of frozen tissue sections

1) TS/A tumor tissues were taken out from -80°C freezer and placed in -20°C freezer for 20 min.

2) Cryostat microtome was cooled down to -22°C.

3) A small amount of O.C.T compound was added on top of a cryostat object disk that was at room temperature.

4) Frozen tumor tissues were positioned in the center of the object disk and transferred back to microtome.

5) Enough O.C.T compound was added to embed the whole tumor tissue before the object disk become solid.

6) The disk was placed in the object disk holder of the microtome and the set screw was tightened to fix the object disk. Enough space was left between the block and the microtome blade.

7) The ratchet was disengaged from the micrometer gear and the block was moved toward the blade edge with forward button.

8) Engage the ratchet on the micrometer gear and turn the flywheel with right hand to cut the tissues until a full section of the specimen was visible.

9) The thickness of cutting section was set to 5 μm and the first 3-5 sections were discarded.

10) The sections were unfolded with the paint bush and picked up with Super Frost Microscope Slides.

11) The sections were stored in -80°C freezer until immunohistochemical staining.

2.6.4.2 Staining process

All staining procedures were performed at room temperature.

1) Frozen tissue sections were fixed with acetone for 10 min and dried in the hood for 20 min.

2) A ring around the section was drawn with a DAKO Pen.

3) The fixed tissue sections were washed with 0.1% Tween-20 in PBS for 5 min.

4) The tissues sections were incubated with peroxide blocking solution for 10 min.

5) The tissue sections were washed with 0.1% Tween-20 in PBS for 30 sec.

6) Streptavidin/biotin blocking kit was applied before the staining when primary antibody is biotinylated. The tissue sections were incubated with streptavidin solution for 15 min.

7) The tissue sections were washed 2 x 5 min with PBS on a shaker.

8) The tissue sections were incubated with biotin solution for 15 min.

9) The tissue sections were washed 3 x 5 min with PBS on a shaker.

10) The tissue sections were incubated with 3% BSA in PBS for 1 h.

11) The tissue sections were washed with 0.1% Tween-20 in PBS for 30 sec.

12) Primary antibody was diluted in 1% BSA/PBS solution and 100 µl of primary antibody solution was added to cover each tissue.

13) The tissue sections were incubated with primary antibody for 1.5 h.

14) The tissue sections were washed 3 x 5 min with PBS and then washed with 0.1% Tween-20 in PBS for 30 sec on a shaker.

15) Secondary antibody was diluted in 1% BSA/PBS solution and 100 µl antibody solution was added to cover each tissue.

16) The tissue sections were incubated with the secondary antibody solution for 45 min.

17) The tissue sections were washed 3 x 5 min with PBS on a shaker.

18) The tissue sections were incubated with AEC chromogen substrate for 5-15 min.

19) Development of the reaction was terminated by washing the tissue sections with PBS for 5 min.

20) The tissue sections were immersed in Mayer's hematoxylin solution for 1 min (Mayer's hematoxylin solution should be filtered before usage).

21) The tissue sections were washed with tap water until blue colors faded away.

22) The tissue sections were mounted with Faramount mounting medium and covered with cover glasses. Stained samples were stored at room temperature.

2.6.4.3 Large tissue scanning technique

1) Stained tumor tissue mounted on top of object glasses were sequentially scanner under 10x objective of Nikon Eclipse Ni-E microscope (JAPAN).

2) The settings for taking sequential image acquisitions were the same for all sections stained with one specific marker.

3) The entire image was assembled with NIS Elements Imaging software.

4) The entire image of whole tumor specimen was analyzed with ImageScope software (version 12.1.0.5029, Aperio Technologies, Inc, 2003-2013, Wetzlar, 35578, Germany).

5) Necrosis area and overlay area was excluded with negative selection tool of ImageScope.

6) The positivity of staining was calculated by Positive Pixel Count Algorithm (dividing the number of positive pixels by the total number of pixels in the selected area).

7) The analysis for each picture was performed by two independent observers from our laboratory.

2.6.5 Immunoprecipitation

1) 10 μl of Protein G Sepharose beads required for each reaction were washed 3 x 5 min with PBS/0.1% Tween 20 solution and centrifuged at 6,000 rpm, 4°C for 5 min.

2) 200 μl of rat anti-SI-CLP antibody (1B8), 2 μg of rat IgG2a in 200 μl of PBS and 200 μl of PBS was mixed with 800 μl of PBS, which was added to pelleted Protein G Sepharose beads. The mixture was incubated on a rotator at 4°C overnight.

3) The Protein G Sepharose beads conjugated with antibody were centrifuged at 6,000 rpm, 4°C for 5 min.

4) The supernatant was carefully aspirated, leaving 30-50 μl of liquid on top of pelleted Protein G Sepharose beads.

5) The Protein G Sepharose beads conjugated with antibody were washed 3 x 5 min with PBS/0.1% Tween 20 solution, followed by centrifugation at 6,000 rpm, 4°C for 5 min.

6) 20 μl of conditioned supernatant of BHK-21 recSFV/SI-CLP cells were mixed with 800 μl of DMEM medium, which was added to the Protein G Sepharose beads.

7) The mixture was incubator on a rotator at 4°C for 3 h.

8) The mixture was centrifuged at 6,000 rpm, 4°C for 5 min.

9) The supernatant was collected in a 1.5 ml of Eppendorf tube, and the Protein G Sepharose beads were washed three times with PBS, followed by centrifugation at 6,000 rpm, 4°C for 5 min.

10) The supernatant and Protein G Sepharose beads conjugated with antibody were dissolved in the same amount of 2x Laemmli sample buffer, which was heated at 95°C for 3 min before loading for Western Blot analysis.

2.6.6 Western blot analysis

1) The gel casting unit was assembled and its integrity was tested by adding 20 ml of ddH$_2$O to the gap of the two glass plates. Separating gel was prepared according to the Table 8.

2) Freshly prepared 10% separating gel was poured between the two glass plates to cover 80% of the gel casting unit.

3) 500 µl of 100% methanol was added immediately on top of the separating gel to get a level top.

4) The methanol was dumped after separating gel was polymerized and washed two times with ddH$_2$O.

5) Stacking gel was prepared according to the Table 8 and poured on top of the separating gel.

6) A comb was inserted immediately into the stacking gel to form wells.

7) After the stacking gel polymerized, the gel casting unit was placed in an electrophoresis unit filled with 1×TGS running buffer.

8) The comb was carefully removed without causing any air-bubbles or twisting the gel-walls.

9) Samples were mixed with the same volume of 2×Laemmli sample buffer supplemented with β-mercaptoethanol.

10) The samples were heated at 95°C for 3 min, and they were centrifuged briefly before loading.

11) 20 µl of sample was added to each well using a micro syringe.

12) Electrophoresis was performed at a constant current of 15-50 mA per gel until the bromophenol blue reached the bottom of the gel.

13) The gel was carefully removed from the glass plates and placed in a plastic container filled with blotting buffer. Filter papers and a nitrocellulose membrane were adjusted to the gel size and immersed into the blotting buffer.

14) The Western Blot cassette was arranged in the following order: spongy pad / 2 filter papers / gel / Nitrocellulose membrane / 2 filter papers / spongy pad.

15) Air bubbles were removed by gently rolling a glass rod over the top. The cassette was tightened and placed in a blotting apparatus filled with blotting buffer, with the membrane towards the positive side of the gel.

16) Blotting was carried out at 250 mA for 3 h.

17) The cassette was taken out from the blotting apparatus and the membrane was placed in a plastic container filled with PBS.

18) The membrane was rinsed with PBS and stained with Ponceau S solution for 10 min to visualize the protein bands.

19) The membrane was washed with ddH2O until the red dye was invisible.

20) The membrane was incubated with 6% milk in PBS at room temperature for 1 h.

21) The membrane was incubated with primary antibody diluted in 1% milk/PBS at 4°C with shaking overnight.

22) The membrane was shortly washed with 0.1% Tween 20 in PBS, and then it was washed 4 x 5 min with 0.1% Tween 20 in PBS at room temperature on a shaker with 5 min.

23) Species specific secondary antibody was diluted in 1% milk/PBS, which was added to cover the membrane.

24) The membrane was incubated at room temperature for 1 h with shaking.

25) The membrane was washed with 0.1% Tween 20 in PBS for 30 sec, and then it was washed 4 x 10 min at room temperature on a shaker.

26) Western HRP substrate from Luminata Forte was added to cover the membrane, which was incubated at room temperature for 3 min.

27) The membrane was packed in a plastic film and developed in an X-ray film processor to display protein band.

Table 7. Composition of acrylamide gels.

Ingredients	10% Separating gel/10ml	5% Stacking gel/ 5ml
ddH2O	4.0 ml	3.4 ml
1.5 M Tris (pH 8.8)	2.5 ml	0.63 ml
10 % APS	0.1 ml	0.05 ml
10 % SDS	0.1 ml	0.05 ml
30% Acrylamide mix	3.3 ml	0.83 ml
TEMED	0.004 ml	0.004 ml

2.6.7 Flow cytometry analysis

All cell staining procedures were performed in FACS tubes. All centrifugation after washing steps were performed at 400 RCF, for 4 min at room temperature. Freshly isolated naive T cells from spleen tissue of BALB/c mice were applied for analyzing the purity of T cells.

1. Freshly isolated naive T cells were washed once with 1 ml of FACS buffer.

2. 1×10^6 cells were re-suspended in 100 µl of FACS buffer.

3. 1 µl of Fc block (BD Biosciences) was added to the samples and incubated for 5 min at 4°C.

4. 1 µg APC conjugated rat anti-CD3 IgG2c antibody diluted in 100 µl of FACS buffer was added to the sample and incubated for 30 min at 4°C.

5. Samples were washed two times with 500 µl FACS buffer.

6. Cells were re-suspended in 200-300 µl FACS buffer before measurement.

7. Samples were analyzed using a BD FACS Canto II.

2.7   RNA related methods

2.7.1   Isolation of total RNA

The E.Z.N.A. total RNA kit I from Omega was used for RNA isolation.

1) 350 µl of RNA lysis buffer was added to $3\text{-}5\text{X}10^6$ cells.

2) The cell lysates were completely disrupted by passing through a Nr.19 needle combined with a 10ml syringe 5-10 times.

3) 350 µl of 70% ethanol were added to the cell lysates and mixed well by pipetting up and down 5-10 times.

4) The sample was added to a RNA spin column placed in a 2ml collection tube without touching the membrane.

5) The RNA spin column was centrifuged for 1 min at 10,000 RCF, and the flow-through was discarded.

6) The RNA spin column was washed once by adding 500 µl of wash buffer I, followed by washing twice in 500 µl wash buffer II.

7) The final flow-through was discarded, and a new 2 ml collection tube was placed under the column.

8) The RNA spin column was centrifuged for 2 min at 16,000 RCF to dry the matrix completely.

9) The RNA spin column was placed in a fresh RNase free Microfuge tube after the last centrifugation.

10) 50 µl of RNase free water preheated at 70°C was added to elute RNA, followed by centrifuging the tube at 16,000 RCF for 2 min.

11) The RNA concentration was determined by measuring the absorption peak at 260 nm wavelength.

12) The quality of RNA samples was analyzed by electrophoresis in the 1% agarose gel.

13) RNA samples were stored at -80°C.

2.7.2 First strand cDNA synthesis

The RevertAid H Minus First Strand Synthesis Kit from Fermentas was used for cDNA synthesis.

1) 1 µl of 10x DNase I buffer with $MgCl_2$ (Fermentas) was added to each RNA sample (up to 1 µg) and mixed well by pipetting.

2) 1 µl of RNase free DNase I (Fermentas) was added to the sample, and the total volume of each sample was adjusted to 12 µl with RNase free water.

3) The sample was incubated at 37°C for 40 min to digest possible fragments of genomic DNA, and then DNase was inactivated by incubating at 70°C for 10 min.

4) 1 µl of Oligo DT primer was added to the sample and mixed by tapping the Eppendorf tube gently.

5) The sample was incubated at 70°C for 5 min.

6) Each cDNA reaction mixture was prepared by mixing 4 µl of reaction buffer (5x) with 1 µl of RiboLock RNase inhibitor, 2 µl of dNTP Mix (10M) and 1 µl of reverse transcriptase.

7) 8 µl of cDNA reaction mixture was added to each sample, which was mixed and spin down before transferring back to Thermoblock.

8) The sample was incubated at 42°C for 60 min and then at 70°C for 10 min.

9) The cDNA samples were diluted 10 times with RNase free water for performing real-time PCR analysis.

2.7.3 Real-time PCR with TaqMan probes

Primers and dual-labeled probes purchased from MWG Biotech are shown from 5' to 3' in the Table 9. Gene expression assay for mouse IL-10, TGF-β and VEGF-A were purchased from Thermo Fisher Scientific company. Probe of target gene contained FAM on the 5' end and a BHQ1 quencher on the 3' end of the sequence. Probe of β-actin gene contained JOE on the 5' end and a BHQ1 on the 3' end of the sequence. Each cDNA sample was analyzed in triplicates. The expression of target gene in each sample was normalized with the expression of β-actin gene in the same sample.

Each reaction mixture for real-time PCR was prepared by mixing:

1) 5 µl of TaqMan Gene Expression Master mix

2) 0.5 µl of 20 x TaqMan Assay

3) 1 µl of diluted cDNA sample

4) 3.5 µl of ddH2O.

Amplification was performed using a Roche LightCycler 480 instrument. The following program was used:

1) Denaturation: at 95°C for 10 min.

2) Annealing and elongation for 1 min at 60°C, followed by denaturation at 95°C for 15 sec; 50 cycles.

3) Cooling: 37°C for 1 min.

Table 8. List of primers used for real-time PCR analysis.

Primers and number	Sequence (5'-3')	Application
Mouse β-actin Forward	AGC CAT GTA CGT AGC CAT CCA	RT-PCR
Mouse β-actin Reverse	TCT CCG GAG TCC ATC ACA ATG	RT-PCR
Mouse β-actin Probe	TGT CCC TGT ATG CCT CTG GTC GTA CCA C	RT-PCR
Mouse CD163 Forward	GTGTGACATGTTCTGATGGA	RT-PCR
Mouse CD163 Reverse	TCTTCCCAGTCAGCTTCT	RT-PCR
Mouse CD163 Probe	TCTCCACCTCCACAATGCCAGCAC	RT-PCR
Mouse CD206 Forward	TGCTTTAACCTGGCATCAG	RT-PCR
Mouse CD206 Reverse	GGAACTGGTTAATCCTGTGAG	RT-PCR
Mouse CD206 Probe	TGAGTGTCACGGAGATCCACGAGCA	RT-PCR
Mouse IL-1β Forward	CTTTGAAGAAGAGCCCATCC	RT-PCR
Mouse IL-1β Reverse	TTCATCTCGGAGCCTGTAG	RT-PCR
Mouse IL-1β Probe	CCTGCTGGTGTGTGACGTTCCCAT	RT-PCR
Mouse IL-6 Forward	GAGGATACCACTCCCAACAGACC	RT-PCR
Mouse IL-6 Reverse	AAGTGCATCATCGTTGTTCATACA	RT-PCR
Mouse IL-6 Probe	TGTCTATACCACTTCACAAGTCGGAGGCT	RT-PCR
Mouse LYVE-1 Forward	GACTCTGGATTGGACTCAAC	RT-PCR
Mouse LYVE-1 Reverse	CTCTGATGATGGACTTCCTG	RT-PCR
Mouse LYVE-1 Probe	AGTGTACGCAGTGGTTGGCAGTGG	RT-PCR
Mouse stabilin-1 Forward	TACTGTTACCGCGTGCAAGACG	RT-PCR
Mouse stabilin-1 Reverse	ATTGGCATAGCCCAGCAGCATC	RT-PCR
Mouse stabilin-1 Probe	TCTTGGCCGCCACTGCCAACTTCTCCACCTTCTAT	RT-PCR
Mouse TNF-α Forward	CTATGTCTCAGCCTCTTCT	RT-PCR
Mouse TNF-α Reverse	GGAACTTCTCATCCCTTTG	RT-PCR
Mouse TNF-α Probe	CAGTAGACAGAAGAGCGTGGTGGC	RT-PCR

2.8 Migration Assay

6.5 mm Transwell with 5 μm or 8 μm pore polycarbonate membrane inserts (Corning) were used for performing migration assay. Purified SI-CLP protein derived from HEK-293 cells used for stimulation was purchased from Cusabio (Wuhan, China), and SI-CLP containing supernatant derived from alphavirus infected BHK-21 cells was provided by Dr. Anna Zajakina (Department of Protein Engineering, Biomedical Research and Study center, Riga, Latvia).

Table 9. Migration model used in the study.

Cell types	Cell amount	Migration buffer	Membrane size (μm)	Migration time (h)	Chemokines
CD14+ human monocytes	5×10^5	Macrophage SFM	5	3	Human CCL-2
Mouse bone marrow derived macrophages	5×10^5	RPMI	5	3	Murine CCL-2
Mouse naive T cells	5×10^5	RPMI	5	3	Murine CCL19
TS/A-EV and TS/A-SI-CLP cells	5×10^5	RPMI	8	16	FCS

1) Cells were re-suspended in migration buffer at a concentration of 5×10^6/ml according to the Table 10.

2) 600 µl of migration buffer was added into the lower chamber without causing any visible air bubbles.

3) 100 µl of the cell suspension was added in the top well of each Transwell carefully without touching the membrane.

4) The whole Transwell plate was incubated at 37°C, 5% CO_2 for 3 or 16 h.

5) The medium in the top well was aspirated and a wet cotton swab was used to remove the cells on the upper side of each insert that had not migrated yet.

6) The inserts were transferred to 24 wells plates with 800 µl of ice cold methanol (100%) inside.

7) The 24 wells plates were placed in a -30°C freezer for 5 min.

8) Methanol was aspirated and the inserts were washed three times in ddH$_2$O for 10 min.

9) Migrated cells at the lower side of inserts were stained with 1 ml of DAPI solution (prepared in PBS at 1: 1000 dilutions) for 5 min at room temperature.

10) The inserts were washed 3 x 5 min in ddH$_2$O.

11) The upper surface of each insert was cleaned again by a wet cotton swab to get rid of residual non-migrated cells.

12) One drop of fluorescent mounting medium was added on top of a Super Frost object slide.

13) The membrane of whole insert was cut off carefully and placed on Super Frost object slides with migrated cells towards the mounting medium directly.

14) A 22 mm x 22 mm coverslip was applied for covering the membrane. The slides were dried at 4°C cooling room and protected from light.

15) 10 random images were taken for each slide under the aid of a fluorescent microscope equipped with a 32x objective. The mean migrated cells for each reaction were calculated via counting the cells in each image.

2.9 Proliferation assay

The Click-iT® EdU Alexa Fluor® 488 Flow Cytometry Assay Kit was used.

1) $3X10^5$ cells were split into one well of 6 wells plates, which were maintained in corresponding medium for 24 h.

2) 10 μM/ml EdU was added to each well and mixed with the medium.

3) The 6 wells plates were incubated at 37°C, 5% CO_2 for 1 h.

4) The cells in each well were collected according to the standard protocol for harvesting adherent cells.

5) Harvested cells were kept in FACS tubes and washed once with 2 ml of FACS buffer.

6) 100 μl of fixative solution (Click-iT® component D) was added to each FACS tube and mixed well with the cells.

7) The FACS tubes were incubated at room temperature for 15 min.

8) 3 ml of 1% BSA in PBS was added to each FACS tube and mixed well with the cells.

9) The supernatant was discarded after centrifugation at 1,200 rpm for 8 min.

10) 100 μl of saponin-based permeabilization and wash reagent (Click-iT® component E) was added to each FACS tube.

11) The FACS tubes were vortexed gently and incubated at room temperature for 15 min.

12) 500 μl of Click-iT® reaction cocktail was added to each FACS tube, which was mixed and incubated at room temperature for 30 min in darkness.

13) The cells in each FACS tube were washed once by adding 3 ml of saponin-based permeabilization and wash reagent.

14) The supernatant was discarded after centrifugation at 1,200 rpm for 8 min.

15) 200 μl of saponin-based permeabilization and wash reagent was added to re-suspend the cell pellet.

16) Cells were analyzed on a BD FACS Canto II. 488 nm excitation with a green emission filter.

2.10 Statistical analysis

When samples are normalized distributed, unpaired t-test was used to compare the difference of mean values in two independent groups, and data are presented as mean ± SD.

When samples are not normalized distributed, nonparametric Mann-Whitney U-test was used to compare the difference of median values in two independent groups, and data are presented as median.

Statistical analysis was performed with the GraphPad Prism 6.05 version (GraphPad Software, Inc., CA 92037 USA). The statistical difference was indicated as * ($P<0.05$), ** ($P<0.01$), *** ($P<0.001$) and **** ($P<0.0001$).

3   Results

3.1   Comparison of tumor growth in stabilin-1 ko mice after injection of TS/A-EV and TS/A-SI-CLP cells

Elevated circulating levels of prototype chitinase-like protein YKL-40 were identified in patients with various types of solid cancer and are predictive for bad clinical outcome[127]. YKL-40 was found to support tumor growth and metastasis in the mouse model for breast cancer[128]. SI-CLP, discovered in our laboratory as a ligand for stabilin-1, is a close structural homologue of YKL-40, however the role of SI-CLP in cancer progression remains to be unknown. First animal model to investigate the role of SI-CLP in breast cancer progression was established in our laboratory (Nan Wang, PhD thesis 2014), and the model was also used in current study. In the model TS/A cells were stably transfected with plasmid expressing full length SI-CLP and control plasmid empty vector (EV), singe cell derived clones were generated and used for the subcutaneous injection into BALB/c mice. This breast carcinoma mouse model was most suitable for investigating the effect of SI-CLP on tumor growth since no endogenous SI-CLP was detected in TS/A-EV cells and TS/A-EV tumor tissue (Figure 6A). Previous data obtained by PhD student Nan Wang suggested that SI-CLP suppresses tumor growth in this model, possibly by decreasing the amount of stabilin-1+ TAM (Nan Wang, PhD thesis, 2014). Knockout of the stabilin-1 gene in BALB/c and C57BL/6 mice significantly inhibited tumor growth and metastasis in a TS/A breast carcinoma model and a B16 melanoma model[68,129]. However, the role of stabilin-1 in SI-CLP mediated suppression of tumor growth was not investigated. Tumor challenge studies were performed in BALB/c stabilin-1 ko mice.

First question that was asked in the present study is whether SI-CLP can also suppress tumor growth in the stabilin-1 ko mice, similarly to wt mice. 2.5×10^6 TS/A-SI-CLP (clone CL-P1D5) or TS/A-EV (clone CL-A1) cells were injected subcutaneously into BALB/c wild type (wt) or stabilin-1 ko mice. Tumor volume at multiple time points (day 7, 10, 14, 18 and 21 post-injection) was measured according to the formula described in the Section 2.4. Mice were killed on day 21 post-injection and tumor was excised and weighed. Three independent tumor injection experiments were performed. In total, sixteen wt mice injected with TS/A-EV cells, seventeen wt mice injected with TS/A-SI-CLP cells, fifteen ko mice injected with TS/A-EV cells and fourteen ko mice injected with TS/A-SI-CLP cells were included in the final statistical analysis. SI-CLP expression levels in BALB/c wt and stabilin-1 ko mice

injected by TS/A-SI-CLP cells were found to be comparable (Figure 6B). At all time-points analysed, the tumor volume in mice injected with TS/A-SI-CLP cells was significantly decreased compared to mice injected with TS/A-EV cells (Figure 7). The tumor volume in BALB/c wt mice injected with TS/A-EV cells was 1.51 times bigger than mice injected with TS/A-SI-CLP cells on day 7 (Figure 7A), 1.71 times on day 10 (Figure 7B), 2.04 times on day 14 (Figure 7C), 1.82 times on day 18 (Figure 7D) and 1.4 times on day 21 post-injection (Figure 7E). In stabilin-1 ko mice, the tumor volume generated by injecting TS/A-EV cells was 2.33 times bigger than those generated by injecting TS/A-SI-CLP cells on day 7 (Figure 7A), 2.34 times on day 10 (Figure 7B), 2 times on day 14 (Figure 7C), 2 times on day 18 (Figure 7D), and 2.24 times on day 21 (Figure 7E). The tumor weight in wt mice injected with TS/A-EV cells was 1.47 times heavier than the mice injected with TS/A-SI-CLP cells, while the tumor weight in ko mice injected with TS/A-EV cells was 2.4 times heavier than those injected with TS/A-SI-CLP cells (Figure 7F). The suppression of tumor growth induced by SI-CLP was more pronounced in stabilin-1 ko mice compared to BALB/c wt mice. Moreover, the tumor volume generated by injecting TS/A-SI-CLP clone in stabilin-1 ko mice was smaller than that generated by injecting the same TS/A-SI-CLP clone in BALB/c wt mice at all time points analysed, but the distinction reached significance only on day 18 and day 21 post-injection.
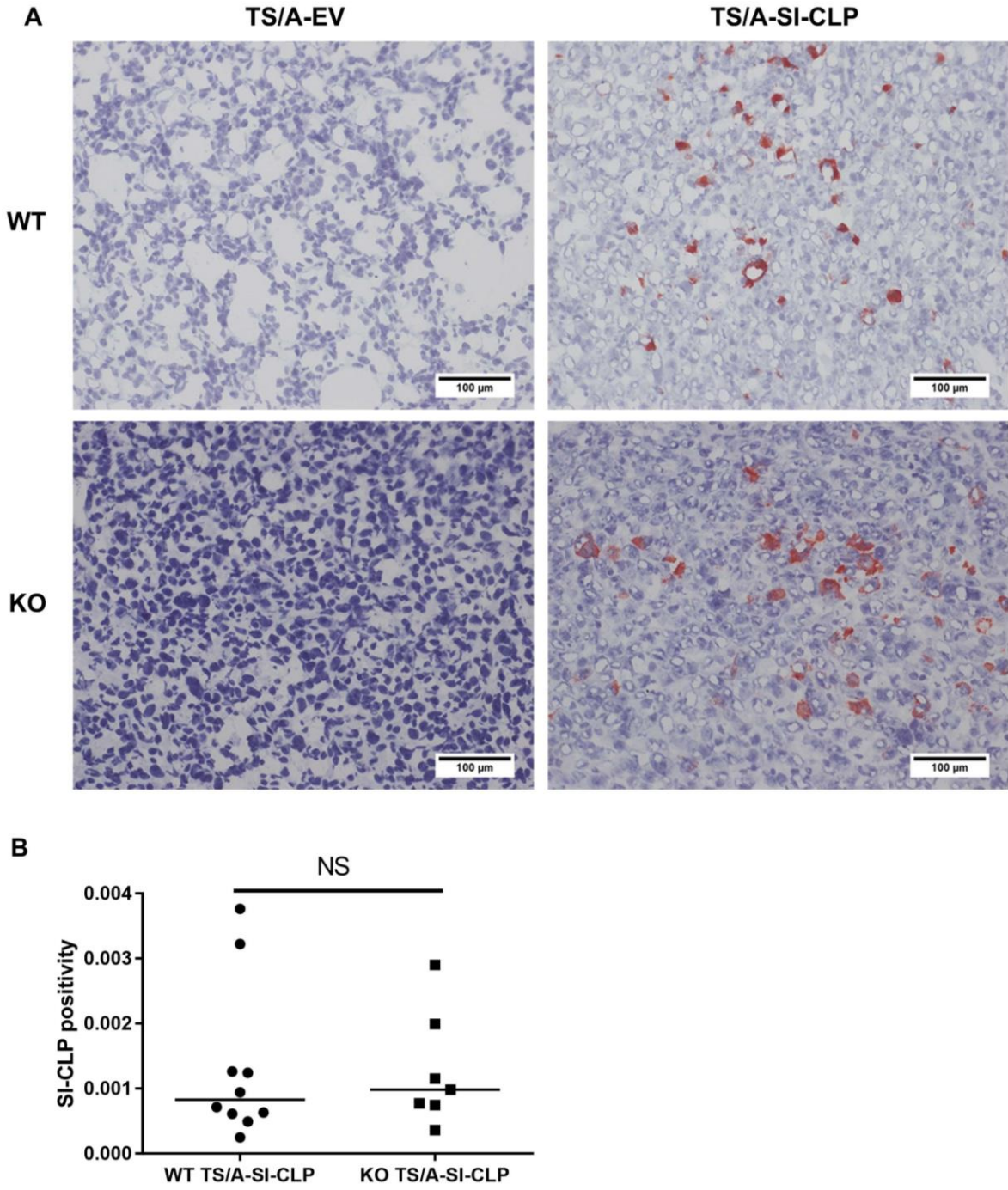
Figure 6. Quantitative analysis of SI-CLP expression in tumors generated by subcutaneous injection of TS/A-SI-CLP cells into BALB/c wt and stabilin-1 ko mice. (A) SI-CLP expression was visualized using rat anti-SI-CLP antibody (1B8), scale bar: 100 μm. (B) Quantitative analysis of SI-CLP positivity in BALB/c wt and stabilin-1 ko mice injected with TS/A-SI-CLP cells (clone P1D5). The Mann-Whitney test was used to compare the median of SI-CLP positivity, and NS indicates no statistical significance.
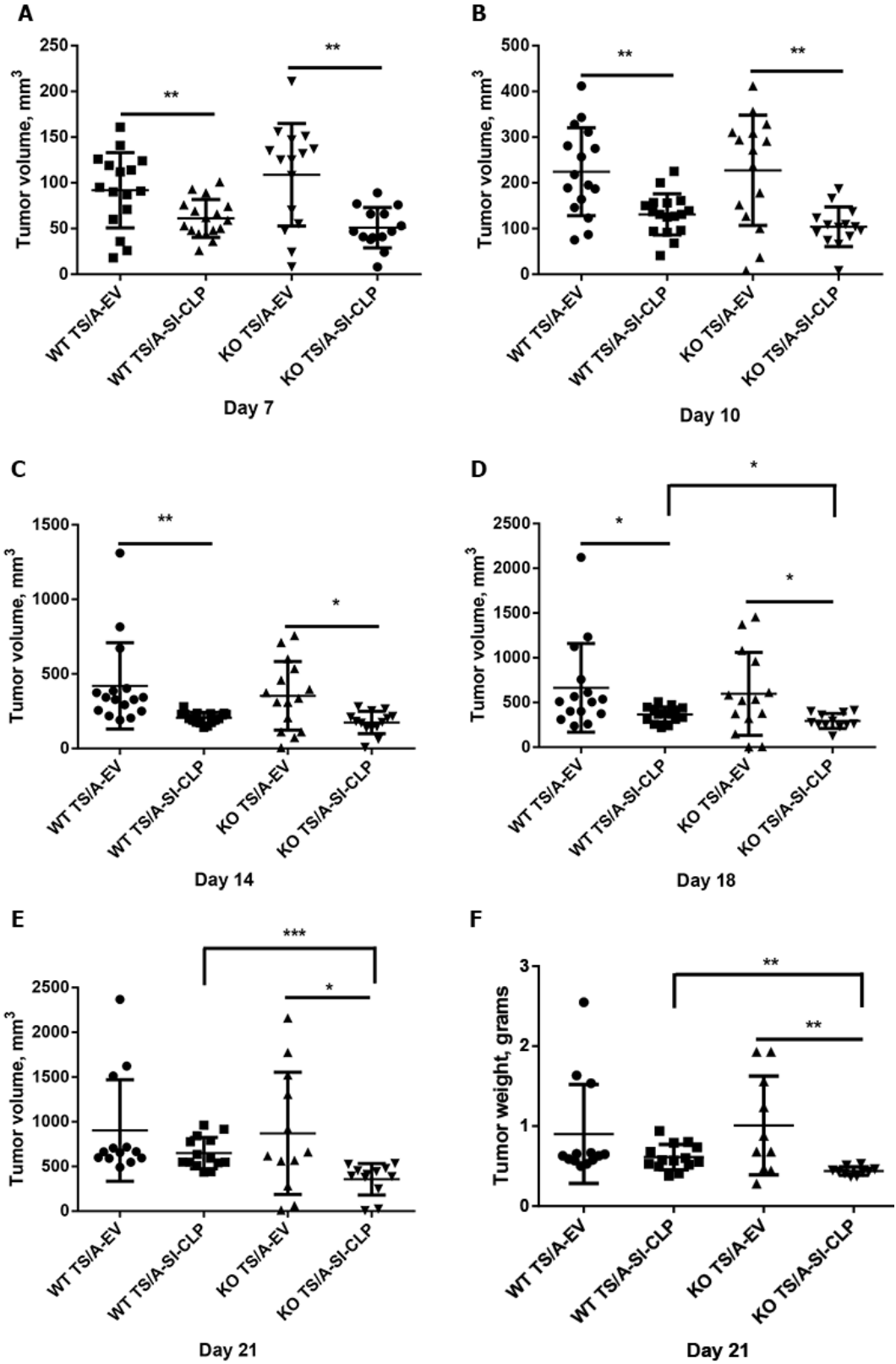
Figure 7. Comparison of tumor growth of TS/A-EV and TS/A-SI-CLP derived tumors in BALB/c wt and stabilin-1 ko mice. (A) Tumor volume on day 7 post-injection. (B) Tumor volume on day 10 post-injection. (C) Tumor volume on day 14 post-injection. (D) Tumor volume on day 18 post-injection. (E) Tumor volume on day 21 post-injection. (F) Tumor weight on day 21 post-injection. An unpaired t-test was used to compare the significance of the difference between two groups, and data are presented as the mean ± SD.

58

3.2 Comparison of proliferation and migration of TS/A-EV and TS/A-SI-CLP cells

Since significant reduction of tumor growth was found in mice injected with TS/A-SI-CLP cells, it was hypothesized that this effect could be due to the differences in the proliferation or migration ability of transfected TS/A cells. The proliferation assay was performed on five TS/A-EV clones (CL-1, CL-A1, CL-A3, CL-A4 and CL-A6) and five TS/A-SI-CLP clones (CL-P1C8, CL-P1D5, CL-P1F10, CL-P2B7 and CL-P2G7). At least two independent experiments were performed for each clone and each experiment was done in triplicates. TS/A-EV and TS/A-SI-CLP cells were maintained in RPMI complete medium until the cell confluence reached 80%. 10 μM/ml EdU (5-ethynyl-2´-deoxyuridine) was added to the medium and incubated with cells at 37°C for 1 h. Alexa Fluor 488 conjugated azide dye was used to stain and quantify proliferating cells. All cells excluding cell debris were gated for proliferation analysis (Figure 8A). Around 39.4% of TS/A-EV cells (Figure 8B) and 50% of TS/A-SI-CLP cells (Figure 8C) were in proliferating status when they were harvested. The proliferation ability of TS/A-SI-CLP cells was slightly increased in comparison to TS/A-EV cells, but the difference did not reach statistical significance (Figure 8D, P=0.0952).

The ability of tumor cells to spread and migrate is vital for tumor progression[130]. The migration assay was performed using four TS/A-EV clones (CL-A1, A3, A4, A6) and four TS/A-SI-CLP clones (P1D5, P1C8, P1F10, P2B7). Two independent experiments were carried out for each clone, and each migration experiment was performed in triplicates. Migration of TS/A-EV and TS/A-SI-CLP cells was first tested with a 5 μm pore polycarbonate membrane insert, but no cells could pass through the membrane. The mean nuclear size of TS/A-EV and TS/A-SI-CLP cells is around 10 μm, so Transwell with a pore size of 8 μm was chosen. A concentration gradient of 2% to 20% FCS was used to recruit FOXQ1 transfected mouse macrophage-like RAW 264.7 cells in our lab (IIya Ovsiy, PhD thesis, 2013), so the concentration gradient of FCS was used to assess the migration ability of SI-CLP transfected TS/A cells. 5×10^5 TS/A-EV and TS/A-SI-CLP cells maintained in RPMI + 2% FCS medium were seeded in the top chamber, and the lower chamber was filled with RPMI + 20% FCS medium. The migration assay was performed in a 37°C incubator for 16 h. Migrated cells adhered on the lower side of the membrane and were visualized with DAPI staining (Figure 9A). Migrated cells were photographed under a fluorescence microscope equipped with a 32x objective and the migrated cells in 10 random images were counted to get the mean values for each clone. The chemotactic index was calculated according to the

following formula: number of migrated cells in experimental group/ the lowest number of migrated cells in control well[131]. More TS/A-SI-CLP cells were found in the lower side of membrane in comparison to TS/A-EV cells, but the difference did not reach statistically significant (Figure 9B, P=0.3429).
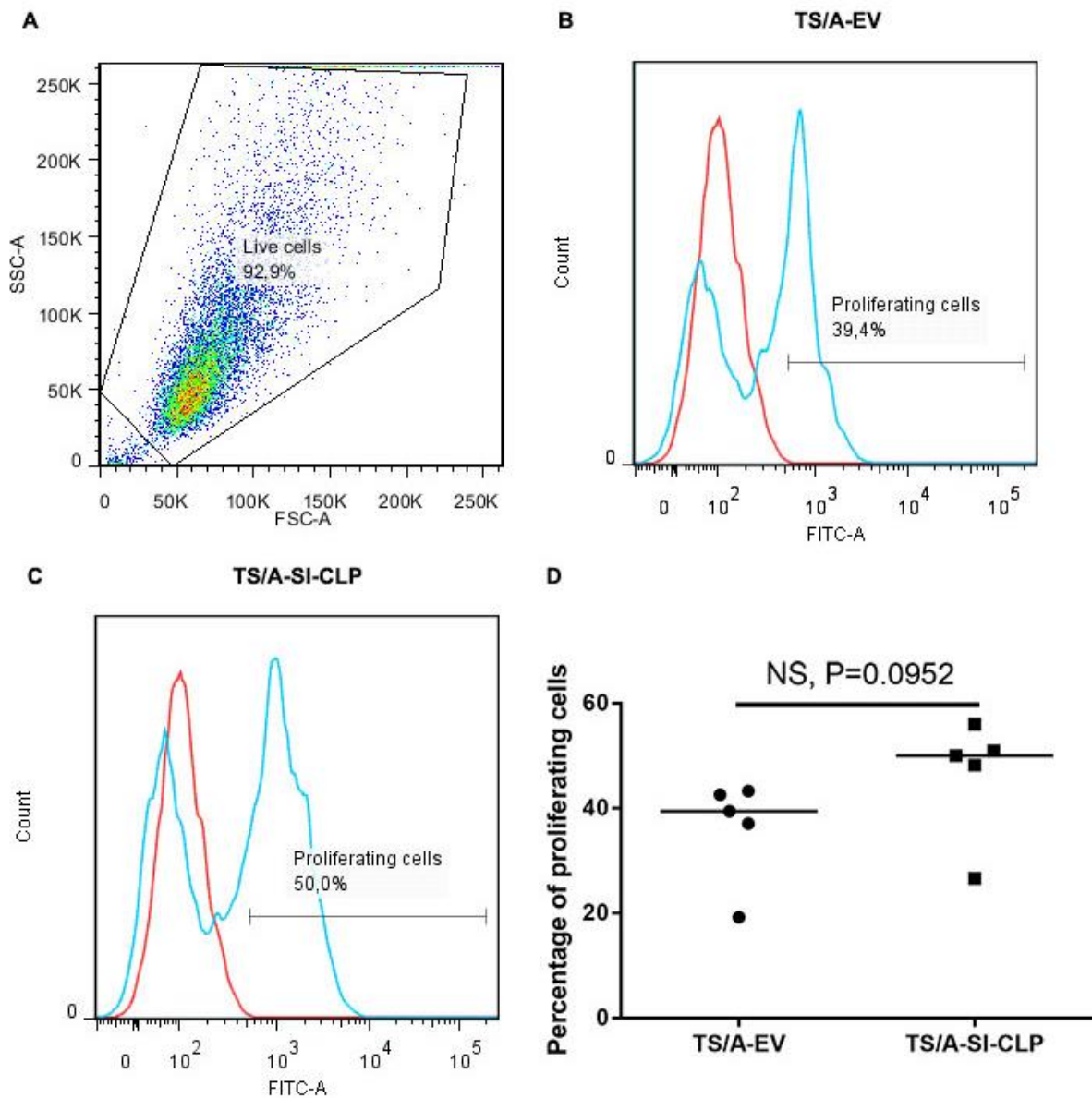
Figure 8. Comparison of the proliferation of TS/A-EV and TS/A-SI-CLP cells. (A) The SSC-A and FSC-A were adjusted to select the correct cell population for analysis. Cell debris was excluded (bottom, left hand corner). (B) Representative histogram demonstrating percentage of proliferating TS/A-EV cells. (C) Representative histogram demonstrating percentage of proliferating TS/A-SI-CLP cells. (D) Comparison of proliferation of TS/A-EV and TS/A-SI-CLP cells. The Mann-Whitney Test was used to compare the significance of difference, and data are presented as the median. NS indicates no statistical significance.
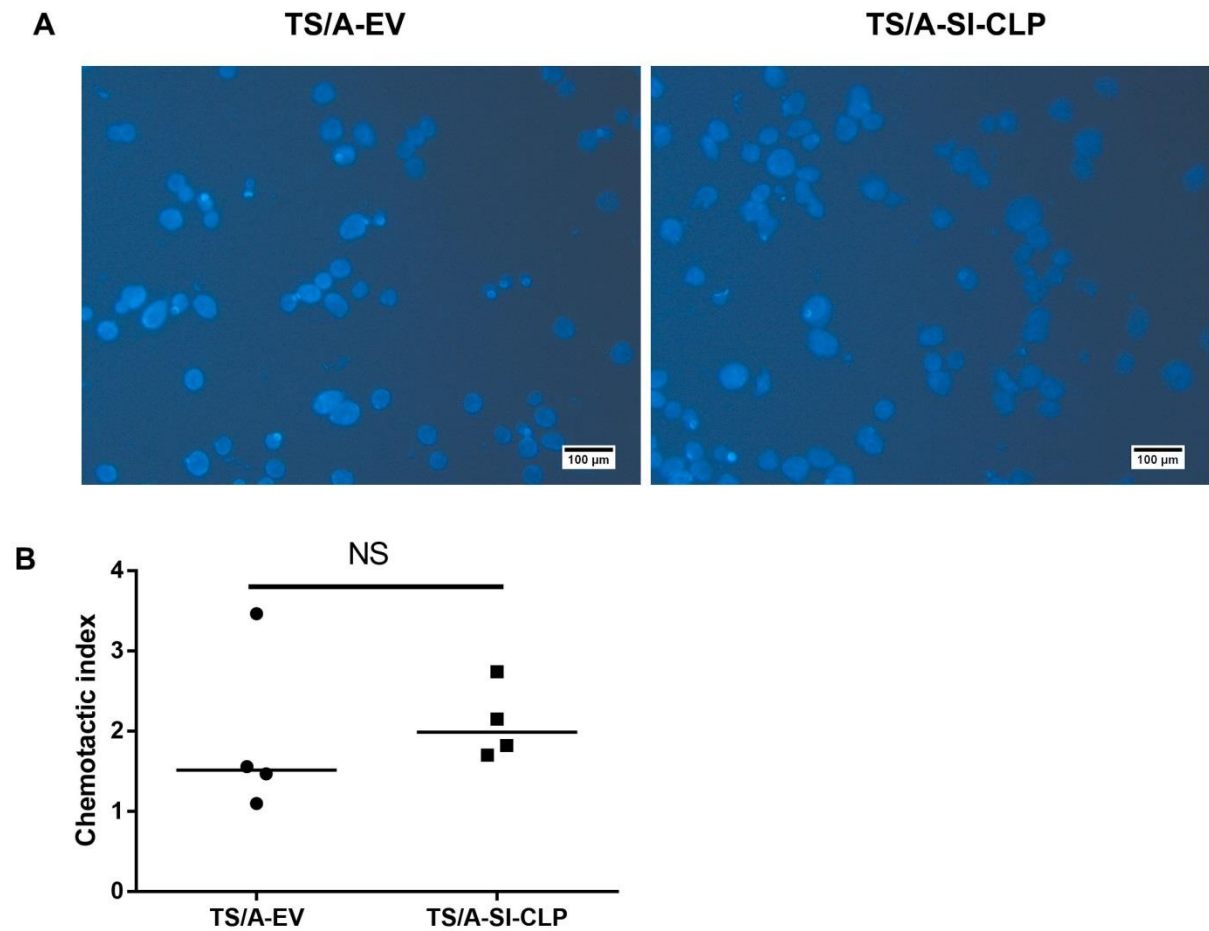
Figure 9. Comparison of the migration of TS/A-EV and TS/A-SI-CLP cells. (A) Representative picture of migrated TS/A-EV and TS/A-SI-CLP cells on the lower side of the membrane was visualized by DAPI staining, scale bar: 100 μm. (B) Comparison of the chemotactic index of migrated TS/A-EV and TS/A-SI-CLP cells. The Mann-Whitney Test was used to compare the significance of difference, and data are presented as the median. NS indicates no statistical significance.

3.3 Comparison of angiogenesis in TS/A-EV and TS/A-SI-CLP tumors

Tumor neovascularization is important for local tumor growth, and YKL-40-mediated support of tumor growth was found to be associated with its pro-angiogenesis activities[9,39,56]. Over-expression of YKL-40 in HCT-116 and MDA-MB-231 cells promoted angiogenesis (evaluated by the levels of CD31+ expression) in mouse models for breast adenocarcinoma and colorectal carcinoma[9]. Thus, it was examined whether SI-CLP affected tumor neovascularization in TS/A tumors. TS/A tumors were found to be highly vascularized and tumor vessels were visualized using antibodies against CD31 protein, the major markers of vascular endothelium. In TS/A tumor tissue, CD31 was found on vessel-like structures and single cells (Figure 10A). The vascularization in BALB/c wt mice was investigated in six TS/A-EV and ten TS/A-SI-CLP tumors, and was found to be unaltered (Figure 10B). In

stabilin-1 ko mice, the expression of CD31 protein was investigated in seven TS/A-SI-CLP tumors and five TS/A-EV tumors from three experiments. CD31 positivity was not affected by SI-CLP in the absence of stabilin-1 expression.
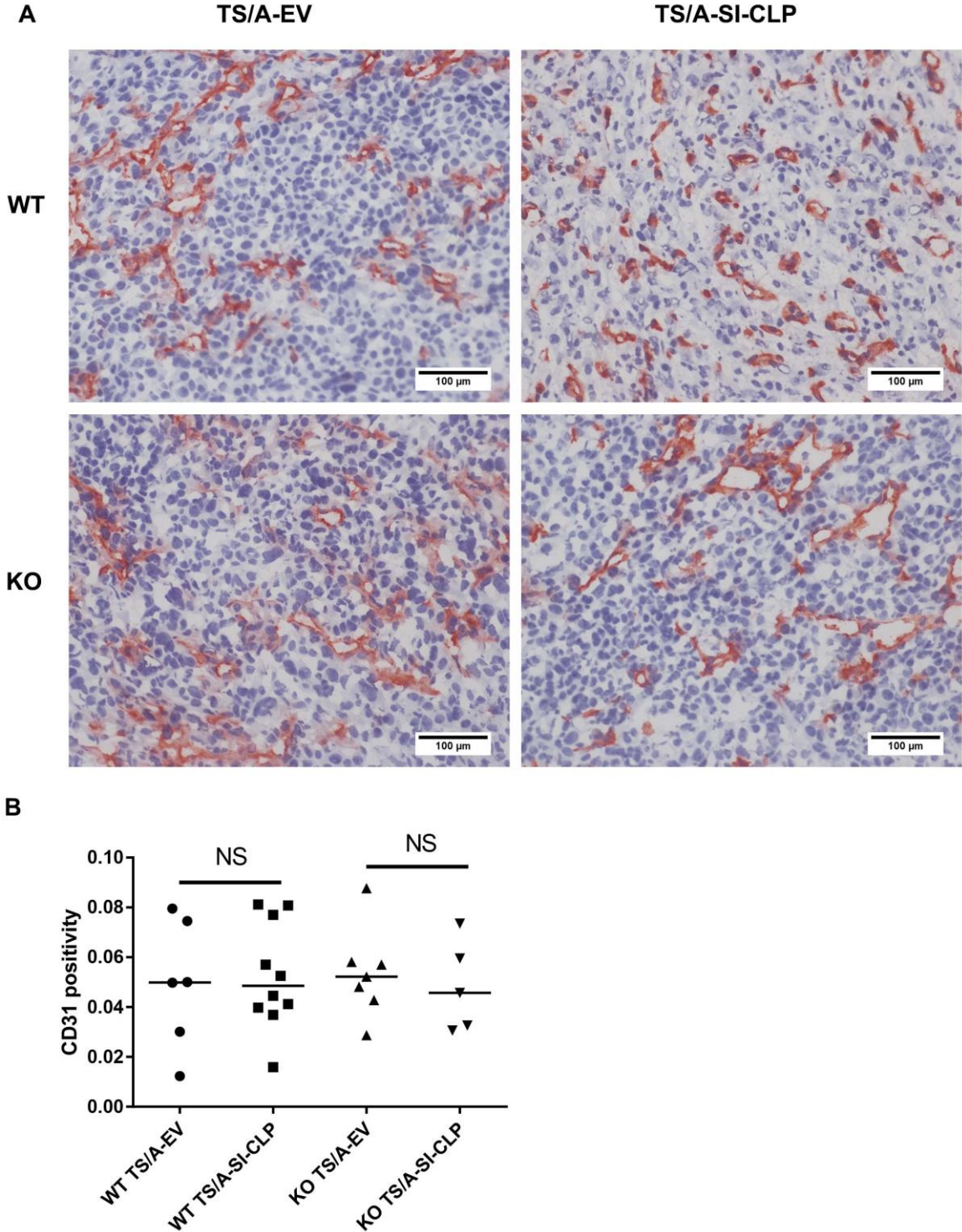
Figure 10. Quantitative analysis of CD31 expression in tumors generated by subcutaneous injection of TS/A-EV and TS/A-SI-CLP cells into BALB/c wt and stabilin-1 ko mice. (A) CD31 expression was visualized using rat anti-mouse CD31 antibody, scale bar: 100 μm. (B) Comparison of the positivity of CD31 protein in BALB/c wt and stabilin-1 ko mice injected with TS/A-EV or TS/A-SI-CLP cells. The Mann-Whitney test was used to compare the significance of difference between two groups, and data are presented as the median. NS indicates no statistical significance.

3.4   Comparison of TAM infiltration in TS/A-EV and TS/A-SI-CLP tumors

Even though TS/A-SI-CLP cells demonstrated slightly enhanced proliferation (25%) and migration ability (31%) in comparison with TS/A-EV cells, the injection of TS/A-SI-CLP cells in both BALB/c wt and stabilin-1 ko mice resulted in attenuated tumor growth in vivo. It was hypothesized that the inhibition of tumor growth could be a result of changes in tumor stroma composition, but not in tumor cells. TAM are important components of tumor stromal cells, which affect tumor progression in multiple ways[86]. Since TAM were reported to promote tumor progression of human breast cancer[82], the infiltration and phenotype of TAM in the TS/A tumor model was also investigated. CD68 was previously used as a pan-macrophage marker in a mouse TS/A mammary tumor model[68], so the positivity of CD68 staining imply the total amount of TAM. Tumors generated by injecting TS/A-EV and TS/A-SI-CLP cells into BALB/c wt and stabilin-1 ko mice were abundantly infiltrated by TAM (Figure 11A).

The positivity of CD68 protein was investigated in ten TS/A-EV tumors and eight TS/A-SI-CLP tumors generated in BALB/c wt mice from three independent tumor injection experiments. For each mouse, three consecutive sections were stained and quantified. In BALB/c wt mice, the positivity of CD68 in TS/A-EV tumors was 2.5 times higher than in TS/A-SI-CLP tumors (Figure 11B). In stabilin-1 ko mice, eight TS/A-EV tumors and eight TS/A-SI-CLP tumors were used to quantify the positivity of CD68 expression. Tumors generated by injecting TS/A-EV cells into stabilin-1 ko mice demonstrated a 1.84 times higher CD68 expression than tumors generated by injecting TS/A-SI-CLP cells into stabilin-1 ko mice (Figure 11B). There was no statistical difference between CD68 positivity in BALB/c wt and stabilin-1 ko mice injected with TS/A-SI-CLP cells, suggesting that the presence of stabilin-1 does not alter SI-CLP induced changes in TAM infiltration.
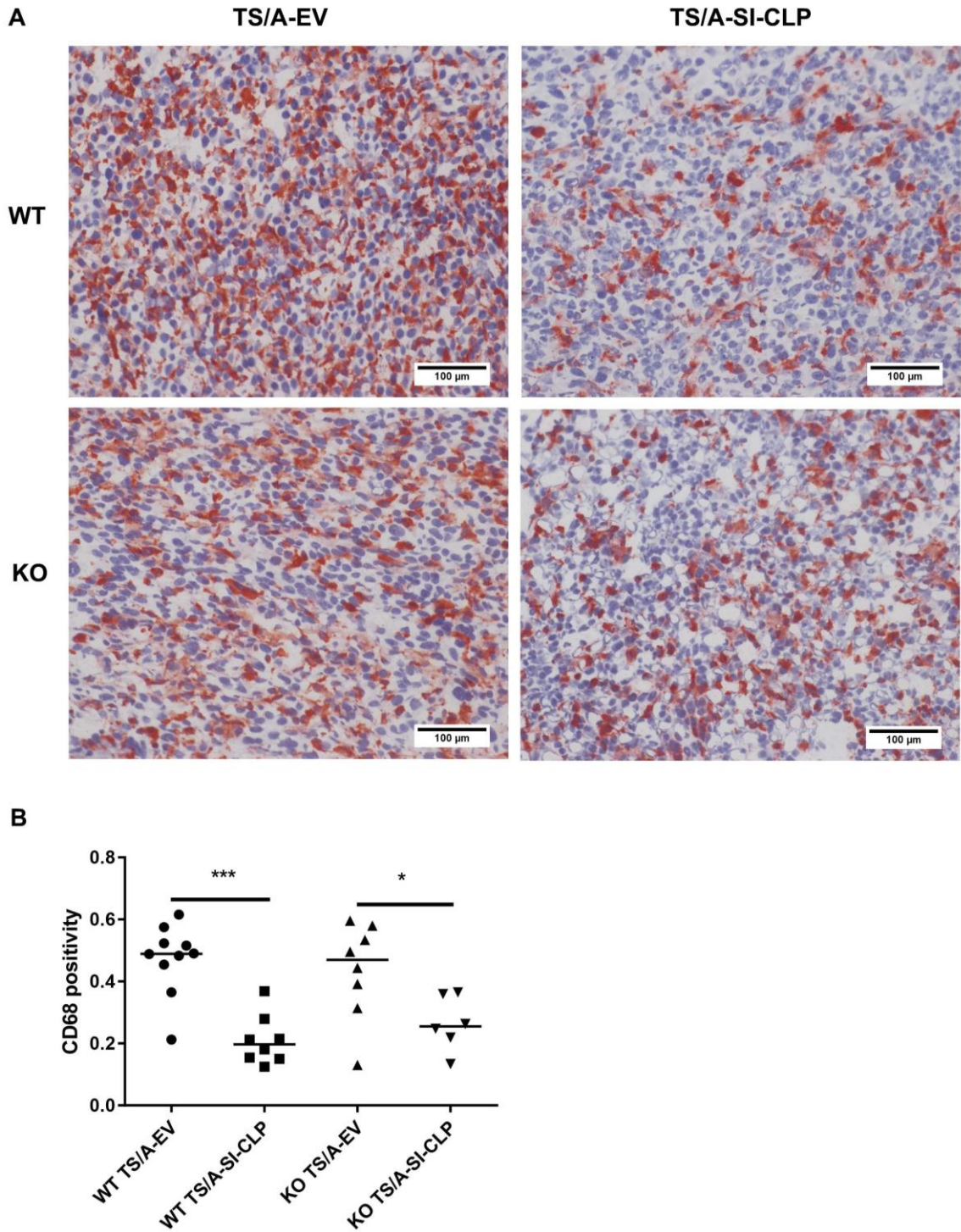
Figure 11. Quantitative analysis of CD68 expression in tumors generated by subcutaneous injection of TS/A-EV and TS/A-SI-CLP cells into BALB/c wt and stabilin-1 ko mice. (A) CD68 was visualised using rat anti-mouse CD68 antibody, scale bar: 100 μm. (B) Comparison of the positivity of CD68 protein in BALB/c wt and stabilin-1 ko mice injected with TS/A-EV or TS/A-SI-CLP cells. The Mann-Whitney test was used to compare the significance of difference between two groups, and data are presented as the median.

3.5 Comparison of other TAM markers in TS/A-EV and TS/A-SI-CLP tumors

Next, the expression of several polarization and activation markers of infiltrating TAM was analyzed in TS/A-SI-CLP and TS/A-EV tumors. CD206 is one of major markers for alternative activation of macrophages, and CD206 positive TAM are found to be proangiogenic[132]. CD206 was abundantly found in TS/A-EV and TS/A-SI-CLP tumor tissues (Figure 12A). The expression of CD206 protein in BALB/c wt mice was investigated in ten TS/A-EV and twelve TS/A-SI-CLP tumors obtained from three independent experiments. In BALB/c wt mice, the expression of CD206 protein in TS/A-EV tumors was 2.26 times higher than TS/A-SI-CLP tumors (Figure 12B). In stabilin-1 ko mice, CD206 expression was investigated in nine TS/A-EV and six TS/A-SI-CLP tumors. Tumors generated by injecting TS/A-EV cells into stabilin-1 ko mice demonstrated 1.68 times higher CD206 expression than tumors generated by injecting TS/A-SI-CLP cells (Figure 12B).

Lymphatic vessel endothelial hyaluronan receptor 1 (LYVE-1) was initially used as a marker of lymphatic endothelial cells, but its expression was also found in a subset of TAM in murine models of TS/A mammary carcinoma (Alexandru Gudima, Master thesis, 2013) and B16F1 melanoma tissues[133]. In TS/A tumors, LYVE-1 protein was rarely found in typical lymph vessel like structures, and was preferentially expressed by single cells that can be identified as macrophages by morphology (Figure 13A). The expression of LYVE-1 protein was investigated in eight wt mice injected with TS/A-EV cells and nine wt mice injected with TS/A-SI-CLP cells from three experiments. In BALB/c wt mice, the positivity of LYVE-1 protein in TS/A-EV tumors was 4 times higher than TS/A-SI-CLP cell tumors (Figure 13B). In stabilin-1 ko mice, LYVE-1 expression was investigated in six TS/A-EV and five TS/A-SI-CLP tumors. In stabilin-1 ko mice, tumors generated by injecting TS/A-EV cells demonstrated a 4.23 times higher LYVE-1 expression than tumors generated by injecting TS/A-SI-CLP cells (Figure 13B). Moreover, the difference of LYVE-1 expression between TS/A-EV and TS/A-SI-CLP tumors in both BALB/c wt and stabilin-1 ko mice was more pronounced compared to CD68 and CD206 markers.

Stabilin-1 is a multifunctional scavenger receptor expressed by TAM and demonstrates tumor-promoting effect in mouse mammary carcinoma and melanoma models[68,129]. The expression of stabilin-1 was compared in twelve BALB/c wt mice injected with TS/A-EV cells and fourteen BALB/c wt mice injected with TS/A-SI-CLP cells from three independent experiments. Stabilin-1 positive cells were abundant found in TS/A-EV and TS/A-SI-CLP

tumors (Figure 14A). Moreover, the positivity of stabilin-1 expression in TS/A-EV tumors was 2.18 times higher than that detected in TS/A-SI-CLP tumors (Figure 14B). As expected, stabilin-1 protein was not detectable in stabilin-1 ko mice (Figure 14A, lower panel).
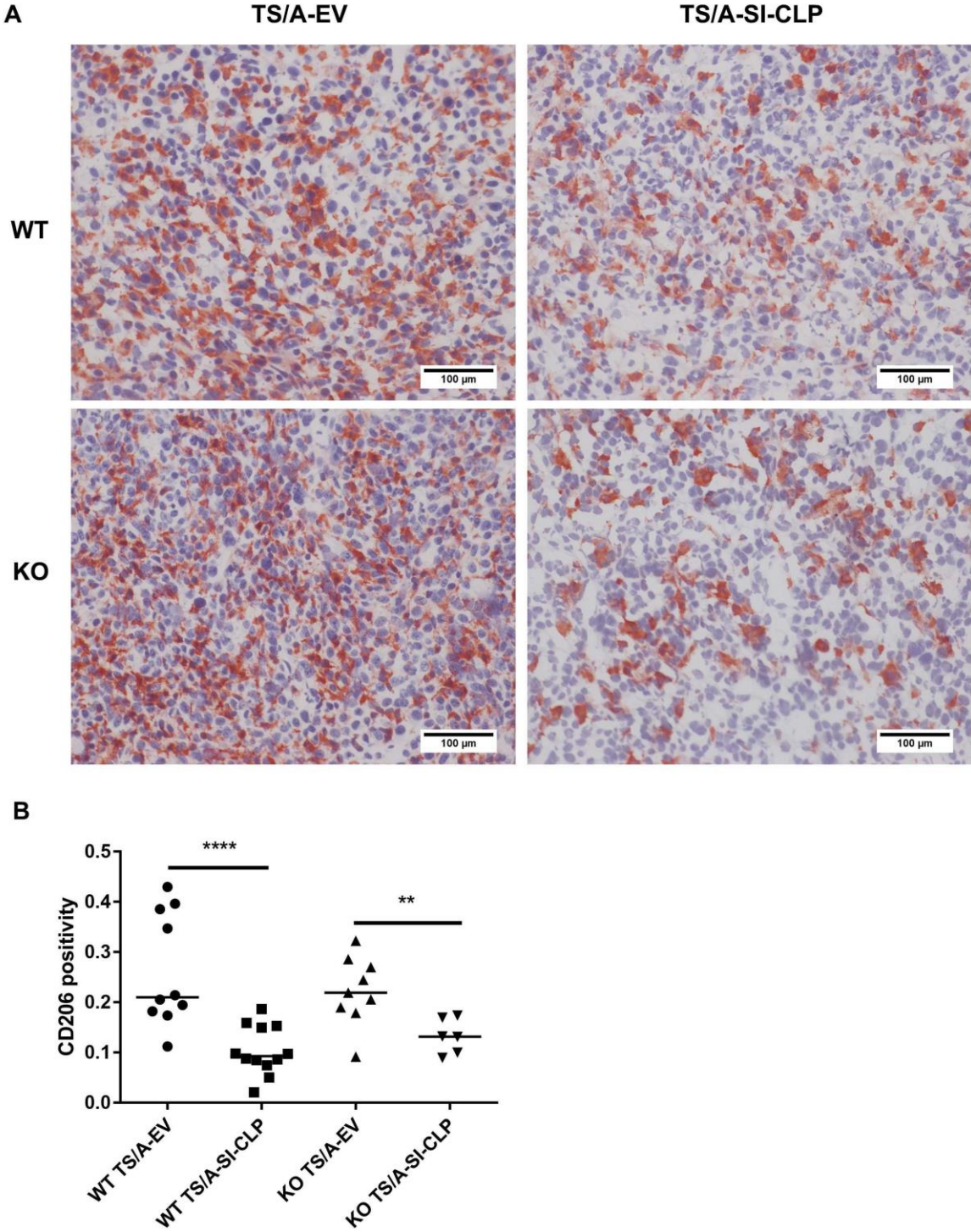
Figure 12. Quantitative analysis of CD206 expression in tumors generated by subcutaneous injection of TS/A-EV and TS/A-SI-CLP cells into BALB/c wt and stabilin-1 ko mice. (A) CD206 was visualised using rat anti-mouse CD206 antibody, scale bar: 100 μm. (B) Comparison of the positivity of CD206 protein in BALB/c wt and stabilin-1 ko mice injected with TS/A-EV or TS/A-SI-CLP cells. The Mann-Whitney test was used to compare the significance of difference between two groups, and data are presented as the median.
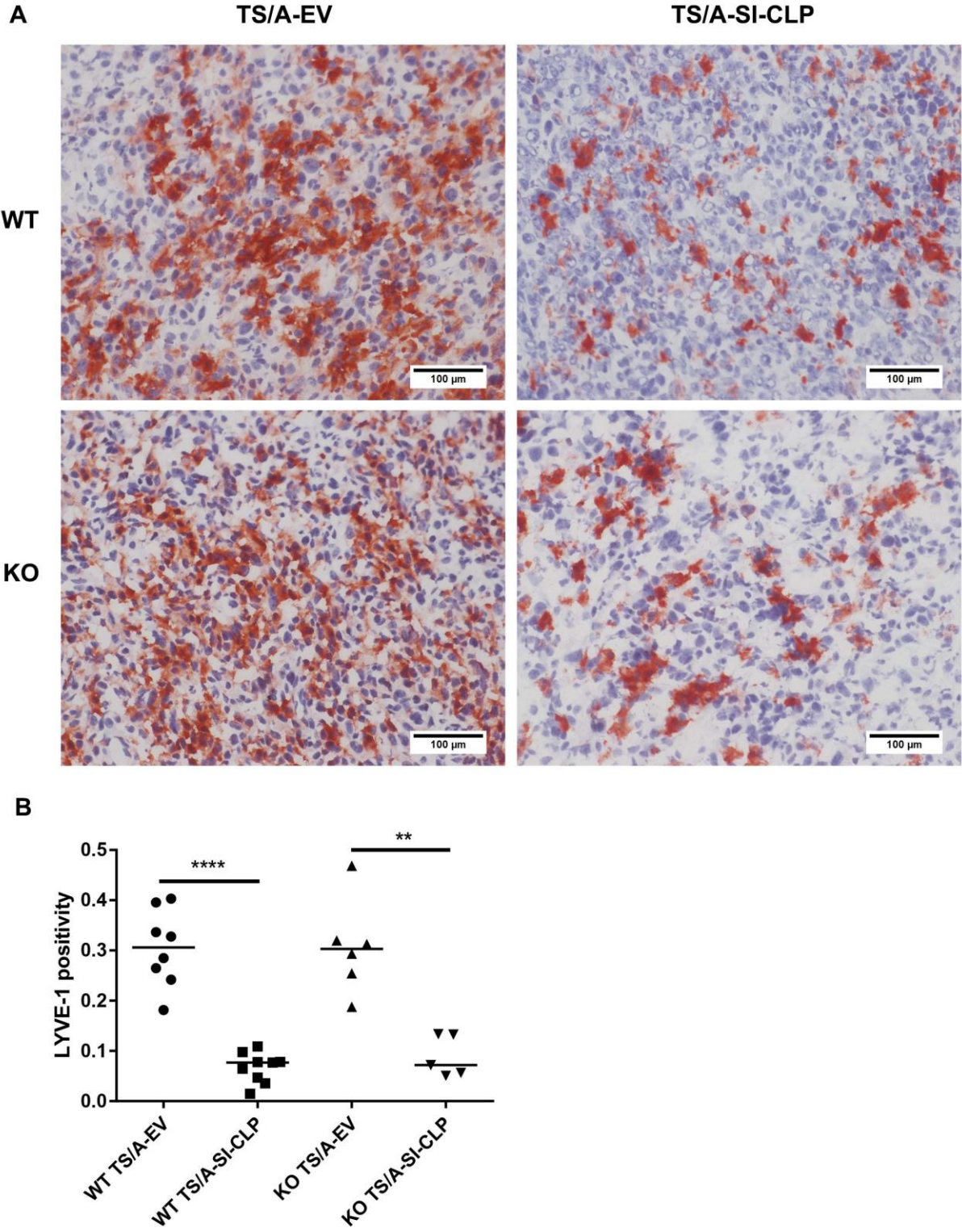
Figure 13. Quantitative analysis of LYVE-1 expression in tumors generated by subcutaneous injection of TS/A-EV and TS/A-SI-CLP cells into BALB/c wt and stabilin-1 ko mice. (A) LYVE-1 was visualised using biotin conjugated rabbit anti-mouse LYVE-1 antibody, scale bar: 100 µm. (B) Comparison of the positivity of LYVE-1 protein in BALB/c wt and stabilin-1 ko mice injected with TS/A-EV or TS/A-SI-CLP cells. The Mann-Whitney test was used to compare the significance of difference between two groups, and data are presented as the median.
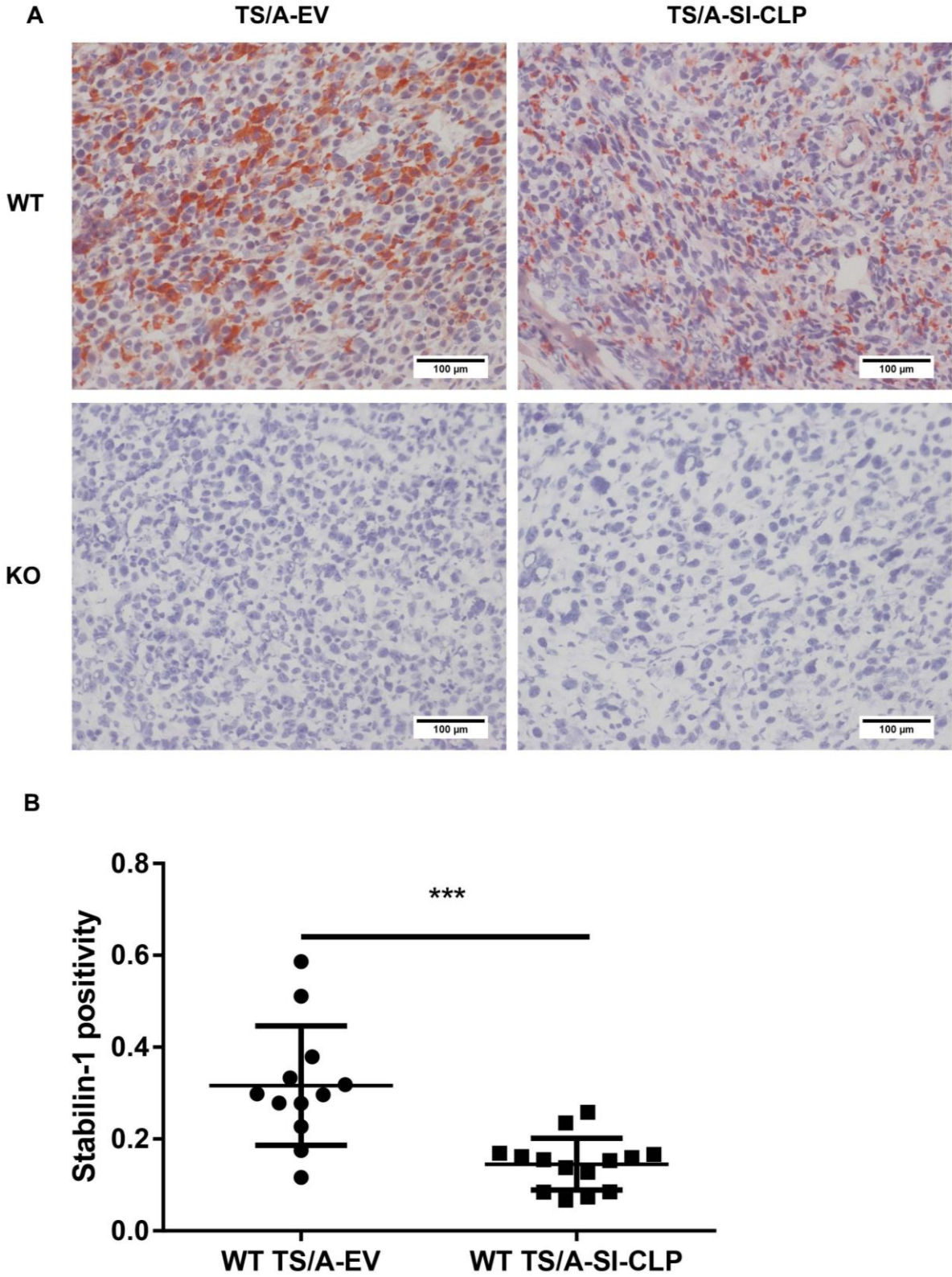
Figure 14. Quantitative analysis of stabilin-1 expression in tumors generated by subcutaneous injection of TS/A-EV and TS/A-SI-CLP cells into BALB/c wt and stabilin-1 ko mice. (A) Stabilin-1 was visualised using rabbit anti-stabilin-1 antibody (RS1), scale bar: 100 μm. (B) Comparison of the positivity of stabilin-1 protein in BALB/c wt mice injected with TS/A-EV or TS/A-SI-CLP cells. An unpaired t-test was used to compare the significance of difference, and data are presented as the mean ± SD.

3.6 Comparison of the expression of T cell markers in TS/A-EV and TS/A-SI-CLP tumors

T cells are important regulators of intratumoral immune reactions including tumor rejection and tumor tolerance. The infiltration of T cells in TS/A tumor models was investigated using antibody against CD3, a commonly used marker of T cells. In BALB/c wt mice, CD3 expression was investigated in twelve TS/A-EV tumors and thirteen TS/A-SI-CLP tumors from three independent experiments. CD3 positive cells were broadly found in TS/A-EV tumors, while much less CD3 positive cells were detected in TS/A-SI-CLP tumors (Figure 15A). In BALB/c wt mice the positivity of CD3 in TS/A-EV tumors was 2.74 times higher than that in TS/A-EV tumors (Figure 15B, P=0.0024), indicating reduced infiltration of T cells into TS/A-SI-CLP tumors. In stabilin-1 ko mice, CD3 expression was investigated in ten TS/A-EV and eight TS/A-SI-CLP tumors. Tumors generated by injecting TS/A-EV cells into stabilin-1 ko mice demonstrated 6 times higher CD3 expression than tumors generated by injecting TS/A-SI-CLP cells into stabilin-1 ko mice (Figure 15B). Moreover, CD3 positivity in BALB/c wt mice injected with TS/A-SI-CLP cells was significantly higher than that in stabilin-1 ko mice injected with TS/A-SI-CLP cells, which suggested the reduction of CD3 positive cells in TS/A-SI-CLP tumors was affected by the absence of stabilin-1 (P=0.0137).

Increased infiltration of CD8 positive T cells in human breast cancer tissue reduces the risk of death[134]. Therefore, we analyzed whether the presence of SI-CLP affects the amount of CD8 positive T cells in the tumor mass. CD8 expression in BALB/c wt mice was assessed in eight TS/A-EV tumors and eleven TS/A-SI-CLP tumors from three experiments. In stabilin-1 ko mice, the expression of CD8 protein was investigated in ten TS/A-EV tumors and five TS/A-SI-CLP tumors. In BALB/c wt mice, there was a tendency for reduced levels of CD8 in TS/A-SI-CLP tumors, while in stabilin-1 ko mice more CD8+ T cells were found in TS/A-SI-CLP tumors. Minor CD8 positive cells were found in TS/A-SI-CLP and TS/A-EV tumors (Figure 16A), while the amounts of CD8 positive T cells was not affected by SI-CLP presence (Figure 16B).
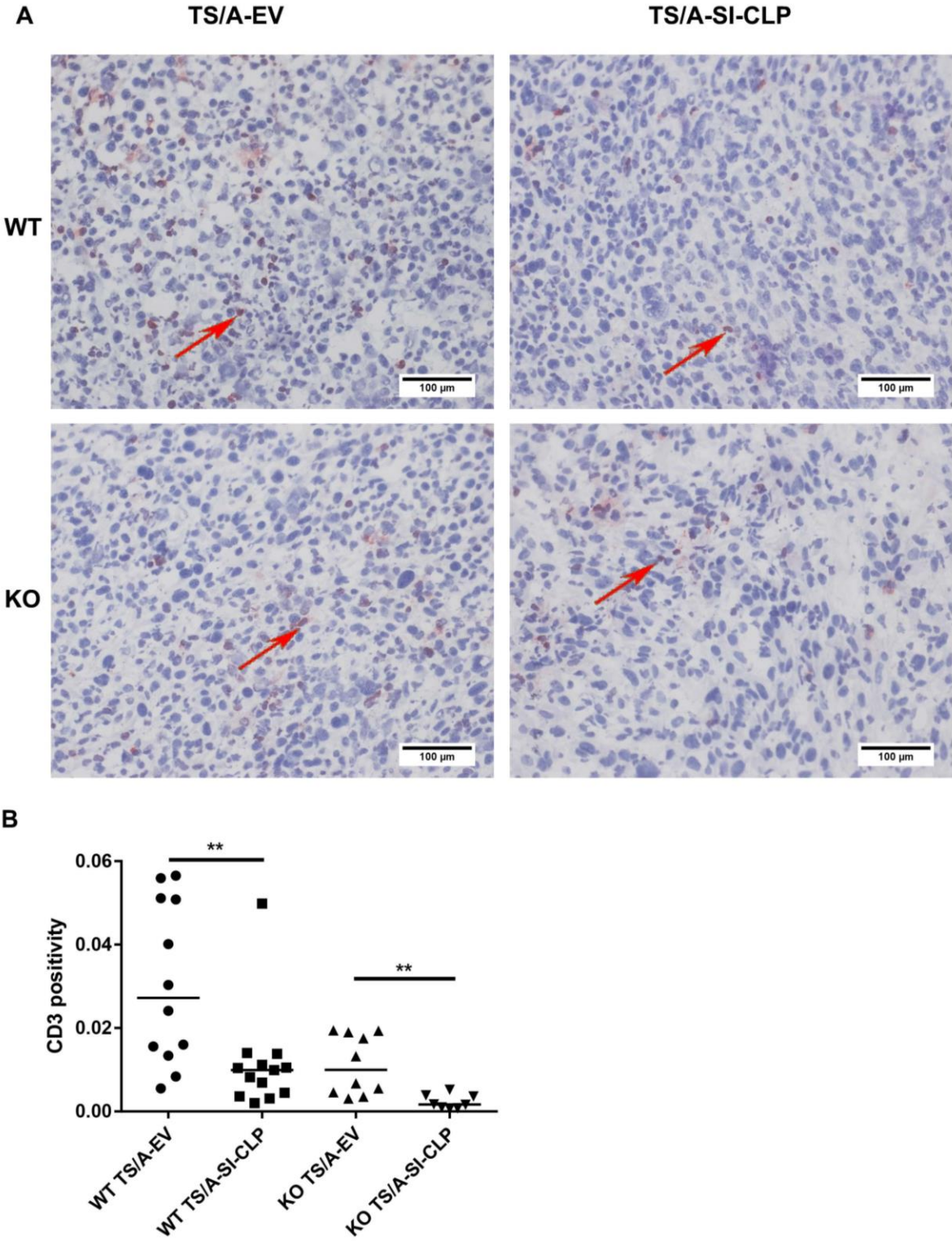
A

B

Figure 15. Quantitative analysis of CD3 expression in tumors generated by subcutaneous injection of TS/A-EV and TS/A-SI-CLP cells into BALB/c wt and stabilin-1 ko mice. (A) CD3 expression was visualized using rat anti-mouse CD3 antibody, scale bar: 100 µm. Red arrows indicate CD3 positive cell. (B) Comparison of the positivity of CD3 protein in BALB/c wt and stabilin-1 ko mice injected with TS/A-EV or TS/A-SI-CLP cells. The Mann-Whitney test was used to compare the significance of difference between two groups, and data are presented as the median.

A

B

Figure 16. Quantitative analysis of CD8 expression in tumors generated by subcutaneous injection of TS/A-EV and TS/A-SI-CLP cells into BALB/c wt and stabilin-1 ko mice. (A) CD8 expression was visualized using rat anti-mouse CD8 antibody, scale bar: 100 μm. (B) Comparison of the positivity of CD8 protein in BALB/c wt and stabilin-1 ko mice injected with TS/A-EV or TS/A-SI-CLP cells. The Mann-Whitney test was used to compare the significance of difference between two groups, and data are presented as the median. NS indicates no statistical significance.

Next, the expression of CD4 (marker of helper T cells) was analyzed. CD4 positive helper T cells suppress tumor immunity by enhancing the function of regulatory T cells[135]. In BALB/c wt mice, the expression of CD4 protein was investigated in twelve TS/A-SI-CLP tumors and ten TS/A-EV tumors from three experiments. In stabili-1 ko mice, the expression of CD4 protein was investigated in nine TS/A-SI-CLP tumors and eight TS/A-EV tumors from three experiments. CD4 expression in TS/A-EV tumors was strong while only single CD4 positive cells were found in TS/A-SI-CLP tumors (Figure 17A). The difference of CD4 expression between TS/A-EV and TS/A-SI-CLP tumors reached 2.25 times in BALB/c wt mice, while the reduction of CD4 expression in TS/A-SI-CLP tumors was 1.9 times in stabilin-1 ko mice (Figure 17B).

A subpopulation of CD4 positive T cells in tumors is known to express transcription factor FoxP3 which specifically marks regulatory T cells (Treg), known to suppress anti-tumor immunity in breast cancer[136]. The expression of FoxP3 protein in BALB/c wt mice was investigated in seven TS/A-EV tumors and nine TS/A-SI-CLP tumors from three experiments. In stabilin-1 ko mice, FoxP3 expression was investigated in seven TS/A-EV tumors and four TS/A-SI-CLP tumors from three experiments. Positive FoxP3 staining was visualized as a red dot in the nuclear area of cells (Figure 18A), and 10 images were taken for each tumor tissue stained with FoxP3 protein under light microscope equipped with a 20x objective. FoxP3 positive cells were counted with ImageJ software, and the mean positive cells were calculated by averaging all FoxP3 positive cells in ten images. In BALB/c wt mice FoxP3 positive Treg cells detected in TS/A-EV tumors were 2.55 times higher than that in TS/A-SI-CLP tumors, while in stabilin-1 ko mice the reduction of FoxP3 positive Treg cells was not significant (Figure 18B, P=0.2939).

PD-1 is a type I membrane receptor specifically expressed by T cells and pro-B cells. The binding of PD-1 with its specific ligands PD-L1 and PD-L2 leads to the apoptosis or deactivation of effector T cells[137]. The application of anti-PD-1 monoclonal antibody in human melanoma patients enhanced the effectiveness of specific T cells killing and prolonged overall survival[138]. The application of anti-PD-1 single agent in patients with advanced triple negative breast cancer was also reported, but the clinical trial results still have to be obtained[139]. In BALB/c wt mice, the expression of PD-1 protein was investigated in seven TS/A-EV tumors and five TS/A-SI-CLP tumors from three experiments. In stabilin-1 ko mice, PD-1 expression was investigated in six TS/A-SI-CLP tumors and five TS/A-EV tumors from three experiments. In BALB/c wt mice, PD-1 positivity in TS/A-EV tumors was 2.2 times

higher than in TS/A-SI-CLP tumors, while the reduction on PD-1 in TS/A-SI-CLP tumors reached 3.8 times in stabilin-1 ko mice (Figure 19).
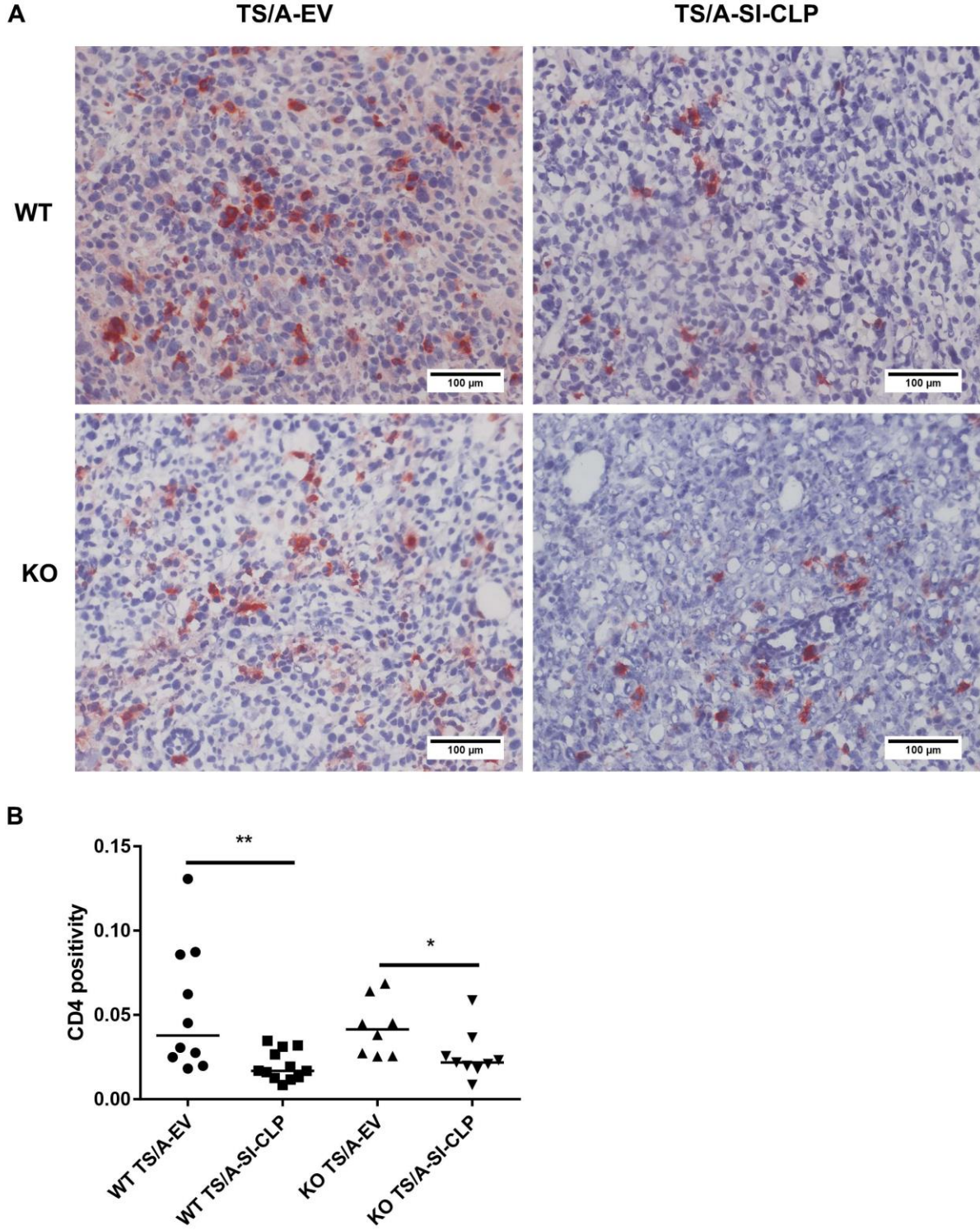
Figure 17. Quantitative analysis of CD4 expression in tumors generated by subcutaneous injection of TS/A-EV and TS/A-SI-CLP cells into BALB/c wt and stabilin-1 ko mice. (A) CD4 expression was visualized using biotin conjugated rat anti-mouse CD4, scale bar: 100 μm. (B) Comparison of the positivity of CD4 protein in BALB/c wt and stabilin-1 ko mice injected with TS/A-EV or TS/A-SI-CLP cells. The Mann-Whitney test was used to compare the significance of difference between two groups, and data are presented as the median.
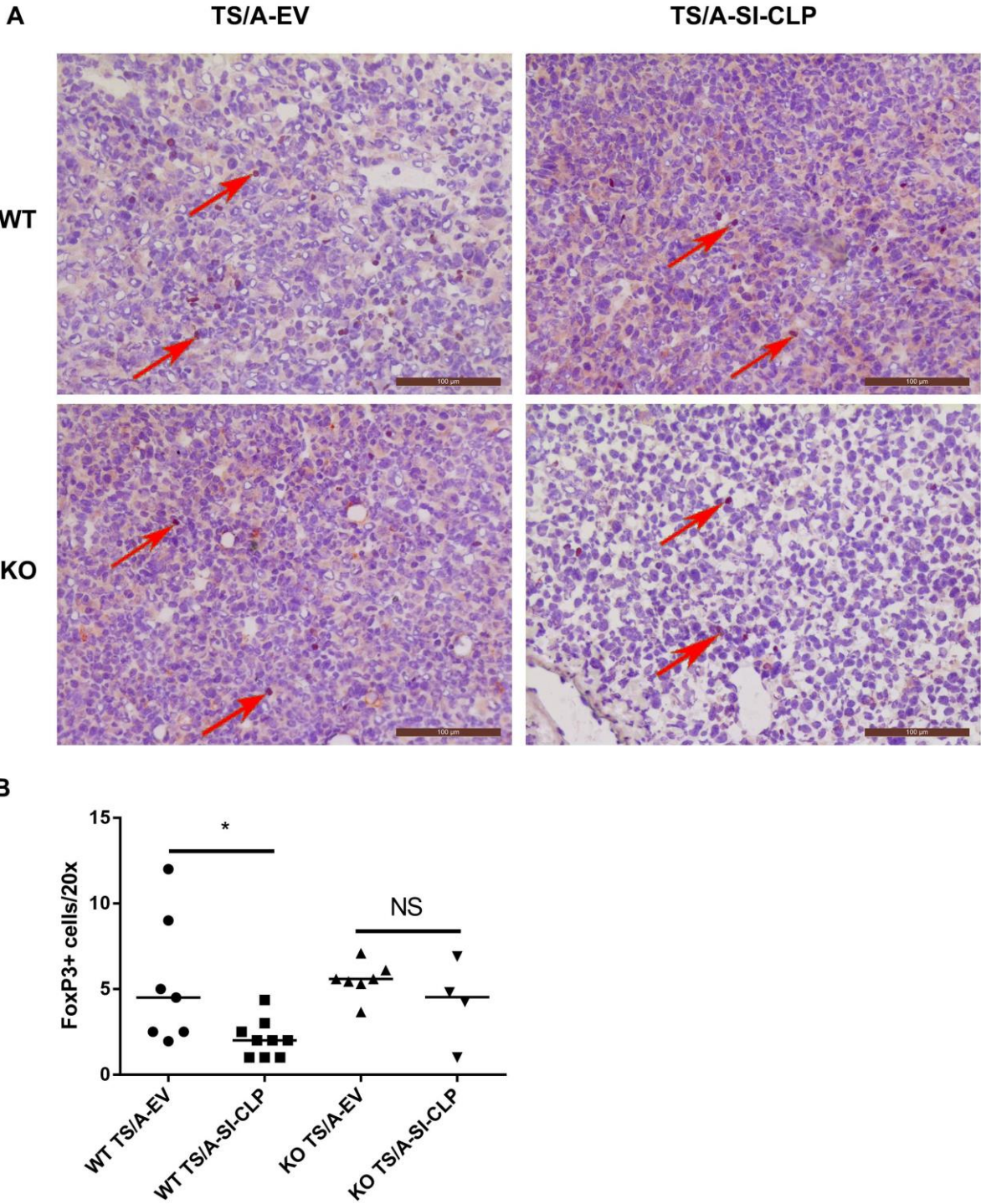
Figure 18. Quantitative analysis of FoxP3 expression in tumors generated by subcutaneous injection of TS/A-EV and TS/A-SI-CLP cells into BALB/c wt and stabilin-1 ko mice. (A) FoxP3 expression was visualized using biotin conjugated rat anti-mouse FoxP3, scale bar: 100 μm. Red arrows indicate FoxP3 positive cell. (B) Comparison of the amount of FoxP3 positive cells in BALB/c wt and stabilin-1 ko mice injected with TS/A-EV or TS/A-SI-CLP cells. The Mann-Whitney test was used to compare the significance of difference between two groups, and data are presented as the median. NS indicates no statistical significance.
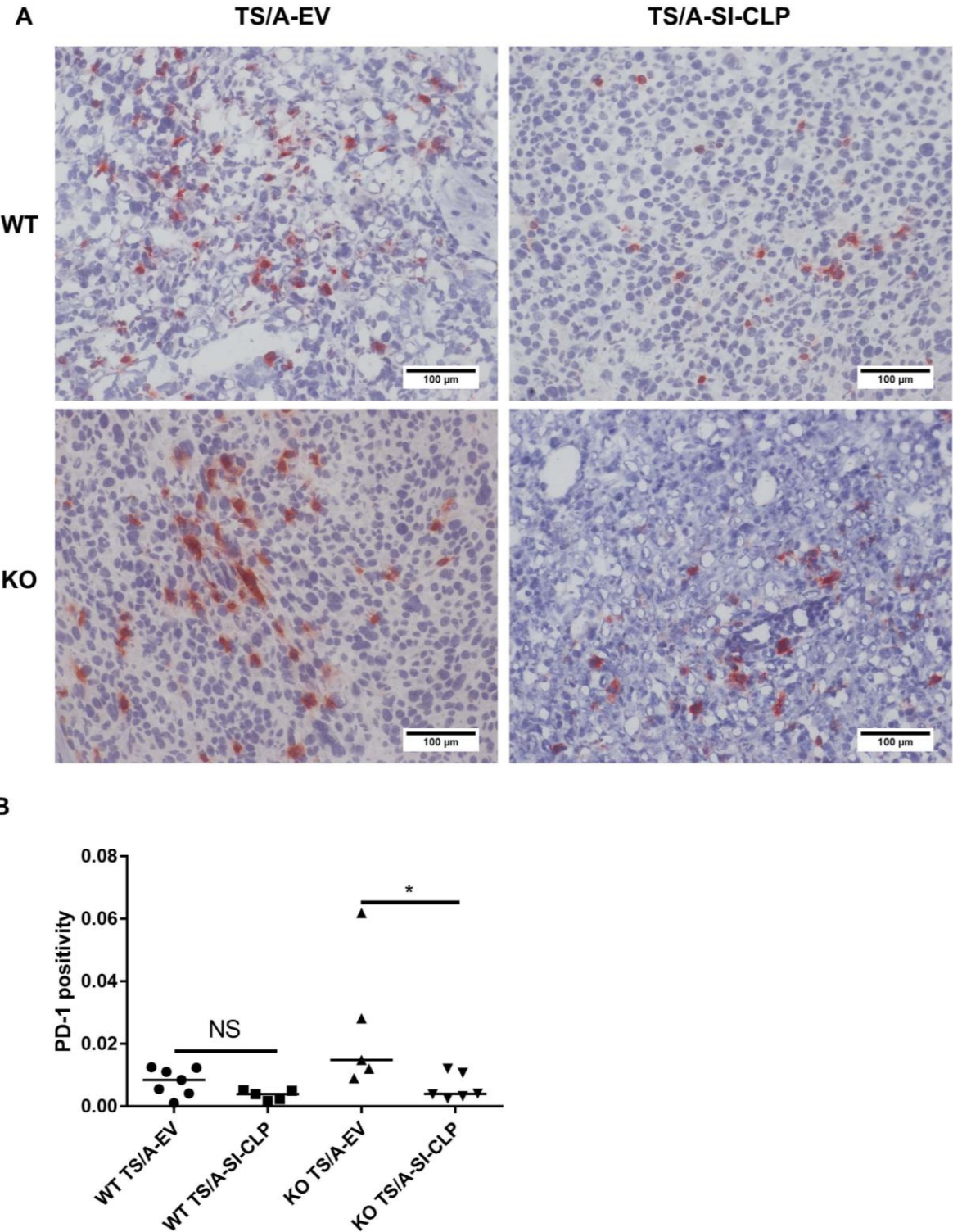
Figure 19. Quantitative analysis of PD-1 expression in tumors generated by subcutaneous injection of TS/A-EV and TS/A-SI-CLP cells into BALB/c wt and stabilin-1 ko mice. (A) PD-1 expression was visualized using goat anti-mouse PD-1 antibody, scale bar: 100 μm. (B) Comparison of the positivity of PD-1 protein in BALB/c wt and stabilin-1 ko mice injected with TS/A-EV or TS/A-SI-CLP cells. The Mann-Whitney test was used to compare the significance of difference between two groups, and data are presented as the median. NS indicates no statistical significance.

3.7 Comparison of other infiltrating immune cells in TS/A-EV and TS/A-SI-CLP tumors

Eosinophils are considered as bystander cells in anti-tumor immunity, but their role in tumor rejection through recruitment of CD8+ T cells has recently been revealed[140]. YM1, one of the chitinase-like proteins, exerts eosinophil chemotactic activity in vivo and in vitro. Thus, it was examined whether SI-CLP expression affected eosinophil infiltration in TS/A-SI-CLP tumors raised in BALB/c wt and stabilin-1 ko mice. Eosinophils were specifically detected using antibodies against Siglec-F protein, and most of eosinophils were localized on the periphery of the tumor mass (Figure 20A). In BALB/c wt mice, the expression of Siglec-F protein was investigated in eleven TS/A-EV tumors and nine TS/A-SI-CLP tumors from three experiments. In stabilin-1 ko mice, Siglec-F expression was investigated in eight TS/A-EV tumors and six TS/A-SI-CLP tumors from three experiments. The expression of the Siglec-F protein in TS/A-EV and TS/A-SI-CLP tumors was not significantly changed, which indicates that the infiltration of eosinophils was not affected by SI-CLP directly (Figure 20B).

The role of neutrophils in tumor progression is controversial[141]. An increased number of neutrophils in breast cancer was reported to facilitate tumor metastasis[142], while in another murine model using 4T1 cells more neutrophils in the orthotopic engrafted tumor inhibited the primary tumor growth and lung metastasis[143]. Neutrophils were detected using antibodies against Gr-1 protein, which was abundantly found in TS/A tumor tissue (Figure 21A). In BALB/c wt mice the amounts of neutrophils were compared in seven TS/A-EV tumors and eight TS/A-SI-CLP tumors, and it was found to be unaltered (Figure 21B). In stabilin-1 ko mice, the amount of neutrophils was investigated in six TS/A-EV tumors and four TS/A-SI-CLP tumors. Similarly, there was no significant difference in neutrophil infiltration (Figure 21B).
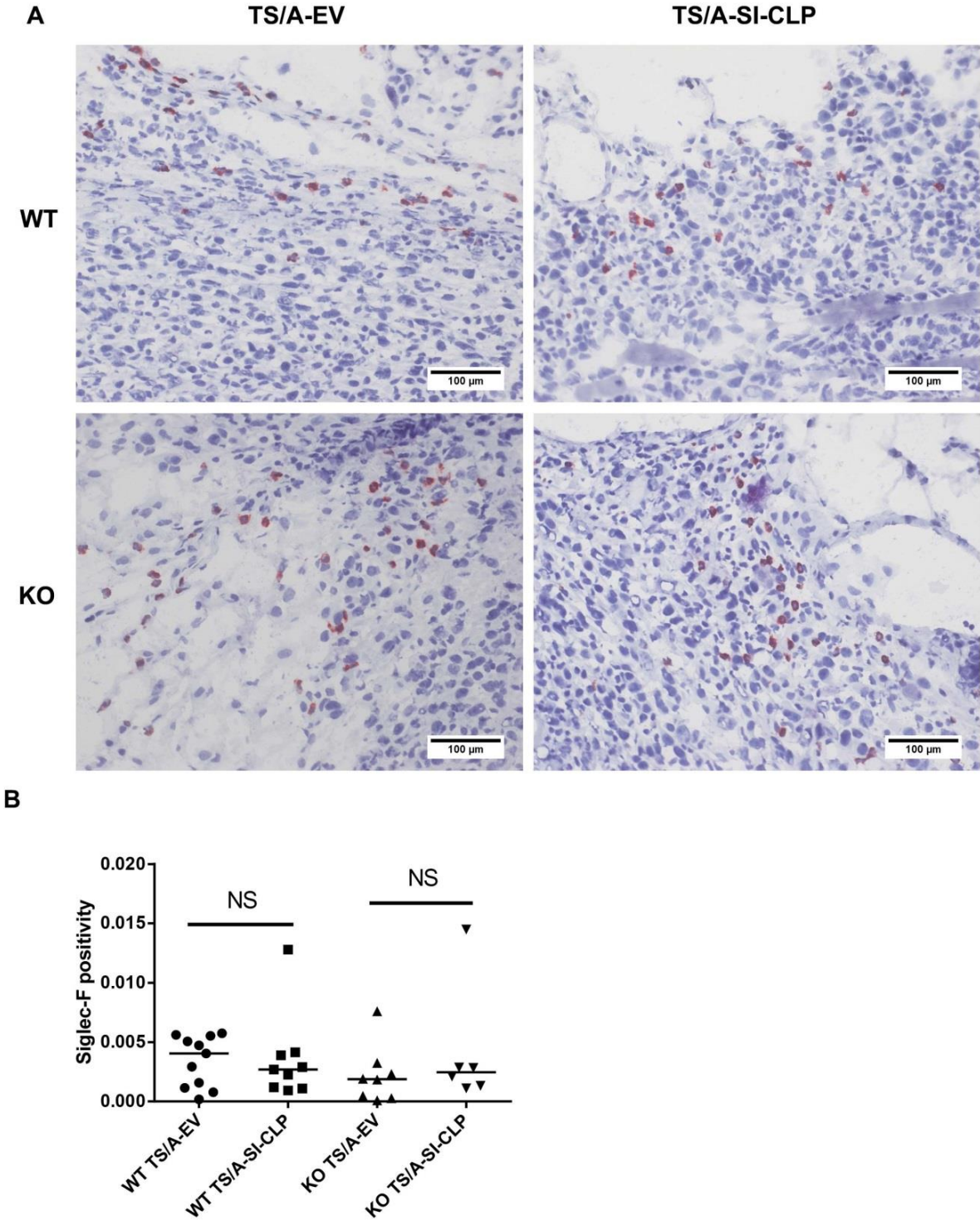
Figure 20. Quantitative analysis of Siglec-F expression in tumors generated by subcutaneous injection of TS/A-EV and TS/A-SI-CLP cells into BALB/c wt and stabilin-1 ko mice. (A) Siglec-F expression was visualized using rat anti-mouse Siglec-F, scale bar: 100 µm. (B) Comparison of the positivity of Siglec-F protein in BALB/c wt and stabilin-1 ko mice injected with TS/A-EV or TS/A-SI-CLP cells. The Mann-Whitney test was used to compare the significance of difference between two groups, and data are presented as the median. NS indicates no statistical significance.
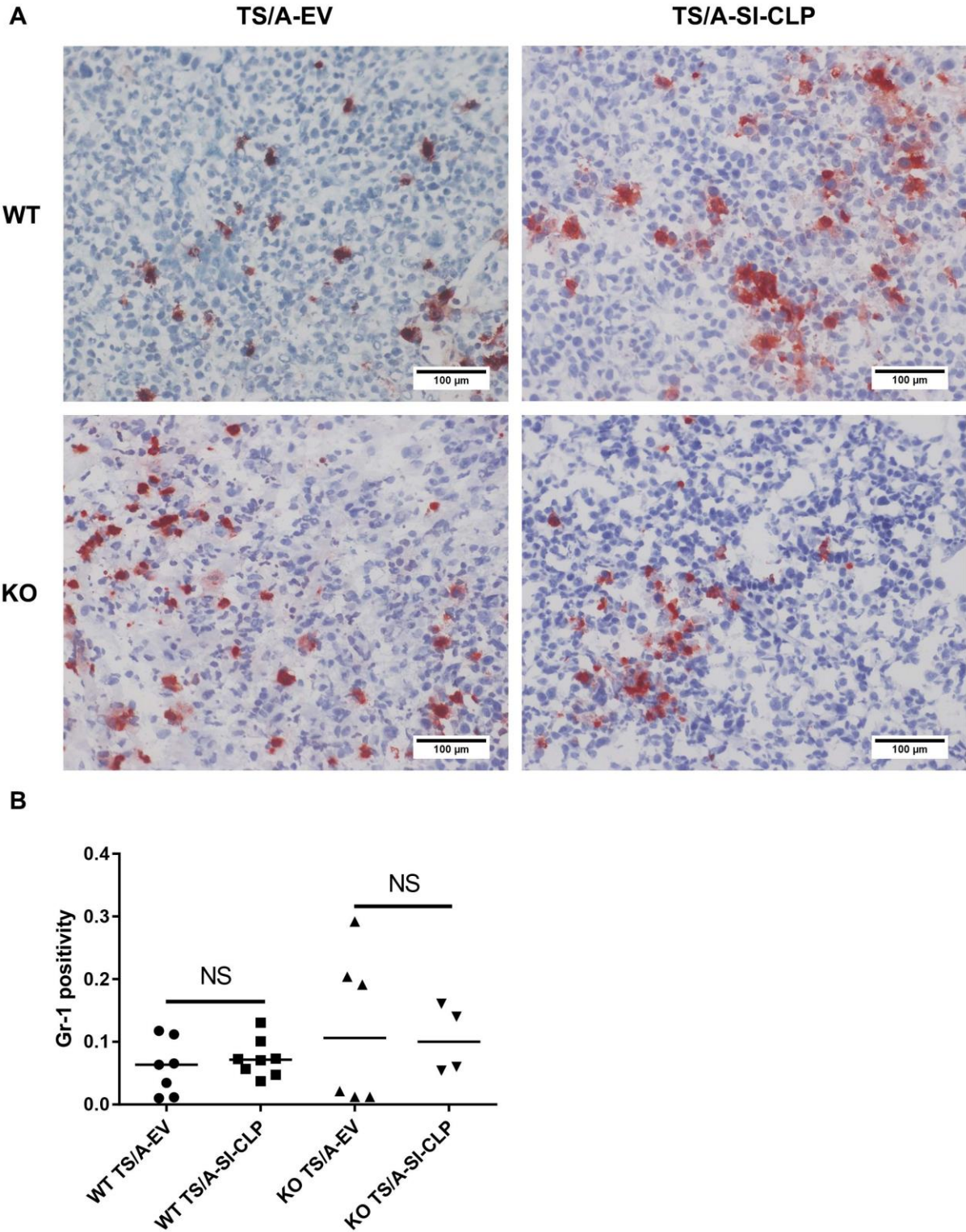
Figure 21. Quantitative analysis of Gr-1 expression in tumors generated by subcutaneous injection of TS/A-EV and TS/A-SI-CLP cells into BALB/c wt and stabilin-1 ko mice. (A) Gr-1 expression was visualized using rat anti-mouse Ly6G antibody, scale bar: 100 μm. (B) Comparison of the positivity of Gr-1 protein in BALB/c wt and stabilin-1 ko mice injected with TS/A-EV or TS/A-SI-CLP cells. The Mann-Whitney test was used to compare the significance of difference between two groups, and data are presented as the median. NS indicates no statistical significance.

3.8 SI-CLP inhibits chemotaxis of murine bone marrow derived macrophages

Since the infiltration of macrophages was inhibited in TS/A-SI-CLP tumors, it was hypothesized that SI-CLP may directly affect macrophage chemotaxis. To test this hypothesis, mouse bone marrow cells were isolated from BALB/c mice and differentiated into macrophages in DMEM medium supplemented with M-CSF for four days. Next, 100 ng/ml of purified murine SI-CLP protein from HEK-293 cells (CUSABIO, China) was incubated with murine bone marrow derived macrophages (BMDM) for 30 min followed by assessment of chemotaxis in response to 100 ng/ml of murine CCL2 protein for 3 h. Each experiment was performed in triplicates, and three mice were used in three independent experiments. 10 random images were taken for each Transwell under fluorescence microscope equipped with a 32x objective, and migrated cells on the lower side of membrane were visualized by DAPI staining. The chemotaxis of BMDM was inhibited after incubation with 100 ng/ml of purified SI-CLP protein for 30 min (Figure 22).

Next, the specific effect of SI-CLP on macrophage migration was confirmed using mouse SI-CLP containing supernatants derived from alphavirus infected BHK-21 cells (provided by Dr. Anna Zajakina, Department of Protein Engineering, Biomedical Research and Study center, Riga, Latvia). SI-CLP containing supernatant (2,5 µl, 5µl, 10 µl and 20µl) from BHK-21 recSFV1/murine SI-CLP cells or control (SI-CLP negative) supernatant of recSFV1/Luc transfected cells were added to $1X10^6$ BMDM suspended in 1 ml of DMEM medium. After 16 hours of incubation at 37°C, BMDM were harvested and diluted in DMEM medium at $5X10^6$/ml. $5X10^5$ BMDM in 100 µl of DMEM medium was seeded in the top well and murine CCL2 was added to the lower chamber as a chemotactic factor. The migration assay was performed in response to CCL2 for 3 h. The migration of BMDM was significantly inhibited after pre-incubation with SI-CLP containing supernatant for all amounts of supernatants used (Figure 23A). Further, to demonstrate the specific effect of SI-CLP on BMDM migration, SI-CLP protein was depleted from supernatants by immunoprecipitation using rat anti-SI-CLP antibody 1B8 immobilized on the protein G beads. Empty protein G bead and beads with immobilized rat IgG were used as a control (Figure 23B). Intact SI-CLP containing supernatant and SI-CLP depleted supernatant from BHK-21 recSFV1/ murine SI-CLP were added to $1X10^6$ BMDM. BMDM were harvested 16 h later and used for the chemotaxis assay. The results showed that the depletion of SI-CLP from BHK-21 recSFV1/

murine SI-CLP supernatant abrogated the inhibitory effect of BHK-21 recSFV1/ murine SI-CLP supernatant on chemotaxis of BMDM (Figure 23C).
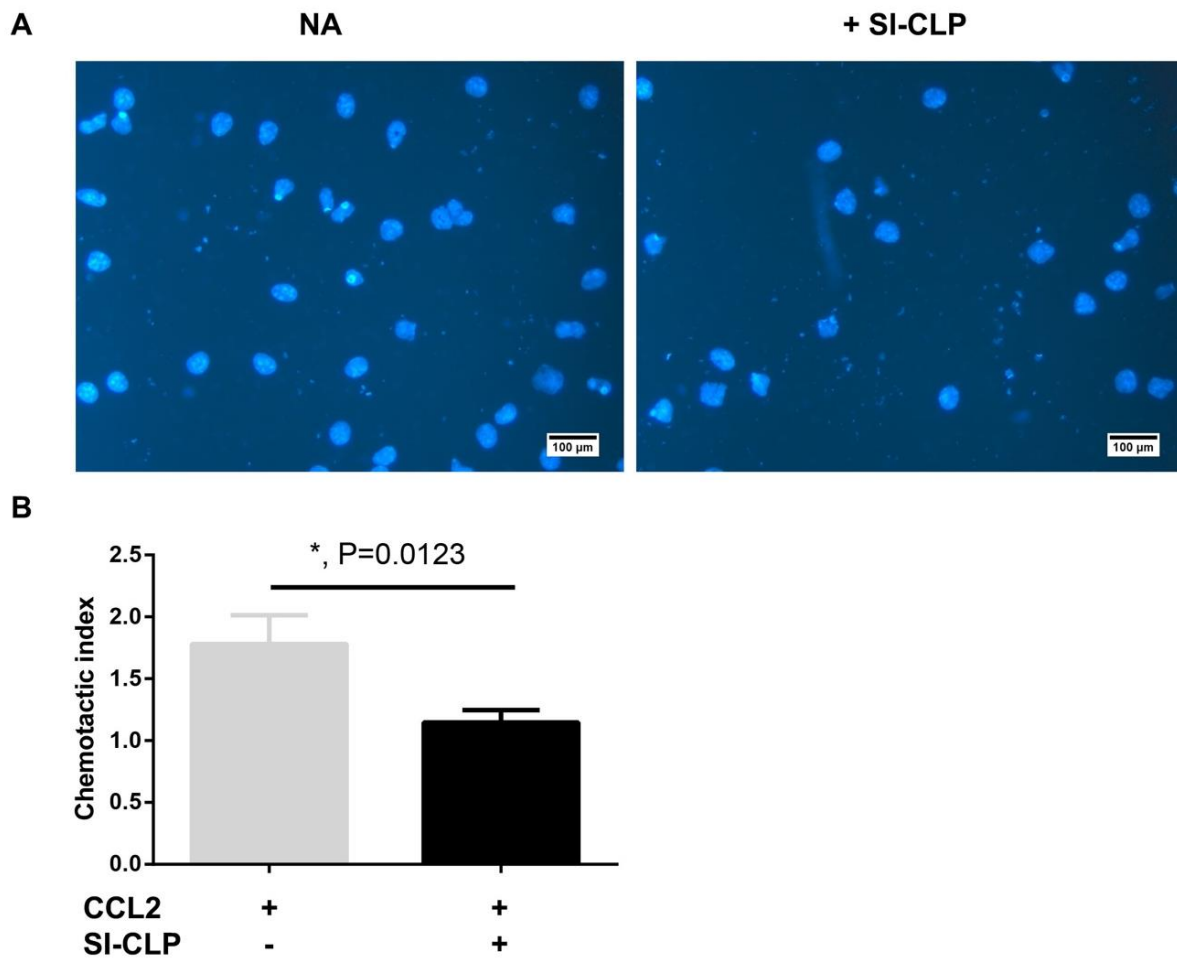
Figure 22. The effect of SI-CLP on the chemotaxis of murine BMDM. (A) Migrated cells on the lower side of membrane were fixed and visualized by DAPI staining, scale bar: 100 µm. (B) Comparison of chemotactic index in BMDM treated with or without SI-CLP protein. An unpaired t-test was used to compare the significance of difference, and data are presented as mean, n=3.
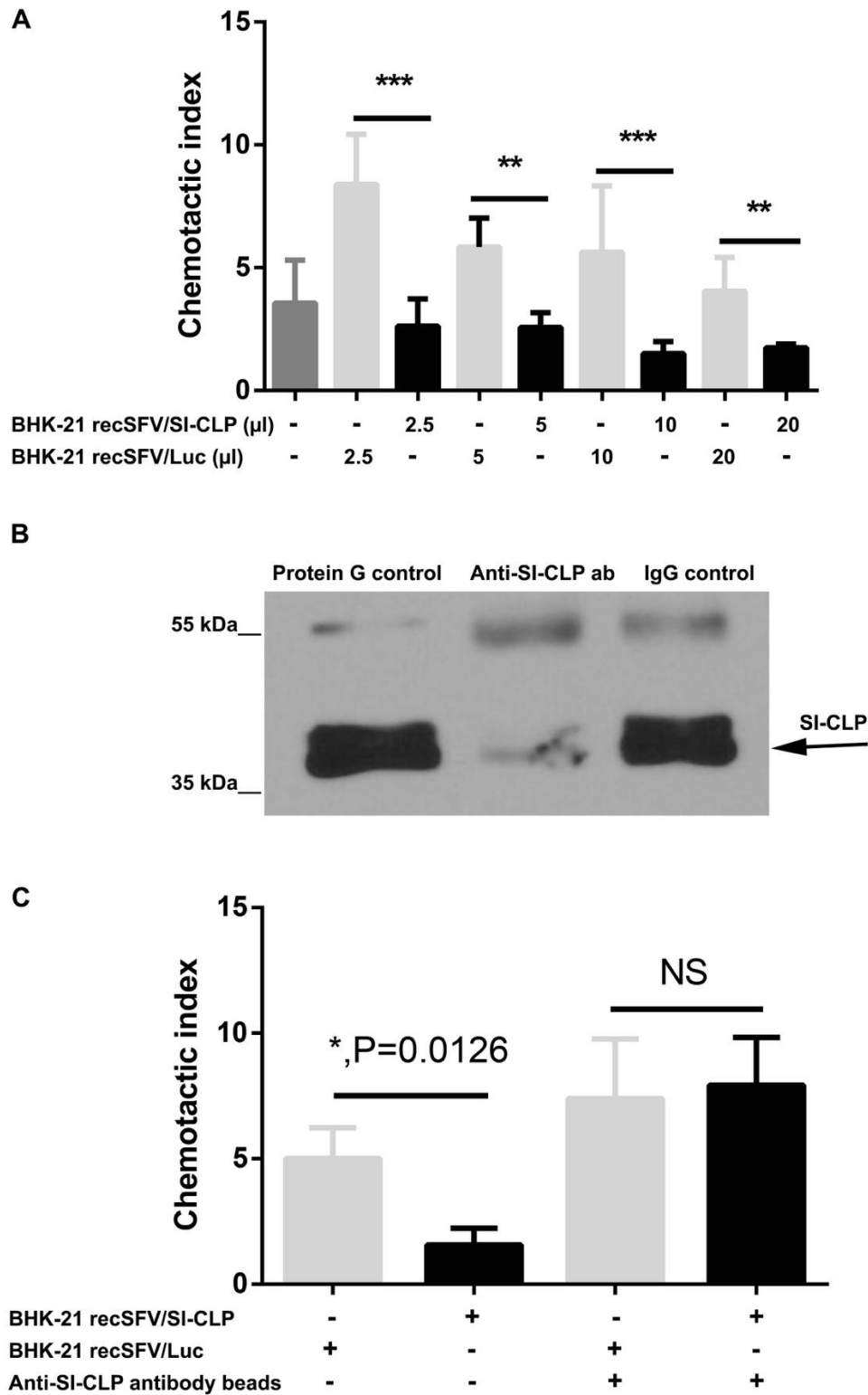
Figure 23. The effect of SI-CLP containing supernatant on chemotaxis of murine BMDM. (A) Comparison of the chemotactic index of BMDMs incubated with BHK-21 recSFV/Luc or BHK-21 recSFV/SI-CLP conditioned supernatant. (B) Western blot image demonstrating depletion of SI-CLP from BHK-21 recSFV/SI-CLP conditioned supernatant after Protein G Sepharose beads conjugated with anti-SI-CLP antibody were added. Protein G Sepharose beads and Protein G Sepharose beads conjugated with rat IgG antibody were used as control. (C) The chemotaxis of murine BMDM after incubation with intact and SI-CLP depleted supernatant of BHK-21 recSFV/SI-CLP. An unpaired t-test was used to compare the significance of difference, and data are presented as the mean ± SD.

Thus, mouse SI-CLP (both commercial recombinant purified as well as alphavirus-derived) demonstrated a clear inhibitory effect on the CCL2-induced chemotaxis of murine BMDM. Therefore, the next question was to analyze whether SI-CLP has inhibitory effect on human monocytes. Freshly isolated CD14+ human monocytes were incubated with 100 ng/ml of recombinant purified human SI-CLP protein produced in HEK-293 cells (CUSABIO, China). Incubation was performed in macrophage SFM medium for 16 h at 37°C. After incubation with SI-CLP, monocytes were harvested and re-suspended in SFM medium at $5X10^6$/ml. Monocytes (100 μl, total amount of $5X10^5$ cells) were placed on the top well of a 5 μm Transwell, and the chemotaxis assay was performed in response to 100 ng/ml human CCL2 protein added to the lower chamber for 3 h. The chemotaxis assay for monocytes derived from each individual donor was performed in triplicates, and five independent donors were used in the assay. Migrated monocytes were found on the lower side of the membrane and in the lower chamber. The representative images of migrated monocytes on the membrane with or without SI-CLP incubation are shown on Figure 24A. Inhibited chemotaxis of human CD14+ monocytes in response to CCL2 was observed in four of five individual donors (BC906-03, BC910-03, BC915-01 and BC915-02) and chemotaxis of the donor BC915-03 was not affected by SI-CLP (Figure 24B). The level of SI-CLP mediated inhibition of monocytes migration was individual for monocyte isolated from individual donors, which is consistence with the study demonstrating donors-specific monocyte reactions to the spectrum of stimuli[144]. The strongest effect was observed for the BC 910-03 (Figure 24).

Figure 24. Effect of SI-CLP on the chemotaxis of human peripheral blood derived CD14+ monocytes. (A) Representative pictures of migrated CD14+ human monocytes on the lower side of membrane with or without SI-CLP incubation, scale bar: 100 μm. (B) Comparison of the chemotactic index of CD14+ human monocytes with or without SI-CLP protein incubation on the membrane (left panel) and in the lower chamber (right panel). Unique code number of individual donors is indicated, and the mean chemotactic index of each donor are presented.

3.9   SI-CLP does not affect the chemotaxis of naive T cells

Since the total amount of CD3 positive cells in TS/A-SI-CLP tumors was decreased compared to that in TS/A-EV tumors, we investigated whether SI-CLP directly affected the chemotaxis of T cells. Naive T cells were isolated from spleen tissue of BALB/c wt mice, and the purity of T cells used in the chemotaxis assay was over 95%. The SSC-A and FSC-A parameters were adjusted to gate all live cells (Figure 25A), and the purity of naive T cells was analyzed using APC conjugated rat anti-mouse CD3 antibody (Figure 25B). Isolated T cells were maintained in RPMI medium for 4 h before performing chemotaxis. 100 ng/ml purified murine SI-CLP protein was added to the T cells, which were harvested 30 min later for performing chemotaxis in response to purified murine CCL19 protein. 5×10^5 naive T cells in 100 μl of RPMI medium were seeded in the top well of a 5 μm Transwell, and 100 ng/ml

of CCL19 were added into the lower chamber as a chemotactic factor. The migration was performed at 37°C, in a 5% CO_2 incubator for 3 h. The migrated cells in the lower chamber were collected and counted by a cell counter (CASY Model TT). No cells were detected on the lower side of the membrane. Statistical analysis revealed that SI-CLP did not affect the chemotaxis of naive T cells either in steady state conditions or in response to CCL19 (Figure 25C). Prolonged incubation time with SI-CLP also did not affect the chemotaxis of naive T cells (Figure 25D).
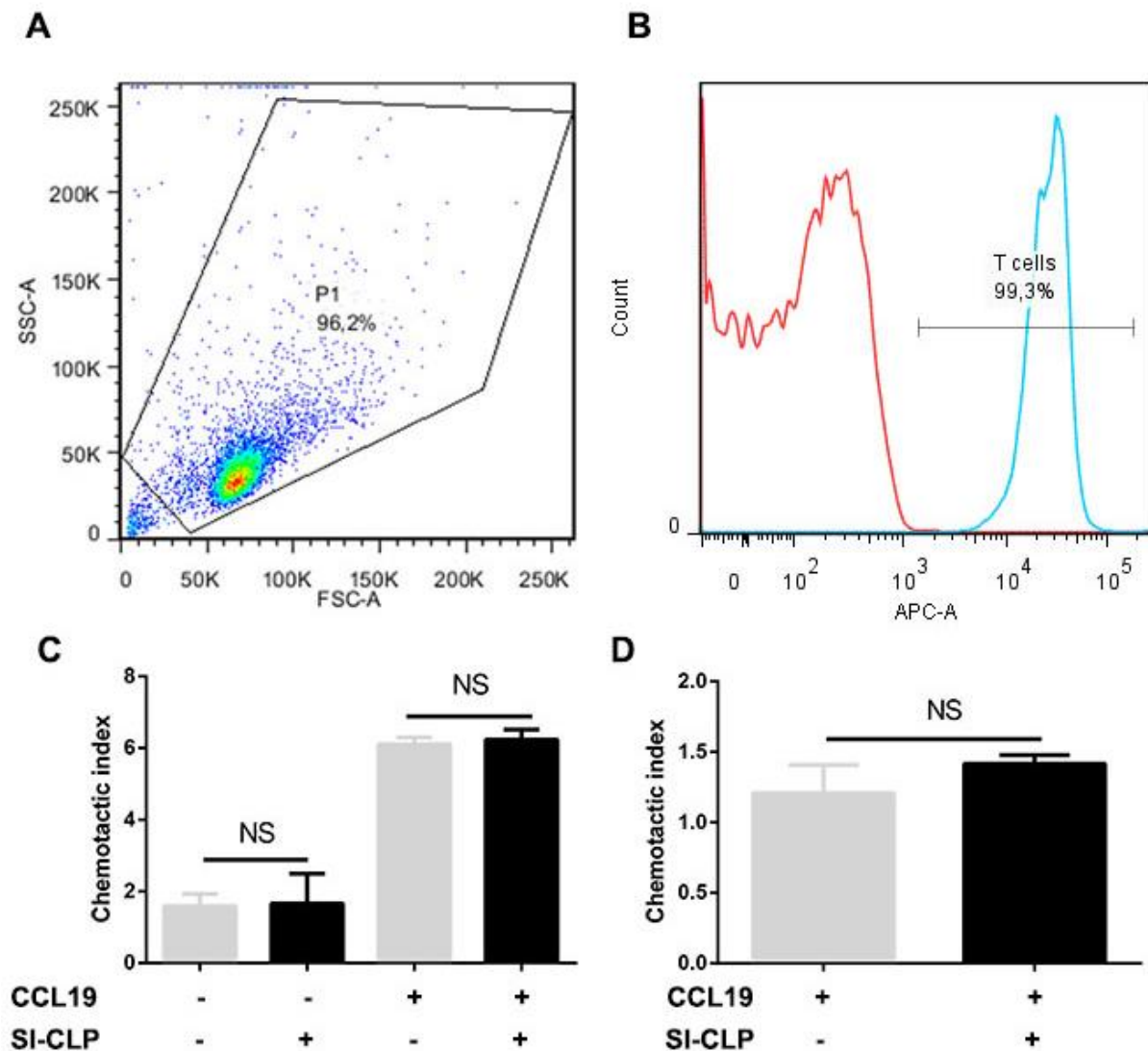

Figure 25. The effect of SI-CLP on the chemotaxis of mouse naive T cells. (A) The SSC-A and FSC-A parameters were adjusted to select all live cells for analysis. Cell debris was excluded (bottom, left hand corner). (B) Purity of isolated T cells was confirmed with APC conjugated rat anti-mouse CD3 antibody. The red line represents staining with APC conjugated rat IgG antibody and the blue line represents staining with APC conjugated rat anti-mouse CD3 antibody. (C) Comparison of the chemotactic index of naive T cells after incubation with SI-CLP for 30 min. (D) Comparison of the chemotactic index of naive T cells after incubation with SI-CLP for 16 h. An unpaired t-test was used to compare the significance of difference, and data are presented as the mean ± SD. NS indicates no statistical significance.

3.10 Analysis of specific markers of polarization in TAM isolated from TS/A-EV and TS/A-SI-CLP tumors

Previous data in vivo and in vitro revealed that the chemotaxis of macrophages was inhibited by SI-CLP. However, specific markers of macrophage activation/polarization, such as CD206, stabilin-1 and LYVE-1, were also suppressed in TS/A-SI-CLP tumors. This reduced expression of TAM markers could be a consequence of reduced TAM infiltration in TS/A-SI-CLP tumors and did not involve changes in the TAM phenotype. Alternatively, reduction in TAM numbers in TS/A-SI-CLP tumors could be accompanied by additional phenotypic changes. To confirm this hypothesis, TAM were isolated from TS/A-EV and TS/A-SI-CLP tumors raised in wt BALB/c mice and assessed for gene expression using RT-PCR analysis.

Four TS/A-SI-CLP (CL-P1D5, P1C8, P1F10 and P2G7) and four TS/A-EV (CL-A1, CL-A3, CL-A6 and CL1) clones were injected subcutaneously into BALB/c wt mice. For each clone, 5 mice were used. The tumor volume and weight on the day of TAM isolation were shown in the Figure 26.
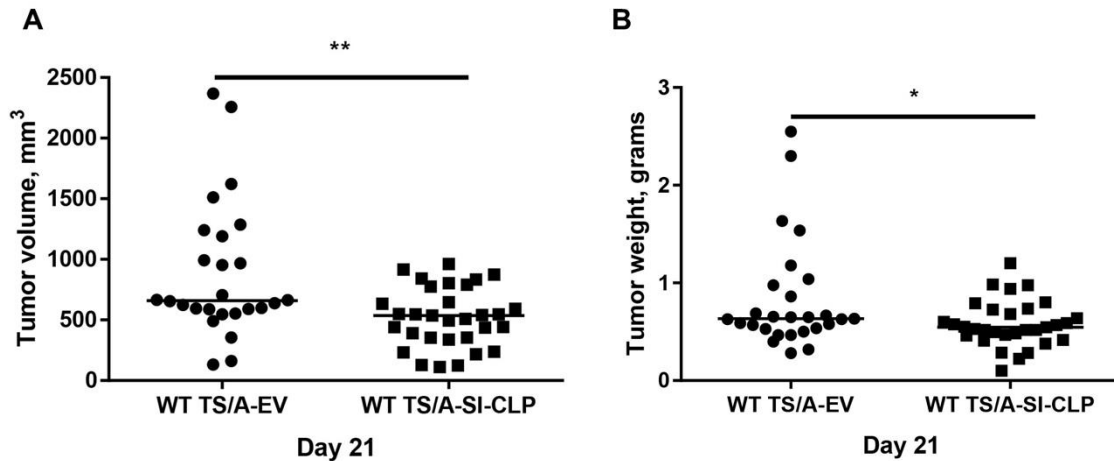
Figure 26. TAM isolated from tumors generated by subcutaneous injection of TS/A-EV and TS/A-SI-CLP cells into BALB/c wt mice. (A) Comparison of tumor volume of TS/A-EV and TS/A-SI-CLP tumors on day 21 post-injection. (B) Comparison of tumor weight of TS/A-EV and TS/A-SI-CLP tumors on day 21 post-injection. The Mann-Whitney test was used to compare the significance of difference between two groups, and data are presented as the median.

TAM were isolated from tumors generated by injecting TS/A-EV cells and tumors generated by injecting TS/A-SI-CLP cells in BALB/c wt mice according to the previously published protocol resulting in the 92-95% TAM purity[68]. As an additional control the purity of TAM was verified by a-CD68 immunofluorescent analysis and demonstrated that over 96%

of TAM were positive for CD68 (Figure 27). Purified TAM were maintained in DMEM complete medium and non-adherent cells were washed away after 30 min. Adherent TAM were used for the RNA isolation. Tumors derived from following TS/A clones were used for TAM isolation: TS/A-EV clones (CL-A1, 4 mice; CL-A3, 3 mice; CL-A6, 3 mice; CL-1, 4 mice), TS/A-SI-CLP clones (P1D5, 4 mice; P1C8, 5 mice; P1F10, 3 mice; P2G7, 5 mice). Pooled RNA samples were generated for each clone and analyzed by RT-PCR for the expression of macrophage markers related to their polarization type and involved in tumor progression.
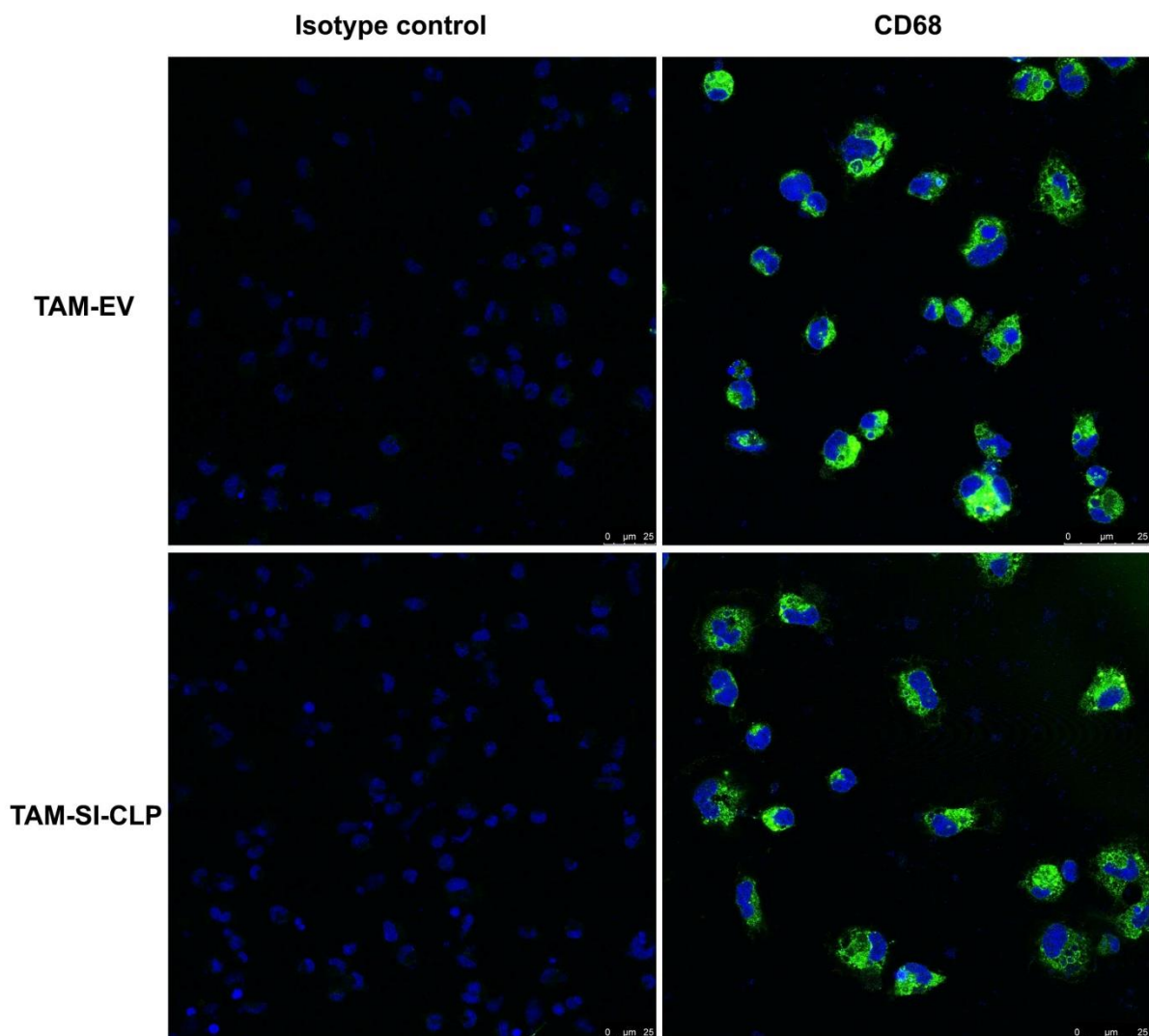
Figure 27. Confocal microscopy analysis of CD68 expression in TAM isolated from BALB/c wt mice injected with TS/A-EV and TS/A-SI-CLP cells. TAM were stained first with rat anti-mouse CD68 antibody or rat isotype control IgG2a, followed by Alexa 488 conjugated donkey anti-rat secondary antibody (shown in green). Blue color visualizes nuclei stained with DRAQ5. Scale bar is 25 µm.

RT-PCR analysis demonstrated that expression of macrophage activation/polarization markers including CD206, LYVE-1, stabilin-1, IL-1 β, IL-6, IL-10, TNF-α, VEGF-A and TGF-β are not significantly changed between TAM isolated from TS/A-EV and TS/A-SI-CLP tumors (Figure 28). These data suggested that expression of SI-CLP in TS/A tumor model does not affect TAM transcriptional profile, related to the type of their polarization and pro-tumor activities.
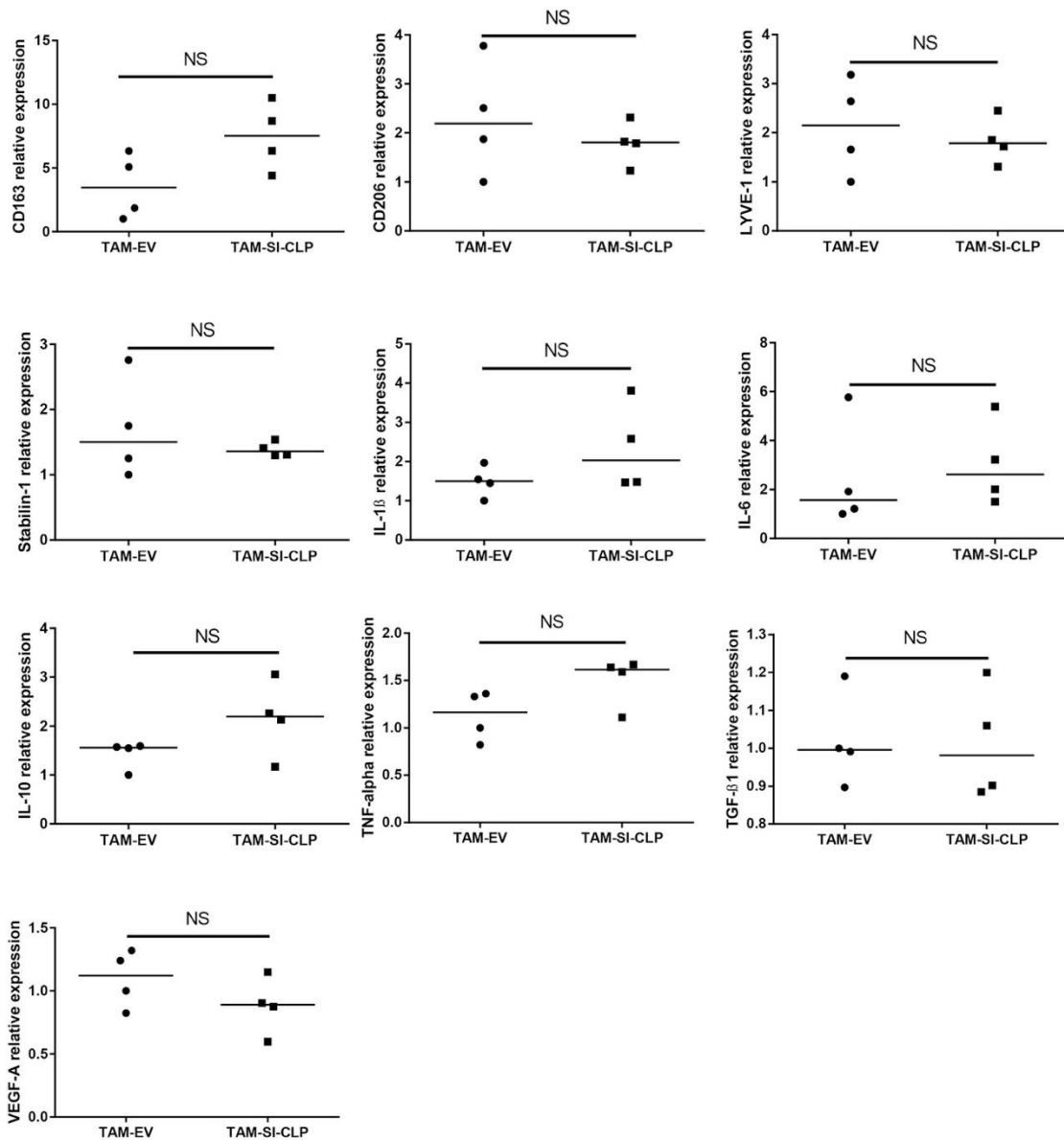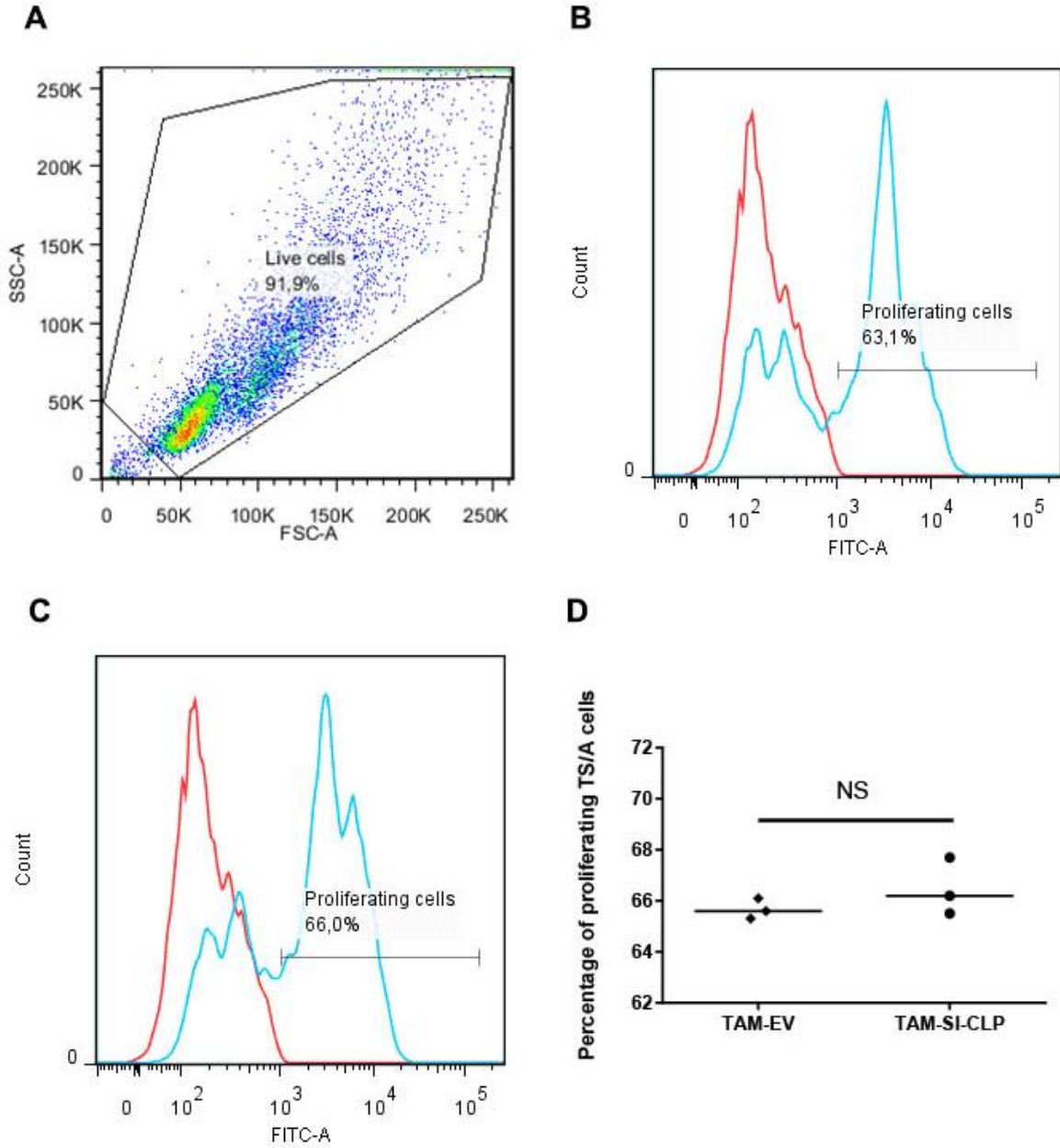

Figure 28. RT-PCR analysis of selected gene expression in TAM isolated from TS/A-EV and TS/A-SI-CLP tumors using real-time PCR. The Mann-Whitney test was used to compare the significance of difference between TAM-EV and TAM-SI-CLP, and data are presented as the median. NS indicates no statistical significance.

3.11 Functional analysis of TAM isolated from TS/A-EV and TS/A-SI-CLP tumors

TAM are known to support tumor cell proliferation and tumor growth by the secretion of growth factors. Next, it was analyzed whether conditioned medium of TAM isolated from TS/A-EV and TS/A-SI-CLP tumors can differentially affect proliferation of TS/A cells in vitro (Figure 29). To obtain conditioned supernatants, $3X10^6$ purified TAM were cultured in DMEM complete medium for 16 h. The TAM-conditioned supernatants were added to DMEM complete medium in a ratio of 1:3 to obtain TAM-DMEM medium. TAM-DMEM medium was used for the cultivation of TS/A cells for 48 h. TS/A cells were harvested and used for the EdU cell proliferation assay. The SSC-A and FSC-A parameters were adjusted to gate all alive cells (Figure 29A). About 63% TS/A cells stimulated by the supernatant derived from TAM-EV were proliferating (Figure 29B), and 66% TS/A cells stimulated by the supernatant derived from TAM-SI-CLP were proliferating (Figure 29C). These results demonstrated supernatants of TAM isolated from TS/A-SI-CLP tumors did not alter TS/A cell proliferation compared to TAM supernatants derived from vector clones (Figure 29D). These data additionally demonstrated that presence of SI-CLP in TS/A model does not affect TAM phenotype, and its tumor suppressive effects is related to the significantly decreased infiltration of TAM.

Figure 29. Flow cytometry analysis of the proliferation of TS/A cells stimulated with TAM-DMEM medium. (A) The SSC-A and FSC-A parameters were adjusted to exclude cell debris (bottom, left hand corner) for flow cytometry analysis. (B) The percentage of proliferating TS/A cells stimulated by supernatants of TAM isolated from TS/A-EV tumors. (C) The percentage of proliferating TS/A cells stimulated by supernatants of TAM isolated from TS/A-SI-CLP tumors. (D) Comparison of the percentage of proliferating TS/A cells stimulated by TAM conditioned medium from TS/A-EV and TS/A-SI-CLP tumors. The Mann-Whitney test was used to compare the significance of difference between two groups, and data are presented as the median. NS indicates no statistical significance.

4 <u>Discussion</u>

4.1 Effect of SI-CLP on tumor growth in stabilin-1 knockout mice.

Chitinases and chitinase-like proteins implicate in the pathological process in a set of human diseases, including cardio-metabolic disorders, allergy, and cancer[1,7]. The best investigated chitinase-like protein in tumor progression is YKL-40. High YKL-40 levels in the circulation of patients with different types of cancer are associated with poor prognosis[127]. YKL-40 participates in each stage of tumor progression including tumor initiation, cancer cell proliferation and migration, as well as tumor angiogenesis[7]. However, the role of other human chitinase-like proteins (SI-CLP and YKL-39) in tumor progression remained unclear. First animal model for the investigation of the function of SI-CLP on breast adenocarcinoma growth was established in our laboratory (Nan Wang, PhD thesis 2014). In this model, subcutaneous injection of TS/A-SI-CLP stably expressing recombinant SI-CLP and control TS/A-EV (empty vector) cells was used and tumor growth was monitored for 21 day. SI-CLP was produced only as recombinant protein by TS/A-SI-CLP cells in this model, while no endogenous proteins was produced by TS/A cells, TAM or other cell types in tumor microenvironment enabling analysis of the effects of ectopically expressed SI-CLP. Preliminary data about the inhibitory role of SI-CLP in mouse model for breast carcinoma were obtained by Dr. Nan Wang (Nan Wang, PhD thesis 2014). It was demonstrated that SI-CLP suppressed tumor growth of TS/A-derived tumors subcutaneously injected in BALB/c mice. This effect correlated with significantly reduced amount of stabilin-1+ TAM. Stabilin-1 is known to directly interact with SI-CLP and to transport the biosynthetic SI-CLP to the lysosomal secretory pathway in alternatively activated macrophages[6]. Stabilin-1 is abundantly expressed on TAM both in human breast cancer and in murine models for breast adenocarcinoma[68,145]. Using stabilin-1 ko mice it was demonstrated that stabilin-1 has a tumor promoting effect in murine breast adenocarcinoma and melanoma models[68,129]. It was hypothesized that SI-CLP released from TS/A cells might change phenotype of stabilin-1+TAM or reduce the infiltration of tumor-promoting stabilin-1+ TAM resulting in inhibited tumor growth. To address this hypothesis, the effect of SI-CLP in the TS/A-model was compared in wild type and stabilin-1 ko mice.

Significant inhibition of tumor growth induced by TS/A-SI-CLP cells was observed in both BALB/c wt and stabilin-1 ko mice at all analyzed time points. The inhibition of SI-CLP on tumor growth was even more pronounced in stabilin-1 ko mice compared to wt mice. On

day 21 after tumor cells injection, the difference in tumor weight between TS/A-EV and TS/A-SI-CLP tumors in wt mice reached 1.47 times, while it reached 2.4 times in ko mice. These results suggest that SI-CLP mediated suppression of tumor growth does not require expression of stabilin-1 on TAM. Moreover, the data suggest that SI-CLP expression in the tumor tissue in combination with the absence of stabilin-1 on TAM have a synergistic suppressive effect on tumor growth. Stabilin-1 was shown to be intracellular sorting receptor for endogenously produced SI-CLP in macrophages[6]. However, it can be also hypothesized that stabilin-1 expressed on TAM can act as an endocytic receptor for the SI-CLP produced by TS/A-SI-CLP cells that results in deprivation of extracellular SI-CLP. This hypothesis can explain the increased tumor-suppressive effect of SI-CLP in the stabilin-1 ko mice compared with wt mice.

YKL-40 was shown to stimulate proliferation of cancer cells lines HEK-293 and U-373 MG cells[41], and increased proliferation induced by YKL-40 was suggested to contribute to the tumor growth in the animal model for colorectal cancer[39]. However, the major mechanisms that promoted tumor growth in this model included recruitment of macrophages and angiogenesis. In our model system expression of the recombinant SI-CLP in TS/A cells has slight stimulatory effects on the TS/A cell proliferation in vitro (around 25% of increase), while SI-CLP has a strong suppressive effect on the tumor growth in vivo. Comparison of the migration ability of TS/A-EV and TS/A-SI-CLP cells in vitro also demonstrated that SI-CLP-mediated suppression of tumor growth cannot be explained by its effect on tumor cell migration. Thus, it was concluded that changes in proliferation and migration of TS/A-SI-CLP cells are not associated with reduced tumor growth in vivo, and prompted us to further investigate the effect of SI-CLP on the composition of tumor microenvironment.

4.2 Effect of SI-CLP on angiogenesis.

The major mechanism of YKL-40-mediated support of tumor growth was assigned to its pro-angiogenic activities[9,39,56]. Over-expression of YKL-40 in HCT-116 and MDA-MB-231 cells promoted angiogenesis (evaluated by the levels of CD31+ expression) in mouse models for breast adenocarcinoma and colorectal carcinoma, while knockdown of the YKL-40 gene in U-87 MG cells decreased angiogenesis in vitro and in vivo[9]. In human breast cancer tissue, the intensity of YKL-40 staining was found to positively correlate with angiogenesis[9]. Moreover, YKL-40 was found to enhance the adhesion and migration of VSMC that supported angiogenesis[38]. All this data suggested that, similarly to YKL-40, SI-CLP can be involved in the regulation of angiogenesis. However, the analysis of CD31 expression in

TS/A-EV and TS/A-SI-CLP tumors using quantitative immunohistochemistry did not detect significant difference in tumor vascularization. Therefore, the suppressive effect of SI-CLP on tumor growth in the TS/A tumor model was not related to the reduced angiogenesis. Therefore, next question raised was whether SI-CLP has an effect on the amount and content of immune cells in tumor microenvironment, where TAM play a key role in the support of primary tumor growth.

4.3   Effect of SI-CLP on TAM infiltration and phenotype.

Since attenuated growth of TS/A-SI-CLP tumors was not attributed to changes in intrinsic properties of tumor cells (proliferation and migration) and angiogenesis, it was hypothesized that the possible mechanism of tumor growth inhibition might involve changes in intratumoral immunity (specifically, alterations in immune cell composition of the tumor microenvironment). The infiltration of immune cells in TS/A-EV and TS/A-SI-CLP tumor tissue was investigated using quantitative immunohistochemistry for the specific immune cell markers. CD68 was used as a general marker of TAM in TS/A tumor tissue and CD68 positivity reflected the abundance of TAM in the tumor mass[68]. CD68 positivity was found to be significantly decreased in TS/A-SI-CLP tumors suggesting that SI-CLP has an inhibiting effect on TAM infiltration. The promoting effects of TAM in the progression of breast cancer are well-documented[85,93,146], and reduced numbers of TAM in the tumor tissue are associated with delayed tumor progression[82]. Higher numbers of TAM in human breast cancer tissue predict a worse prognosis[97]. Other markers expressed on TAM include CD206 and stabilin-1. CD206 was identified as a prototype marker for alternative macrophage activation[147]. CD206 is considered as a specific marker of tumor-supporting macrophages, and selective depletion of CD206 positive TAM in TS/A-derived tumors inhibits tumor growth and metastasis[132]. Stabilin-1 is a multifunctional clearance/sorting receptor expressed by alternatively activated macrophages[148]. We and others have recently demonstrated that stabilin-1 positive TAM facilitate tumor growth and metastasis in murine breast adenocarcinoma and melanoma models[68,129]. Decreased levels of CD206 and stabilin-1 expression in TS/A-SI-CLP tumors suggested that SI-CLP can inhibit intratumoral accumulation of TAM with tumor supporting activities that result in the delayed tumor growth. This assumption was supported by the fact that the fold change in CD206 and stabilin-1 expression was comparable to the fold change of CD68. LYVE-1 is a frequently used as classical marker of lymphatic endothelium, however it can also be expressed by TAM subsets in murine model of TS/A mammary adenocarcinoma (Alexandru Gudima, Master thesis, 2012) and B16F1 melanoma[133]. LYVE-1 is frequently co-

expressed with CD68 and stabilin-1 in TS/A tumor, while part of LYVE-1 can be also found on vessel-like structures that do no express macrophages markers (Alexandru Gudima, Master thesis, 2012). Reduction of LYVE-1 expression identified by quantitative immunohistochemical analysis in the TS/A-SI-CLP tumors was more pronounced compared with the reduction of CD206 and stabilin-1 expression, that can be explained by the additional suppressive effects of SI-CLP on lymphangiogenesis. In stabilin-1 ko mice, the effect of SI-CLP on reducing the amount of CD68+, CD206+ and LYVE-1+ cells was comparable to wt mice, indicating that similarly to the effect on tumor growth, effect of SI-CLP on TAM content does not depend on stabilin-1 expression on TAM.

The results of immunohistochemical analysis on TS/A-EV and TS/A-SI-CLP tumors suggest that SI-CLP influences the infiltration of macrophages to TAM-SI-CLP tumors. The chemotactic effects of chitinase-like proteins on immune cells have been already reported previously for YM-1 and YKL-40[37,39]. YM1 was shown to induce the chemotaxis of bone marrow cells, eosinophils and T cells, but not macrophages derived from peritoneal exudate[37]. YKL-40 was shown to enhance the chemotaxis of human monocyte-like THP-1 cells[39]. Since SI-CLP shares similarity with YM1 and YKL-40, it was reasonable to assess whether SI-CLP has an effect on macrophage chemotaxis. In vitro experiment in a Transwell system demonstrated that purified SI-CLP protein as a chemotactic agent added to the lower chamber did not induce the chemotaxis of murine BMDM and human monocytes (data not shown). However, pre-incubation of BMDM with commercial purified SI-CLP or conditioned SI-CLP-containing supernatant of BHK-21 cells infected with SI-CLP producing alphavirus resulted in the significant reduction of BMDM migration induced by CCL2. The specificity of this effect was additionally confirmed by the depletion of SI-CLP from BHK-21 supernatants using immunoprecipitation. Inhibition of CCL2-induced migration was also demonstrated for human freshly purified CD14+ monocytes pre-incubated with commercial purified human SI-CLP. Thus, in contrast to the promoting effects of YM1 and YKL-40 in macrophage migration, SI-CLP demonstrated an inhibiting effect, that corresponds to the decreased amount of TAM in infiltrating TS/A-SI-CLP tumor compared to TS/A-EV tumors. Despite substantial similarity between SI-CLP, YKL-40 and YM1, SI-CLP clearly inhibited chemotaxis of macrophages whereas YKL-40 and YM1 facilitated chemotaxis of macrophages. This functional difference between closely related proteins suggest that macrophage infiltration in tumors can be coordinately regulated by chitinase-like protein networks. The mechanism of SI-CLP mediated inhibition of macrophage chemotaxis is currently unknown. It can be hypothesized that binding of SI-CLP with primary macrophages

may decrease the availability of CCR2 receptor on the cell surface of macrophages, which interferes the CCL2-CCR2 interaction. The binding of CCL2 with CCR2 is mediated by glycosaminoglycan, and formation of CCL2 tetramers induced by heparin is important for binding with glycosaminoglycan[149]. Like YKL-40, SI-CLP possesses strong affinity to heparin, and might interfere with tetramer formation of CCL2 through competitive binding with heparin.

The results of quantitative histology on tumor sections as well as the results of chemotactic tests in vitro provided strong arguments that SI-CLP inhibits macrophage influx in the tumor mass. However, it was necessary to examine whether SI-CLP has an additional effect on the phenotype of infiltrating TAM since the expression of macrophage activation markers including CD206 and stabilin-1 differed between TS/A-EV and TS/A-SI-CLP tumors. In order to examine whether SI-CLP expression affects the TAM phenotype, TAM were isolated from TS/A-EV and TS/A-SI-CLP tumors and expression of surface markers and cytokines was analyzed by RT-PCR. However, the gene expression of CD206, LYVE-1 and stabilin-1 was not significantly changed between TAM isolated from TS/A-EV and TS/A-SI-CLP tumors, indicating that the decrease of tumor supporting TAM (CD206+, stabilin-1+ TAM) results from the reduction of the amount of TAM in TS/A-SI-CLP tumors, but not by the direct effect of SI-CLP on TAM activation. The expression of other markers of macrophage polarization, including CD163, IL-1β, IL-6, TNF-α, and TGF-β, was also similar in TS/A-EV and TS/A-SI-CLP derived TAM. Thus, the analysis did not reveal any significant effect of the presence of SI-CLP in the tumor microenvironment on macrophage phenotype. The data suggested that the expression of SI-CLP in TS/A tumor model does not affect these genes related to the type of TAM polarization.

TAM are known to support the local tumor growth by enhancing the secretion of cytokines and growth factors that promote the proliferation of tumor cells[97,98]. In order to test whether TAM isolated from TS/A-SI-CLP have reduced tumor-promoting effect compared to TAM isolated from TS/A-EV tumors, TAM conditioned medium was used to stimulate TS/A cells. Conditioned medium of TAM strongly supported the proliferation of TS/A cells, but the supportive activity did not vary between TAM isolated from TS/A-EV and TS/A-SI-CLP tumors. Therefore, the major effect of SI-CLP that explained the suppression of tumor growth was the inhibition of infiltration of TAM with tumor-promoting phenotype.

4.4 Effect of SI-CLP on other immune cell recruitment.

TAM are key cells of tumor microenvironment that also affect infiltration and phenotype of other innate and adaptive immune cells. Moreover, chitinase-like protein YM1 has a direct chemotactic effect on eosinophils and T cells[37]. Therefore, we investigated how the presence of SI-CLP in tumor mass can influence the content and amount of various types of immune cells in the tumor microenvironment. The amount of T cells in TS/A-EV and TS/A-SI-CLP tumors was investigated by quantitative immunohistological analysis of CD3, and less CD3+ cells were found in the TS/A-SI-CLP tumors in both BALB/c wt and stabilin-1 ko mice. CD8+ cytotoxic T cells play a crucial role in tumor rejection, while FoxP3+ regulatory T cells (Tregs) support tumor tolerance. Minor amount of CD8+ cells was found in the TS/A-EV and TS/A-SI-CLP tumors, and the presence of SI-CLP did not have statistically significant effect on the amount of CD8+ cells neither in wt nor in the stabilin-1 ko mice. However, significantly less CD4+ and FoxP3+ positive cells were found in TS/A-SI-CLP tumors. The effect of SI-CLP on the reduction of FoxP3+ cells did not depend on the expression of stabilin-1 on TAM and was similar in wt and stabilin-1 ko mice.

Since the amount of T cells was reduced in the TS/A-SI-CLP tumors, it was hypothesized that the infiltration of T cells can be inhibited by SI-CLP protein, similar to its effect on macrophages. The effect of SI-CLP on the chemotaxis of T cells was studied in vitro using naïve T cells isolated from spleen of BALB/c mice. However, purified mouse SI-CLP did not show an inhibitory effect on T-cell migration towards CCL19 (positive control for chemotaxis of T cells) suggesting that reduced infiltration of T cells in the tumor tissue is due to reduced number of TAM in TS/A-SI-CLP tumor tissue. In addition, SI-CLP-mediated reduction of TAM can also explain reduced amount of FoxP3+ cells in the TS/A-SI-CLP tumors. Further analysis of other types of immune cells that regulate tumor growth demonstrated that the infiltration of eosinophils and neutrophils was not significantly changed between TS/A-EV and TS/A-SI-CLP tumors.

In summary, the present study demonstrated that SI-CLP has a pronounced suppressive effect on the growth of breast adenocarcinoma, where SI-CLP inhibits recruitment of TAM with tumor-promoting phenotype. The inhibitory effect of SI-CLP on recruiting pro-tumor TAM has to be further examined in the experimental models for different types of cancer, for example colorectal cancer and glioblastoma, where TAM play a crucial role in the tumor progression. In perspective, tumor-suppressive properties of SI-CLP can be considered for the design of novel therapeutic approaches to target tumor-supportive TAM.

5 **Summary**

SI-CLP belongs to the family of chitinase-like proteins that combine properties of cytokines and growth factors. SI-CLP was identified as an intracellular ligand for the multifunctional receptor stabilin-1, expressed on tumor-associated macrophages (TAM). YKL-40, a homologue of SI-CLP, has tumor-promoting activities in animal models for glioblastoma, colorectal carcinoma and breast adenocarcinoma, and elevated levels of YKL-40 in human serum correlate with poor prognosis in various types of cancer. In contrast, previous data obtained in our laboratory demonstrated that SI-CLP has an inhibitory effect on tumor growth in mouse model for breast adenocarcinoma correlating with decreased amount of stabilin-1+TAM. However, the mechanisms of SI-CLP-mediated suppression of tumor growth remain to be unknown. The aims of the present study were to identify the functional role and possible mechanism of SI-CLP effects in cancer development using mouse model for breast adenocarcinoma. The effects of SI-CLP on the biology of cancer cells, tumor angiogenesis, and phenotype and amounts of immune cells in tumor microenvironment were analyzed. To examine whether expression of stabilin-1 on TAM is critical for the tumor-suppressive effect of SI-CLP, TS/A cells stably transfected with SI-CLP (TS/A-SI-CLP) and with the control empty vector (control TS/A-EV) were injected subcutaneously into BALB/c wt and stabilin-1 knockout (ko) mice. The suppressive effects of SI-CLP on tumor growth in the stabilin-1 ko mice were similar to wt mice at all time points analyzed (from day 7 until day 21), indicating that SI-CLP does not require stabilin-1 expression on TAM for its intratumoral effects. In vitro analysis of TS/A-SI-CLP and TS/A-EV demonstrated that SI-CLP does not suppress TS/A cell proliferation or migration. Quantitative immunohistochemistry demonstrated that the presence of SI-CLP does not affect tumor angiogenesis and infiltration of neutrophils and eosinophils in vivo. However, SI-CLP significantly inhibited infiltration of TAM in tumor mass without changing their tumor-supporting phenotype. The direct inhibitory effect of SI-CLP on the CCL2 induced recruitment of mouse bone-marrow derived macrophages and human monocytes was demonstrated in vitro. Reduced amount of TAM in TS/A tumor tissue correlated with the decreased amount of FoxP3+ cells, while SI-CLP had no direct effect on T-cell migration in vitro. In summary, the results of the study demonstrated that SI-CLP suppresses growth on breast adenocarcinoma primarily by inhibiting the infiltration of tumor-associated macrophages and reducing tumor-supportive activities of tumor microenvironment.

6 **References**

1. Lee, CG, Da Silva, CA, Dela Cruz, CS, Ahangari, F, Ma, B, Kang, MJ, He, CH, Takyar, S, Elias, JA: Role of chitin and chitinase/chitinase-like proteins in inflammation, tissue remodeling, and injury. *Annual review of physiology,* 73**:** 479-501, 2011.
2. Elias, JA, Homer, RJ, Hamid, Q, Lee, CG: Chitinases and chitinase-like proteins in T(H)2 inflammation and asthma. *J Allergy Clin Immunol,* 116**:** 497-500, 2005.
3. Mauch, F, Mauch-Mani, B, Boller, T: Antifungal Hydrolases in Pea Tissue : II. Inhibition of Fungal Growth by Combinations of Chitinase and beta-1,3-Glucanase. *Plant physiology,* 88**:** 936-942, 1988.
4. Chang, NCA, Hung, SI, Hwa, KY, Kato, I, Chen, JE, Liu, CH, Chang, AC: A macrophage protein, Ym1, transiently expressed during inflammation is a novel mammalian lectin. *Journal of Biological Chemistry,* 276**:** 17497-17506, 2001.
5. Boot, RG, Blommaart, EFC, Swart, E, Ghauharali-van der Vlugt, K, Bijl, N, Moe, C, Place, A, Aerts, JMFG: Identification of a novel acidic mammalian chitinase distinct from chitotriosidase. *Journal of Biological Chemistry,* 276**:** 6770-6778, 2001.
6. Kzhyshkowska, J, Mamidi, S, Gratchev, A, Kremmer, E, Schmuttermaier, C, Krusell, L, Haus, G, Utikal, J, Schledzewski, K, Scholtze, J, Goerdt, S: Novel stabilin-1 interacting chitinase-like protein (SI-CLP) is up-regulated in alternatively activated macrophages and secreted via lysosomal pathway. *Blood,* 107**:** 3221-3228, 2006.
7. Kzhyshkowska, J, Yin, S, Liu, T, Riabov, V, Mitrofanova, I: Role of chitinase-like proteins in cancer. *Biol Chem,* 397**:** 231-247, 2016.
8. Fusetti, F, Pijning, T, Kalk, KH, Bos, E, Dijkstra, BW: Crystal structure and carbohydrate-binding properties of the human cartilage glycoprotein-39. *J Biol Chem,* 278**:** 37753-37760, 2003.
9. Shao, R, Hamel, K, Petersen, L, Cao, QJ, Arenas, RB, Bigelow, C, Bentley, B, Yan, W: YKL-40, a secreted glycoprotein, promotes tumor angiogenesis. *Oncogene,* 28**:** 4456-4468, 2009.
10. Meng, G, Zhao, Y, Bai, X, Liu, Y, Green, TJ, Luo, M, Zheng, X: Structure of human stabilin-1 interacting chitinase-like protein (SI-CLP) reveals a saccharide-binding cleft with lower sugar-binding selectivity. *J Biol Chem,* 285**:** 39898-39904, 2010.
11. Xiao, WC, Meng, G, Zhao, YM, Yuan, HH, Li, TT, Peng, YY, Zhao, Y, Luo, M, Zhao, WM, Li, ZG, Zheng, XF: Human Secreted Stabilin-1-Interacting Chitinase-like Protein Aggravates the Inflammation Associated With Rheumatoid Arthritis and Is a Potential Macrophage Inflammatory Regulator in Rodents. *Arthritis Rheumatol,* 66**:** 1141-1152, 2014.
12. Schimpl, M, Rush, CL, Betou, M, Eggleston, IM, Recklies, AD, van Aalten, DMF: Human YKL-39 is a pseudo-chitinase with retained chitooligosaccharide-binding properties. *Biochemical Journal,* 446**:** 149-157, 2012.
13. Bigg, HF, Wait, R, Rowan, AD, Cawston, TE: The mammalian chitinase-like lectin, YKL-40, binds specifically to type I collagen and modulates the rate of type I collagen fibril formation. *Journal of Biological Chemistry,* 281**:** 21082-21095, 2006.
14. Renkema, GH, Boot, RG, Au, FL, Donker-Koopman, WE, Strijland, A, Muijsers, AO, Hrebicek, M, Aerts, JM: Chitotriosidase, a chitinase, and the 39-kDa human cartilage glycoprotein, a chitin-binding lectin, are homologues of family 18 glycosyl hydrolases secreted by human macrophages. *European journal of biochemistry / FEBS,* 251**:** 504-509, 1998.
15. Shackelton, LM, Mann, DM, Millis, AJT: Identification of a 38-Kda Heparin-Binding Glycoprotein (Gp38k) in Differentiating Vascular Smooth-Muscle Cells as a Member of a Group of Proteins Associated with Tissue Remodeling. *Journal of Biological Chemistry,* 270**:** 13076-13083, 1995.
16. Ranok, A, Wongsantichon, J, Robinson, RC, Suginta, W: Structural and thermodynamic insights into chitooligosaccharide binding to human cartilage chitinase 3-like protein 2 (CHI3L2 or YKL-39). *J Biol Chem,* 290**:** 2617-2629, 2015.
17. Hakala, BE, White, C, Recklies, AD: Human cartilage gp-39, a major secretory product of articular chondrocytes and synovial cells, is a mammalian member of a chitinase protein family. *J Biol Chem,* 268**:** 25803-25810, 1993.

18. Lee, CG, Hartl, D, Lee, GR, Koller, B, Matsuura, H, Da Silva, CA, Sohn, MH, Cohn, L, Homer, RJ, Kozhich, AA, Humbles, A, Kearley, J, Coyle, A, Chupp, G, Reed, J, Flavell, RA, Elias, JA: Role of breast regression protein 39 (BRP-39)/chitinase 3-like-1 in Th2 and IL-13-induced tissue responses and apoptosis. *J Exp Med,* 206**:** 1149-1166, 2009.

19. Petersson, M, Bucht, E, Granberg, B, Stark, A: Effects of arginine-vasopressin and parathyrold hormone-related protein (1-34) on cell proliferation and production of YKL-40 in cultured chondrocytes from patients with rheumatoid arthritis and osteoarthritis. *Osteoarthr Cartilage,* 14**:** 652-659, 2006.

20. Volck, B, Price, PA, Johansen, JS, Sorensen, O, Benfield, TL, Nielsen, HJ, Calafat, J, Borregaard, N: YKL-40, a mammalian member of the chitinase family, is a matrix protein of specific granules in human neutrophils. *P Assoc Am Physician,* 110**:** 351-360, 1998.

21. Ku, BM, Lee, YK, Ryu, J, Jeong, JY, Choi, J, Eun, KM, Shin, HY, Kim, DG, Hwang, EM, Yoo, JC, Park, JY, Roh, GS, Kim, HJ, Cho, GJ, Choi, WS, Paek, SH, Kang, SS: CHI3L1 (YKL-40) is expressed in human gliomas and regulates the invasion, growth and survival of glioma cells. *International journal of cancer Journal international du cancer,* 128**:** 1316-1326, 2011.

22. Faibish, M, Francescone, R, Bentley, B, Yan, W, Shao, R: A YKL-40-neutralizing antibody blocks tumor angiogenesis and progression: a potential therapeutic agent in cancers. *Molecular cancer therapeutics,* 10**:** 742-751, 2011.

23. Hu, B, Trinh, K, Figueira, WF, Price, PA: Isolation and sequence of a novel human chondrocyte protein related to mammalian members of the chitinase protein family. *Journal of Biological Chemistry,* 271**:** 19415-19420, 1996.

24. Knorr, T, Obermayr, F, Bartnik, E, Zien, A, Aigner, T: YKL-39 (chitinase 3-like protein 2), but not YKL-40 (chitinase 3-like protein 1), is up regulated in osteoarthritic chondrocytes. *Ann Rheum Dis,* 62**:** 995-998, 2003.

25. Steck, E, Breit, S, Breusch, SJ, Axt, M, Richter, W: Enhanced expression of the human chitinase 3-like 2 gene (YKL-39) but not chitinase 3-like 1 gene (YKL-40) in osteoarthritic cartilage. *Biochem Bioph Res Co,* 299**:** 109-115, 2002.

26. <Julia Kzhyshkowska,Biomarker Insights 2008.pdf>.

27. Jin, HM, Copeland, NG, Gilbert, DJ, Jenkins, NA, Kirkpatrick, RB, Rosenberg, M: Genetic characterization of the murine Ym1 gene and identification of a cluster of highly homologous genes. *Genomics,* 54**:** 316-322, 1998.

28. Harbord, M, Novelli, M, Canas, B, Power, D, Davis, C, Godovac-Zimmermann, J, Roes, J, Segal, AW: Ym1 is a neutrophil granule protein that crystallizes in p47(phox)-deficient mice. *Journal of Biological Chemistry,* 277**:** 5468-5475, 2002.

29. Raes, G, De Baetselier, P, Noel, W, Beschin, A, Brombacher, F, Hassanzadeh, G: Differential expression of FIZZ1 and Ym1 in alternatively versus classically activated macrophages. *J Leukocyte Biol,* 71**:** 597-602, 2002.

30. Lee, E, Yook, J, Haa, K, Chang, HW: Induction of Ym1/2 in mouse bone marrow-derived mast cells by IL-4 and identification of Ym1/2 in connective tissue type-like mast cells derived from bone marrow cells cultured with IL-4 and stem cell factor. *Immunol Cell Biol,* 83**:** 468-474, 2005.

31. Goren, I, Pfeilschifter, J, Frank, S: Uptake of Neutrophil-Derived Ym1 Protein Distinguishes Wound Macrophages in the Absence of Interleukin-4 Signaling in Murine Wound Healing. *American Journal of Pathology,* 184**:** 3249-3261, 2014.

32. Nair, MG, Cochrane, DW, Allen, JE: Macrophages in chronic type 2 inflammation have a novel phenotype characterized by the abundant expression of Ym1 and Fizz1 that can be partly replicated in vitro. *Immunol Lett,* 85**:** 173-180, 2003.

33. Park, JA, Drazen, JM, Tschumperlin, DJ: The Chitinase-like Protein YKL-40 Is Secreted by Airway Epithelial Cells at Base Line and in Response to Compressive Mechanical Stress. *Journal of Biological Chemistry,* 285**:** 29817-29825, 2010.

34. Chen, CC, Pekow, J, Llado, V, Kanneganti, M, Lau, CW, Mizoguchi, A, Mino-Kenudson, M, Bissonnette, M, Mizoguchi, E: Chitinase 3-like-1 expression in colonic epithelial cells as a potentially novel marker for colitis-associated neoplasia. *Am J Pathol,* 179**:** 1494-1503, 2011.

35. Malinda, KM, Ponce, L, Kleinman, HK, Shackelton, LM, Millis, AJT: Gp38k, a protein synthesized by vascular smooth muscle cells, stimulates directional migration of human umbilical vein endothelial cells. *Experimental Cell Research,* 250**:** 168-173, 1999.

36. Welch, JS, Escoubet-Lozach, L, Sykes, DB, Liddiard, K, Greaves, DR, Glass, CK: T(H)2 cytokines and allergic challenge induce YM1 expression in macrophages by a STAT6-dependent mechanism. *Journal of Biological Chemistry,* 277**:** 42821-42829, 2002.

37. Owhashi, M, Arita, H, Hayai, N: Identification of a novel eosinophil chemotactic cytokine (ECF-L) as a chitinase family protein. *Journal of Biological Chemistry,* 275**:** 1279-1286, 2000.

38. Nishikawa, KC, Millis, AJ: gp38k (CHI3L1) is a novel adhesion and migration factor for vascular cells. *Exp Cell Res,* 287**:** 79-87, 2003.

39. Kawada, M, Seno, H, Kanda, K, Nakanishi, Y, Akitake, R, Komekado, H, Kawada, K, Sakai, Y, Mizoguchi, E, Chiba, T: Chitinase 3-like 1 promotes macrophage recruitment and angiogenesis in colorectal cancer. *Oncogene,* 31**:** 3111-3123, 2012.

40. Tang, H, Sun, Y, Shi, ZQ, Huang, H, Fang, Z, Chen, JQ, Xiu, QY, Li, B: YKL-40 Induces IL-8 Expression from Bronchial Epithelium via MAPK (JNK and ERK) and NF-kappa B Pathways, Causing Bronchial Smooth Muscle Proliferation and Migration. *Journal of Immunology,* 190**:** 438-446, 2013.

41. Areshkov, PO, Avdieiev, SS, Balynska, OV, Leroith, D, Kavsan, VM: Two closely related human members of chitinase-like family, CHI3L1 and CHI3L2, activate ERK1/2 in 293 and U373 cells but have the different influence on cell proliferation. *Int J Biol Sci,* 8**:** 39-48, 2012.

42. Recklies, AD, White, C, Ling, H: The chitinase 3-like protein human cartilage glycoprotein 39 (HC-gp39) stimulates proliferation of human connective-tissue cells and activates both extracellular signal-regulated kinase- and protein kinase B-mediated signalling pathways. *The Biochemical journal,* 365**:** 119-126, 2002.

43. Tang, H, Sun, Y, Shi, Z, Huang, H, Fang, Z, Chen, J, Xiu, Q, Li, B: YKL-40 induces IL-8 expression from bronchial epithelium via MAPK (JNK and ERK) and NF-kappaB pathways, causing bronchial smooth muscle proliferation and migration. *J Immunol,* 190**:** 438-446, 2013.

44. Iwamoto, FM, Hottinger, AF, Karimi, S, Riedel, E, Dantis, J, Jahdi, M, Panageas, KS, Lassman, AB, Abrey, LE, Fleisher, M, DeAngelis, LM, Holland, EC, Hormigo, A: Serum YKL-40 is a marker of prognosis and disease status in high-grade gliomas. *Neuro Oncol,* 13**:** 1244-1251, 2011.

45. Hormigo, A, Gu, B, Karimi, S, Riedel, E, Panageas, KS, Edgar, MA, Tanwar, MK, Rao, JS, Fleisher, M, DeAngelis, LM, Holland, EC: YKL-40 and matrix metalloproteinase-9 as potential serum biomarkers for patients with high-grade gliomas. *Clin Cancer Res,* 12**:** 5698-5704, 2006.

46. Shao, R, Cao, QJ, Arenas, RB, Bigelow, C, Bentley, B, Yan, W: Breast cancer expression of YKL-40 correlates with tumour grade, poor differentiation, and other cancer markers. *Br J Cancer,* 105**:** 1203-1209, 2011.

47. Tschirdewahn, S, Reis, H, Niedworok, C, Nyirady, P, Szendroi, A, Schmid, KW, Shariat, SF, Kramer, G, vom Dorp, F, Rubben, H, Szarvas, T: Prognostic effect of serum and tissue YKL-40 levels in bladder cancer. *Urol Oncol,* 32**:** 663-669, 2014.

48. Kjaergaard, AD, Nordestgaard, BG, Johansen, JS, Bojesen, SE: Observational and genetic plasma YKL-40 and cancer in 96,099 individuals from the general population. *International journal of cancer Journal international du cancer*, 2015.

49. Hogdall, EV, Ringsholt, M, Hogdall, CK, Christensen, IJ, Johansen, JS, Kjaer, SK, Blaakaer, J, Ostenfeld-Moller, L, Price, PA, Christensen, LH: YKL-40 tissue expression and plasma levels in patients with ovarian cancer. *BMC Cancer,* 9**:** 8, 2009.

50. Xu, CH, Yu, LK, Hao, KK: Serum YKL-40 level is associated with the chemotherapy response and prognosis of patients with small cell lung cancer. *PLoS One,* 9**:** e96384, 2014.

51. Schmidt, H, Johansen, JS, Sjoegren, P, Christensen, IJ, Sorensen, BS, Fode, K, Larsen, J, von der Maase, H: Serum YKL-40 predicts relapse-free and overall survival in patients with American Joint Committee on Cancer stage I and II melanoma. *J Clin Oncol,* 24**:** 798-804, 2006.

52. Johansen, JS, Brasso, K, Iversen, P, Teisner, B, Garnero, P, Price, PA, Christensen, IJ: Changes of biochemical markers of bone turnover and YKL-40 following hormonal treatment for metastatic prostate cancer are related to survival. *Clin Cancer Res,* 13**:** 3244-3249, 2007.

53. Cintin, C, Johansen, JS, Christensen, IJ, Price, PA, Sorensen, S, Nielsen, HJ: Serum YKL-40 and colorectal cancer. *Br J Cancer,* 79**:** 1494-1499, 1999.

54. Johansen, JS, Christensen, IJ, Jorgensen, LN, Olsen, J, Rahr, HB, Nielsen, KT, Laurberg, S, Brunner, N, Nielsen, HJ: Serum YKL-40 in risk assessment for colorectal cancer: a prospective study of 4,496 subjects at risk of colorectal cancer. *Cancer Epidemiol Biomarkers Prev,* 24**:** 621-626, 2015.

55. Francescone, RA, Scully, S, Faibish, M, Taylor, SL, Oh, D, Moral, L, Yan, W, Bentley, B, Shao, R: Role of YKL-40 in the angiogenesis, radioresistance, and progression of glioblastoma. *J Biol Chem,* 286**:** 15332-15343, 2011.

56. Shao, R, Francescone, R, Ngernyuang, N, Bentley, B, Taylor, SL, Moral, L, Yan, W: Anti-YKL-40 antibody and ionizing irradiation synergistically inhibit tumor vascularization and malignancy in glioblastoma. *Carcinogenesis,* 35**:** 373-382, 2014.

57. Low, D, Subramaniam, R, Lin, L, Aomatsu, T, Mizoguchi, A, Ng, A, DeGruttola, AK, Lee, CG, Elias, JA, Andoh, A, Mino-Kenudson, M, Mizoguchi, E: Chitinase 3-like 1 induces survival and proliferation of intestinal epithelial cells during chronic inflammation and colitis-associated cancer by regulating S100A9. *Oncotarget,* 2015.

58. Saidi, A, Javerzat, S, Bellahcene, A, De Vos, J, Bello, L, Castronovo, V, Deprez, M, Loiseau, H, Bikfalvi, A, Hagedorn, M: Experimental anti-angiogenesis causes upregulation of genes associated with poor survival in glioblastoma. *International journal of cancer Journal international du cancer,* 122**:** 2187-2198, 2008.

59. Jensen, BV, Johansen, JS, Price, PA: High levels of serum HER-2/neu and YKL-40 independently reflect aggressiveness of metastatic breast cancer. *Clinical Cancer Research,* 9**:** 4423-4434, 2003.

60. Lu, KV, Jong, KA, Rajasekaran, AK, Cloughesy, TF, Mischel, PS: Upregulation of tissue inhibitor of metalloproteinases (TIMP)-2 promotes matrix metalloproteinase (MMP)-2 activation and cell invasion in a human glioblastoma cell line. *Lab Invest,* 84**:** 8-20, 2004.

61. He, CH, Lee, CG, Dela Cruz, CS, Lee, CM, Zhou, Y, Ahangari, F, Ma, B, Herzog, EL, Rosenberg, SA, Li, Y, Nour, AM, Parikh, CR, Schmidt, I, Modis, Y, Cantley, L, Elias, JA: Chitinase 3-like 1 regulates cellular and tissue responses via IL-13 receptor alpha2. *Cell Rep,* 4**:** 830-841, 2013.

62. Ma, B, Herzog, EL, Lee, CG, Peng, X, Lee, CM, Chen, X, Rockwell, S, Koo, JS, Kluger, H, Herbst, RS, Sznol, M, Elias, JA: Role of chitinase 3-like-1 and semaphorin 7a in pulmonary melanoma metastasis. *Cancer Res,* 75**:** 487-496, 2015.

63. Libreros, S, Garcia-Areas, R, Keating, P, Carrio, R, Iragavarapu-Charyulu, VL: Exploring the role of CHI3L1 in "pre-metastatic" lungs of mammary tumor-bearing mice. *Frontiers in physiology,* 4**:** 392, 2013.

64. Qian, BZ, Li, J, Zhang, H, Kitamura, T, Zhang, J, Campion, LR, Kaiser, EA, Snyder, LA, Pollard, JW: CCL2 recruits inflammatory monocytes to facilitate breast-tumour metastasis. *Nature,* 475**:** 222-225, 2011.

65. Nahrendorf, M, Swirski, FK, Aikawa, E, Stangenberg, L, Wurdinger, T, Figueiredo, JL, Libby, P, Weissleder, R, Pittet, MJ: The healing myocardium sequentially mobilizes two monocyte subsets with divergent and complementary functions. *J Exp Med,* 204**:** 3037-3047, 2007.

66. Gordon, S, Pluddemann, A, Martinez Estrada, F: Macrophage heterogeneity in tissues: phenotypic diversity and functions. *Immunol Rev,* 262**:** 36-55, 2014.

67. Mosser, DM, Edwards, JP: Exploring the full spectrum of macrophage activation. *Nature reviews Immunology,* 8**:** 958-969, 2008.

68. Riabov, V, Yin, S, Song, B, Avdic, A, Schledzewski, K, Ovsiy, I, Gratchev, A, Llopis Verdiell, M, Sticht, C, Schmuttermaier, C, Schonhaber, H, Weiss, C, Fields, AP, Simon-Keller, K, Pfister, F, Berlit, S, Marx, A, Arnold, B, Goerdt, S, Kzhyshkowska, J: Stabilin-1 is expressed in human breast cancer and supports tumor growth in mammary adenocarcinoma mouse model. *Oncotarget,* 2016.

69. Aderem, A, Underhill, DM: Mechanisms of phagocytosis in macrophages. *Annu Rev Immunol,* 17**:** 593-623, 1999.

70. Underhill, DM, Ozinsky, A: Toll-like receptors: key mediators of microbe detection. *Curr Opin Immunol,* 14**:** 103-110, 2002.

71. Gordon, S: The macrophage: Past, present and future. *Eur J Immunol,* 37**:** S9-S17, 2007.

72. Hoeve, MA, Gallagher, IJ, Leech, MD, Howie, SE, Allen, JE: IL-4 is required for optimal induction of Ym1 and RELM alpha in helminth infection and airway inflammation. *Immunology,* 120**:** 28-28, 2007.

73. Zhang, J, Gratchev, A, Riabov, V, Mamidi, S, Schmuttermaier, C, Krusell, L, Kremmer, E, Workman, G, Sage, EH, Jalkanen, S, Goerdt, S, Kzhyshkowska, J: A novel GGA-binding site is required for intracellular sorting mediated by stabilin-1. *Mol Cell Biol,* 29**:** 6097-6105, 2009.

74. Ramachandra, L, Simmons, D, Harding, CV: MHC molecules and microbial antigen processing in phagosomes. *Current Opinion in Immunology,* 21**:** 98-104, 2009.

75. Murray, PJ, Allen, JE, Biswas, SK, Fisher, EA, Gilroy, DW, Goerdt, S, Gordon, S, Hamilton, JA, Ivashkiv, LB, Lawrence, T, Locati, M, Mantovani, A, Martinez, FO, Mege, JL, Mosser, DM, Natoli, G, Saeij, JP, Schultze, JL, Shirey, KA, Sica, A, Suttles, J, Udalova, I, van Ginderachter, JA, Vogel, SN, Wynn, TA: Macrophage activation and polarization: nomenclature and experimental guidelines. *Immunity,* 41**:** 14-20, 2014.

76. Gordon, S, Martinez, FO: Alternative Activation of Macrophages: Mechanism and Functions. *Immunity,* 32**:** 593-604, 2010.

77. Fong, CHY, Bebien, M, Didierlaurent, A, Nebauer, R, Hussell, T, Broide, D, Karin, M, Lawrence, T: An antiinflammatory role for IKK beta through the inhibition of "classical" macrophage activation. *J Exp Med,* 205**:** 1269-1276, 2008.

78. Martinez, FO, Gordon, S: The M1 and M2 paradigm of macrophage activation: time for reassessment. *F1000Prime Rep,* 6**:** 13, 2014.

79. Gratchev, A, Kzhyshkowska, J, Kothe, K, Muller-Molinet, I, Kannookadan, S, Utikal, J, Goerdt, S: Mphi1 and Mphi2 can be re-polarized by Th2 or Th1 cytokines, respectively, and respond to exogenous danger signals. *Immunobiology,* 211**:** 473-486, 2006.

80. Stout, RD, Suttles, J: Functional plasticity of macrophages: reversible adaptation to changing microenvironments. *J Leukoc Biol,* 76**:** 509-513, 2004.

81. Xue, J, Schmidt, SV, Sander, J, Draffehn, A, Krebs, W, Quester, I, De Nardo, D, Gohel, TD, Emde, M, Schmidleithner, L, Ganesan, H, Nino-Castro, A, Mallmann, MR, Labzin, L, Theis, H, Kraut, M, Beyer, M, Latz, E, Freeman, TC, Ulas, T, Schultze, JL: Transcriptome-Based Network Analysis Reveals a Spectrum Model of Human Macrophage Activation. *Immunity,* 40**:** 274-288, 2014.

82. Bingle, L, Brown, NJ, Lewis, CE: The role of tumour-associated macrophages in tumour progression: implications for new anticancer therapies. *Journal of Pathology,* 196**:** 254-265, 2002.

83. Lin, EY, Li, JF, Gnatovskiy, L, Deng, Y, Zhu, L, Grzesik, DA, Qian, H, Xue, XN, Pollard, JW: Macrophages regulate the angiogenic switch in a mouse model of breast cancer. *Cancer Research,* 66**:** 11238-11246, 2006.

84. Noy, R, Pollard, JW: Tumor-associated macrophages: from mechanisms to therapy. *Immunity,* 41**:** 49-61, 2014.

85. Lin, EY, Pollard, JW: Tumor-associated macrophages press the angiogenic switch in breast cancer. *Cancer Res,* 67**:** 5064-5066, 2007.

86. Riabov, V, Gudima, A, Wang, N, Mickley, A, Orekhov, A, Kzhyshkowska, J: Role of tumor associated macrophages in tumor angiogenesis and lymphangiogenesis. *Frontiers in physiology,* 5**:** 75, 2014.

87. Junker, N, Johansen, JS, Andersen, CB, Kristjansen, PE: Expression of YKL-40 by peritumoral macrophages in human small cell lung cancer. *Lung Cancer,* 48**:** 223-231, 2005.

88. Casazza, A, Laoui, D, Wenes, M, Rizzolio, S, Bassani, N, Mambretti, M, Deschoemaeker, S, Van Ginderachter, JA, Tamagnone, L, Mazzone, M: Impeding macrophage entry into hypoxic tumor areas by Sema3A/Nrp1 signaling blockade inhibits angiogenesis and restores antitumor immunity. *Cancer cell,* 24**:** 695-709, 2013.

89. Lin, EY, Li, JF, Gnatovskiy, L, Deng, Y, Zhu, L, Grzesik, DA, Qian, H, Xue, XN, Pollard, JW: Macrophages regulate the angiogenic switch in a mouse model of breast cancer. *Cancer Res,* 66**:** 11238-11246, 2006.

90. Chen, JJ, Yao, PL, Yuan, A, Hong, TM, Shun, CT, Kuo, ML, Lee, YC, Yang, PC: Up-regulation of tumor interleukin-8 expression by infiltrating macrophages: its correlation with tumor angiogenesis and patient survival in non-small cell lung cancer. *Clin Cancer Res,* 9**:** 729-737, 2003.

91. Chen, P, Huang, Y, Bong, R, Ding, Y, Song, N, Wang, X, Song, X, Luo, Y: Tumor-associated macrophages promote angiogenesis and melanoma growth via adrenomedullin in a paracrine and autocrine manner. *Clin Cancer Res,* 17**:** 7230-7239, 2011.

92. Nishie, A, Ono, M, Shono, T, Fukushi, J, Otsubo, M, Onoue, H, Ito, Y, Inamura, T, Ikezaki, K, Fukui, M, Iwaki, T, Kuwano, M: Macrophage infiltration and heme oxygenase-1 expression correlate with angiogenesis in human gliomas. *Clin Cancer Res,* 5**:** 1107-1113, 1999.

93. Lin, L, Chen, YS, Yao, YD, Chen, JQ, Chen, JN, Huang, SY, Zeng, YJ, Yao, HR, Zeng, SH, Fu, YS, Song, EW: CCL18 from tumor-associated macrophages promotes angiogenesis in breast cancer. *Oncotarget,* 6**:** 34758-34773, 2015.

94. Bronckaers, A, Gago, F, Balzarini, J, Liekens, S: The dual role of thymidine phosphorylase in cancer development and chemotherapy. *Med Res Rev,* 29**:** 903-953, 2009.

95. Hotchkiss, KA, Ashton, AW, Klein, RS, Lenzi, ML, Zhu, GH, Schwartz, EL: Mechanisms by which tumor cells and monocytes expressing the angiogenic factor thymidine phosphorylase mediate human endothelial cell migration. *Cancer Research,* 63**:** 527-533, 2003.

96. Sierra, JR, Corso, S, Caione, L, Cepero, V, Conrotto, P, Cignetti, A, Piacibello, W, Kumanogoh, A, Kikutani, H, Comoglio, PM, Tamagnone, L, Giordano, S: Tumor angiogenesis and progression are enhanced by Sema4D produced by tumor-associated macrophages. *J Exp Med,* 205**:** 1673-1685, 2008.

97. Pollard, JW: Tumour-educated macrophages promote tumour progression and metastasis. *Nature reviews Cancer,* 4**:** 71-78, 2004.

98. Giraudo, E, Inoue, M, Hanahan, D: An amino-bisphosphonate targets MMP-9-expressing macrophages and angiogenesis to impair cervical carcinogenesis. *Journal of Clinical Investigation,* 114**:** 623-633, 2004.

99. Zeisberger, SM, Odermatt, B, Marty, C, Zehnder-Fjallman, AHM, Ballmer-Hofer, K, Schwendener, RA: Clodronate-liposome-mediated depletion of tumour-associated macrophages: a new and highly effective antiangiogenic therapy approach. *Brit J Cancer,* 95**:** 272-281, 2006.

100. Galmbacher, K, Heisig, M, Hotz, C, Wischhusen, J, Galmiche, A, Bergmann, B, Gentschev, I, Goebel, W, Rapp, UR, Fensterle, J: Shigella mediated depletion of macrophages in a murine breast cancer model is associated with tumor regression. *PLoS One,* 5**:** e9572, 2010.

101. Mizutani, K, Sud, S, McGregor, NA, Martinovski, G, Rice, BT, Craig, MJ, Varsos, ZS, Roca, H, Pienta, KJ: The Chemokine CCL2 Increases Prostate Tumor Growth and Bone Metastasis through Macrophage and Osteoclast Recruitment. *Neoplasia,* 11**:** 1235-1242, 2009.

102. Robinson, SC, Scott, KA, Wilson, JL, Thompson, RG, Proudfoot, AEI, Balkwill, FR: A chemokine receptor antagonist inhibits experimental breast tumor growth. *Cancer Research,* 63**:** 8360-8365, 2003.

103. Kaler, P, Augenlicht, L, Klampfer, L: Macrophage-derived IL-1 beta stimulates Wnt signaling and growth of colon cancer cells: a crosstalk interrupted by vitamin D-3. *Oncogene,* 28**:** 3892-3902, 2009.

104. Wang, H, Lathia, JD, Wu, QL, Wang, JL, Li, ZZ, Heddleston, JM, Eyler, CE, Elderbroom, J, Gallagher, J, Schuschu, J, MacSwords, J, Cao, YT, McLendon, RE, Wang, XF, Hjelmeland, AB, Rich, JN: Targeting Interleukin 6 Signaling Suppresses Glioma Stem Cell Survival and Tumor Growth. *Stem Cells,* 27**:** 2393-2404, 2009.

105. Sansone, P, Storci, G, Tavolari, S, Guarnieri, T, Giovannini, C, Taffurelli, M, Ceccarelli, C, Santini, D, Paterini, P, Marcu, KB, Chieco, P, Bonafe, M: IL-6 triggers malignant features in mammospheres from human ductal breast carcinoma and normal mammary gland. *Journal of Clinical Investigation,* 117**:** 3988-4002, 2007.

106. Lin, WW, Karin, M: A cytokine-mediated link between innate immunity, inflammation, and cancer. *Journal of Clinical Investigation,* 117**:** 1175-1183, 2007.

References

107. Wyckoff, JB, Wang, Y, Lin, EY, Li, JF, Goswami, S, Stanley, ER, Segall, JE, Pollard, JW, Condeelis, J: Direct visualization of macrophage-assisted tumor cell intravasation in mammary tumors. *Cancer Research,* 67**:** 2649-2656, 2007.

108. Wyckoff, J, Wang, WG, Lin, EY, Wang, YR, Pixley, F, Stanley, ER, Graf, T, Pollard, JW, Segall, J, Condeelis, J: A paracrine loop between tumor cells and macrophages is required for tumor cell migration in mammary tumors. *Cancer Research,* 64**:** 7022-7029, 2004.

109. Condeelis, J, Pollard, JW: Macrophages: Obligate partners for tumor cell migration, invasion, and metastasis. *Cell,* 124**:** 263-266, 2006.

110. Qian, BZ, Pollard, JW: Macrophage Diversity Enhances Tumor Progression and Metastasis. *Cell,* 141**:** 39-51, 2010.

111. Kessenbrock, K, Plaks, V, Werb, Z: Matrix metalloproteinases: regulators of the tumor microenvironment. *Cell,* 141**:** 52-67, 2010.

112. Gocheva, V, Wang, HW, Gadea, BB, Shree, T, Hunter, KE, Garfall, AL, Berman, T, Joyce, JA: IL-4 induces cathepsin protease activity in tumor-associated macrophages to promote cancer growth and invasion. *Gene Dev,* 24**:** 241-255, 2010.

113. Li, Y, Zhao, L, Shi, B, Ma, S, Xu, Z, Ge, Y, Liu, Y, Zheng, D, Shi, J: Functions of miR-146a and miR-222 in Tumor-associated Macrophages in Breast Cancer. *Sci Rep,* 5**:** 18648, 2015.

114. Chen, J, Yao, Y, Gong, C, Yu, F, Su, S, Chen, J, Liu, B, Deng, H, Wang, F, Lin, L, Yao, H, Su, F, Anderson, KS, Liu, Q, Ewen, ME, Yao, X, Song, E: CCL18 from tumor-associated macrophages promotes breast cancer metastasis via PITPNM3. *Cancer cell,* 19**:** 541-555, 2011.

115. Wani, N, Nasser, MW, Ahirwar, DK, Zhao, H, Miao, Z, Shilo, K, Ganju, RK: C-X-C motif chemokine 12/C-X-C chemokine receptor type 7 signaling regulates breast cancer growth and metastasis by modulating the tumor microenvironment. *Breast cancer research : BCR,* 16**:** R54, 2014.

116. Vlaicu, P, Mertins, P, Mayr, T, Widschwendter, P, Ataseven, B, Hogel, B, Eiermann, W, Knyazev, P, Ullrich, A: Monocytes/macrophages support mammary tumor invasivity by co-secreting lineage-specific EGFR ligands and a STAT3 activator. *BMC Cancer,* 13**:** 197, 2013.

117. Kim, R, Emi, M, Tanabe, K, Arihiro, K: Tumor-driven evolution of immunosuppressive networks during malignant progression. *Cancer Research,* 66**:** 5527-5536, 2006.

118. Kelly, JM, Darcy, PK, Markby, JL, Godfrey, DI, Takedo, K, Yagita, H, Smyth, MJ: Induction of tumor-specific T cell memory by NK cell-mediated tumor rejection. *Nat Immunol,* 3**:** 83-90, 2002.

119. Riella, LV, Paterson, AM, Sharpe, AH, Chandraker, A: Role of the PD-1 pathway in the immune response. *Am J Transplant,* 12**:** 2575-2587, 2012.

120. Belai, EB, de Oliveira, CE, Gasparoto, TH, Ramos, RN, Torres, SA, Garlet, GP, Cavassani, KA, Silva, JS, Campanelli, AP: PD-1 blockage delays murine squamous cell carcinoma development. *Carcinogenesis,* 35**:** 424-431, 2014.

121. Rodriguez, PC, Quiceno, DG, Zabaleta, J, Ortiz, B, Zea, AH, Piazuelo, MB, Delgado, A, Correa, P, Brayer, J, Sotomayor, EM, Antonia, S, Ochoa, JB, Ochoa, AC: Arginase I production in the tumor microenvironment by mature myeloid cells inhibits T-cell receptor expression and antigen-specific T-cell responses. *Cancer Research,* 64**:** 5839-5849, 2004.

122. Adeegbe, DO, Nishikawa, H: Natural and induced T regulatory cells in cancer. *Frontiers in immunology,* 4, 2013.

123. Buldakov, M, Zavyalova, M, Krakhmal, N, Telegina, N, Vtorushin, S, Mitrofanova, I, Riabov, V, Yin, S, Song, B, Cherdyntseva, N, Kzhyshkowska, J: CD68+, but not stabilin-1+ tumor associated macrophages in gaps of ductal tumor structures negatively correlate with the lymphatic metastasis in human breast cancer. *Immunobiology*, 2015.

124. Condeelis, J, Singer, RH, Segall, JE: The great escape: when cancer cells hijack the genes for chemotaxis and motility. *Annu Rev Cell Dev Biol,* 21**:** 695-718, 2005.

125. Abraham, D, Zins, K, Sioud, M, Lucas, T, Schafer, R, Stanley, ER, Aharinejad, S: Stromal cell-derived CSF-1 blockade prolongs xenograft survival of CSF-1-negative neuroblastoma. *International Journal of Cancer,* 126**:** 1339-1352, 2010.

126. Schledzewski, K, Geraud, C, Arnold, B, Wang, S, Grone, HJ, Kempf, T, Wollert, KC, Straub, BK, Schirmacher, P, Demory, A, Schonhaber, H, Gratchev, A, Dietz, L, Thierse, HJ,

Kzhyshkowska, J, Goerdt, S: Deficiency of liver sinusoidal scavenger receptors stabilin-1 and -2 in mice causes glomerulofibrotic nephropathy via impaired hepatic clearance of noxious blood factors. *J Clin Invest,* 121**:** 703-714, 2011.

127. Johansen, JS, Schultz, NA, Jensen, BV: Plasma YKL-40: a potential new cancer biomarker? *Future Oncol,* 5**:** 1065-1082, 2009.

128. Libreros, S, Garcia-Areas, R, Shibata, Y, Carrio, R, Torroella-Kouri, M, Iragavarapu-Charyulu, V: Induction of proinflammatory mediators by CHI3L1 is reduced by chitin treatment: decreased tumor metastasis in a breast cancer model. *International journal of cancer Journal international du cancer,* 131**:** 377-386, 2012.

129. Karikoski, M, Marttila-Ichihara, F, Elima, K, Rantakari, P, Hollmen, M, Kelkka, T, Gerke, H, Huovinen, V, Irjala, H, Holmdahl, R, Salmi, M, Jalkanen, S: Clever-1/Stabilin-1 Controls Cancer Growth and Metastasis. *Clin Cancer Res*, 2014.

130. Friedl, P, Wolf, K: Tumour-cell invasion and migration: diversity and escape mechanisms. *Nature reviews Cancer,* 3**:** 362-374, 2003.

131. van Gils, JM, Derby, MC, Fernandes, LR, Ramkhelawon, B, Ray, TD, Rayner, KJ, Parathath, S, Distel, E, Feig, JL, Alvarez-Leite, JI, Rayner, AJ, McDonald, TO, O'Brien, KD, Stuart, LM, Fisher, EA, Lacy-Hulbert, A, Moore, KJ: The neuroimmune guidance cue netrin-1 promotes atherosclerosis by inhibiting the emigration of macrophages from plaques. *Nat Immunol,* 13**:** 136-143, 2012.

132. Movahedi, K, Schoonooghe, S, Laoui, D, Houbracken, I, Waelput, W, Breckpot, K, Bouwens, L, Lahoutte, T, De Baetselier, P, Raes, G, Devoogdt, N, Van Ginderachter, JA: Nanobody-based targeting of the macrophage mannose receptor for effective in vivo imaging of tumor-associated macrophages. *Cancer Res,* 72**:** 4165-4177, 2012.

133. Schledzewski, K, Falkowski, M, Moldenhauer, G, Metharom, P, Kzhyshkowska, J, Ganss, R, Demory, A, Falkowska-Hansen, B, Kurzen, H, Ugurel, S, Geginat, G, Arnold, B, Goerdt, S: Lymphatic endothelium-specific hyaluronan receptor LYVE-1 is expressed by stabilin-1+, F4/80+, CD11b+ macrophages in malignant tumours and wound healing tissue in vivo and in bone marrow cultures in vitro: implications for the assessment of lymphangiogenesis. *J Pathol,* 209**:** 67-77, 2006.

134. Ali, HR, Provenzano, E, Dawson, SJ, Blows, FM, Liu, B, Shah, M, Earl, HM, Poole, CJ, Hiller, L, Dunn, JA, Bowden, SJ, Twelves, C, Bartlett, JM, Mahmoud, SM, Rakha, E, Ellis, IO, Liu, S, Gao, D, Nielsen, TO, Pharoah, PD, Caldas, C: Association between CD8+ T-cell infiltration and breast cancer survival in 12,439 patients. *Annals of oncology : official journal of the European Society for Medical Oncology / ESMO,* 25**:** 1536-1543, 2014.

135. Bailey, SR, Nelson, MH, Himes, RA, Li, Z, Mehrotra, S, Paulos, CM: Th17 cells in cancer: the ultimate identity crisis. *Frontiers in immunology,* 5**:** 276, 2014.

136. Watanabe, MA, Oda, JM, Amarante, MK, Cesar Voltarelli, J: Regulatory T cells and breast cancer: implications for immunopathogenesis. *Cancer metastasis reviews,* 29**:** 569-579, 2010.

137. Dranoff, G: Balancing tumor immunity and inflammatory pathology. *Nat Med,* 19**:** 1100-1101, 2013.

138. Hamid, O, Robert, C, Daud, A, Hodi, FS, Hwu, WJ, Kefford, R, Wolchok, JD, Hersey, P, Joseph, RW, Weber, JS, Dronca, R, Gangadhar, TC, Patnaik, A, Zarour, H, Joshua, AM, Gergich, K, Elassaiss-Schaap, J, Algazi, A, Mateus, C, Boasberg, P, Tumeh, PC, Chmielowski, B, Ebbinghaus, SW, Li, XN, Kang, SP, Ribas, A: Safety and Tumor Responses with Lambrolizumab (Anti-PD-1) in Melanoma. *New Engl J Med,* 369**:** 134-144, 2013.

139. Nanda, R, Chow, LQ, Dees, EC, Berger, R, Gupta, S, Geva, R, Pusztai, L, Pathiraja, K, Aktan, G, Cheng, JD, Karantza, V, Buisseret, L: Pembrolizumab in Patients With Advanced Triple-Negative Breast Cancer: Phase Ib KEYNOTE-012 Study. *J Clin Oncol,* 34**:** 2460-2467, 2016.

140. Carretero, R, Sektioglu, IM, Garbi, N, Salgado, OC, Beckhove, P, Hammerling, GJ: Eosinophils orchestrate cancer rejection by normalizing tumor vessels and enhancing infiltration of CD8(+) T cells. *Nat Immunol,* 16**:** 609-617, 2015.

141. Di Carlo, E, Forni, G, Lollini, P, Colombo, MP, Modesti, A, Musiani, P: The intriguing role of polymorphonuclear neutrophils in antitumor reactions. *Blood,* 97**:** 339-345, 2001.

142. Wculek, SK, Malanchi, I: Neutrophils support lung colonization of metastasis-initiating breast cancer cells. *Nature,* 528**:** 413-417, 2015.

References

143. Granot, Z, Henke, E, Comen, EA, King, TA, Norton, L, Benezra, R: Tumor entrained neutrophils inhibit seeding in the premetastatic lung. *Cancer cell,* 20**:** 300-314, 2011.

144. Moganti, K, Li, F, Schmuttermaier, C, Riemann, S, Kluter, H, Gratchev, A, Harmsen, MC, Kzhyshkowska, J: Hyperglycemia induces mixed M1/M2 cytokine profile in primary human monocyte-derived macrophages. *Immunobiology*, 2016.

145. Mitrofanova, I, Zavyalova, M, Telegina, N, Buldakov, M, Riabov, V, Cherdyntseva, N, Kzhyshkowska, J: Tumor-associated macrophages in human breast cancer parenchyma negatively correlate with lymphatic metastasis after neoadjuvant chemotherapy. *Immunobiology*, 2016.

146. Luo, Y, Zhou, H, Krueger, J, Kaplan, C, Lee, SH, Dolman, C, Markowitz, D, Wu, W, Liu, C, Reisfeld, RA, Xiang, R: Targeting tumor-associated macrophages as a novel strategy against breast cancer. *J Clin Invest,* 116**:** 2132-2141, 2006.

147. Martinez-Pomares, L: The mannose receptor. *J Leukoc Biol,* 92**:** 1177-1186, 2012.

148. Kzhyshkowska, J: Multifunctional receptor stabilin-1 in homeostasis and disease. *ScientificWorldJournal,* 10**:** 2039-2053, 2010.

149. Lau, EK, Paavola, CD, Johnson, Z, Gaudry, JP, Geretti, E, Borlat, F, Kungl, AJ, Proudfoot, AE, Handel, TM: Identification of the glycosaminoglycan binding site of the CC chemokine, MCP-1: implications for structure and function in vivo. *J Biol Chem,* 279**:** 22294-22305, 2004.

7 **Curriculum Vitae**

Personal data

Name	Shuiping
Family name	Yin
Date of birth	August 6th, 1987.
Place of birth	Susong, Anhui province, China
Nationality	chinese
Marital status	Single
Father	Xianlong Yin
Mother	Xianghua Yu

School history

1993-1998	Yanling primary school, Susong, Anhui province, China
1998-2001	Xinqian middle school, Susong, Anhui province, China
2001-2004	Susong high school, Susong, Anhui province, China

University experience

2004-2011	Study at Anhui Medical University P.R. China
	Bachelor's degree in medicine
	Master's degree in Urology
2011-2012	Master degree of translational medical research
	Medical Faculty Mannheim, University of Heidelberg, Germany
2012-2016	Post-graduate study at the Medical Faculty Mannheim,
	University of Heidelberg, Germany

8 <u>Acknowledgement</u>